

IN-SITU ASPHALT MASTER CURVE CONSTRUCTION USING NON-  
DESTRUCTIVE TESTING TECHNIQUES

By

Edmund Pierre Surette

Submitted in partial fulfilment of the requirements  
for the degree of Doctor of Philosophy

at

Dalhousie University  
Halifax, Nova Scotia  
December 2014

© Copyright by Edmund Pierre Surette, 2014

## DEDICATION PAGE

The author would like to dedicate this thesis to his recently deceased father.

Dad, your continued support, love, motivation, and friendship has always provided me the strength to persevere. I love you.

# TABLE OF CONTENTS

|   |      |
|---|------|
| LIST OF TABLES .....  | v    |
| LIST OF FIGURES .....   | vi   |
| ABSTRACT .....  | viii |
| LIST OF SYMBOLS USED.....   | ix   |
| ACKNOWLEDGEMENTS.....   | xii  |
| CHAPTER 1 INTRODUCTION.....   | 1    |
| 1.1    BACKGROUND.....  | 1    |
| 1.2    THESIS OBJECTIVES .....  | 6    |
| CHAPTER 2 SUMMARY OF PAPER OBJECTIVES .....   | 7    |
| CHAPTER 3 PAPER 1: USE OF GPR AND MASW TO COMPLEMENT<br>BACKCALCULATED MODULI AND DESIGN LIFE<br>CALCULATIONS ..... | 10   |
| 3.1    ABSTRACT .....   | 10   |
| 3.2    INTRODUCTION .....   | 11   |
| 3.3    FALLING WEIGHT DEFLECTOMETER .....   | 12   |
| 3.4    GROUND PENETRATING RADAR .....   | 14   |
| 3.5    SEISMIC SURFACE WAVE PROPAGATION METHODS.....  | 16   |
| 3.6    DYNAMIC MODULUS MASTER CURVE .....   | 17   |
| 3.7    EXPERIMENTAL TESTING AND RESULTS.....  | 19   |
| 3.7.1    Site Description .....   | 19   |
| 3.7.2    Coring and Trenching.....  | 21   |
| 3.7.3    Dynamic Modulus and Master Curve .....   | 21   |
| 3.7.4    Temperature Measurement.....   | 22   |
| 3.7.5    Ground Penetrating Radar .....   | 23   |
| 3.7.6    Surface Wave Testing .....   | 25   |
| 3.7.7    Falling Weight Deflectometer .....   | 27   |
| 3.7.8    Design Parameters.....   | 31   |
| 3.8    CONCLUSIONS .....  | 33   |
| 3.9    REFERENCES .....   | 34   |
| CHAPTER 4 PAPER 2: ROBUST MASTER CURVE DETERMINATION USING<br>COMPLIMENTARY MASW TECHNIQUES .....                   | 39   |

|   |   |     |
|---|---|-----|
| 4.1   | ABSTRACT .....                                  | 39  |
| 4.2   | KEYWORDS .....                                  | 39  |
| 4.3   | INTRODUCTION .....                              | 40  |
| 4.4   | DETERMINATION OF DYNAMIC MODULUS .....          | 43  |
| 4.4.1   | Laboratory Testing AASHTO TP 62 .....           | 43  |
| 4.4.2   | Multichannel Analysis of Surface Waves .....    | 44  |
| 4.4.3   | MEPDG Dynamic Modulus Predictive Equation ..... | 45  |
| 4.5   | DYNAMIC MODULUS MASTER CURVE CONSTRUCTION ..... | 46  |
| 4.5.1   | Log-Log Viscosity Relationship (MEPDG).....     | 46  |
| 4.5.2   | Arrhenius .....                                 | 47  |
| 4.5.3   | WLF.....  | 47  |
| 4.5.4   | Second Order Polynomial .....                   | 48  |
| 4.6   | EXPERIMENTAL TESTING AND RESULTS.....           | 48  |
| 4.7   | IMPACT ON PAVEMENT DESIGN.....                  | 56  |
| 4.8   | CONCLUSIONS.....                                | 59  |
| 4.9   | REFERENCES .....                                | 60  |
| CHAPTER 5 PAPER 3: IN-SITU ASPHALT MASAER CURVE CONSTRUCTION<br>USING NON-DESTRUCTIVE TESTING TECHNIQUES..... |   | 66  |
| 5.1   | ABSTRACT .....                                  | 66  |
| 5.2   | KEYWORDS .....                                  | 67  |
| 5.3   | INTRODUCTION .....                              | 67  |
| 5.4   | FIELD AND LABORATORY TESTING .....              | 71  |
| 5.5   | DATA ANALYSIS AND DISCUSSION .....              | 76  |
| 5.6   | CONCLUSIONS.....                                | 89  |
| 5.7   | REFERENCES .....                                | 91  |
| CHAPTER 6 DISCUSSION .....  |   | 96  |
| CHAPTER 7 CONCLUSION.....   |   | 105 |
| REFERENCES .....  |   | 110 |

## LIST OF TABLES

|          |   |    |
|----------|---|----|
| Table 1  | Asphalt core thicknesses. ....  | 21 |
| Table 2  | Moduli results from Station 10. ....  | 29 |
| Table 3  | Moduli results from Station 180. ....   | 29 |
| Table 4  | SN <sub>eff</sub> with and without GPR thickness data for Station 10 and Station 180..                          | 32 |
| Table 5  | SN <sub>eff</sub> with and without GPR thickness data for entire 200 m section. ....                            | 32 |
| Table 6  | Remaining service life. ....  | 33 |
| Table 7  | Typical values of Poisson’s ratio versus temperature (NCHRP, 2004). ....  | 49 |
| Table 8  | Master curve and shift parameters. ....   | 51 |
| Table 9  | Frequency and temperature corrected dynamic modulus. ....   | 54 |
| Table 10 | Predicted fatigue design period. ....   | 58 |
| Table 11 | Field testing dates. ....   | 74 |
| Table 12 | Master curve parameters. ....   | 78 |
| Table 13 | Frequency and temperature shifted dynamic modulus Barrington. ....  | 82 |
| Table 14 | Frequency and temperature shifted dynamic modulus Miramichi. ....   | 83 |
| Table 15 | Coefficients of the developed predictive equation for establishing $\alpha'$ for a PG58-28 asphalt binder. .... | 87 |
| Table 16 | Coefficients of standard equation. ....   | 88 |
| Table 17 | Frequency and temperature shifted dynamic modulus Tantallon. ....   | 89 |

## LIST OF FIGURES

|           |   |    |
|-----------|---|----|
| Figure 1  | Typical pavement cross section. ....  | 20 |
| Figure 2  | Dynamic modulus master curve.....   | 22 |
| Figure 3  | GPR antenna sled.....   | 23 |
| Figure 4  | Longitudinal GPR results.....   | 24 |
| Figure 5  | Transverse GPR results.....   | 24 |
| Figure 6  | GPR granular material thickness.....  | 25 |
| Figure 7  | MSOR test setup. ....   | 26 |
| Figure 8  | Phase velocity dispersion curve for Station 10 center lane.....   | 27 |
| Figure 9  | Dynatest 8082 HWD.....  | 28 |
| Figure 10 | Backcalculated moduli results for 200 m section. ....   | 30 |
| Figure 11 | Raw deflection data Station 10. ....  | 30 |
| Figure 12 | Phase velocity dispersion curve from plate sample. ....   | 50 |
| Figure 13 | Combinations of dynamic modulus data sets and master curve models.....                                      | 52 |
| Figure 14 | Plot of master curve versus laboratory $E^*$ . ....   | 53 |
| Figure 15 | Average relative error for the frequency and temperature shifted $E^*$ .....                                | 55 |
| Figure 16 | Master curve constructed using a combination of AASHTO TP 62 and MASW data and the polynomial equation..... | 56 |
| Figure 17 | Phase-velocity dispersion curve Barrington site.....  | 77 |
| Figure 18 | Constructed master curves; (a) Barrington Site, (b) Miramichi Site. ....                                    | 79 |
| Figure 19 | Plot of master curve versus laboratory $E^*$ for Barrington. ....   | 80 |
| Figure 20 | Plot of master curve versus laboratory $E^*$ for Miramichi.....   | 80 |
| Figure 21 | Average relative error for the frequency and temperature shifted $E^*$ Barrington. ....                     | 82 |

|           |  |     |
|-----------|--|-----|
| Figure 22 | Average relative error for the frequency and temperature shifted $E^*$<br>Miramichi..... | 83  |
| Figure 23 | FWD temperature correction Barrington Site.....  | 84  |
| Figure 24 | Summary of Seasonal Nondestructive Test Data.....  | 85  |
| Figure 25 | Constructed damaged master curves.....   | 87  |
| Figure 26 | Comparison of MASW and resonant frequency moduli.....                                    | 104 |

## **ABSTRACT**

For in-situ asphalt concrete characterization, the MEDPG recommends using the falling weight deflectometer (FWD) to determine the dynamic modulus in combination with the construction of the master curve using the predictive equation. If there is adequate asphalt concrete thickness, asphalt cores may be tested using AASHTO TP 62 to determine the dynamic modulus and construct the master curve, however these cores may not be representative of the actual pavement condition since they may be extracted from select areas showing minimum damage. Both the predictive equation and AASHTO TP 62 require destructive core extraction and can be too costly for many transportation agencies.

Recently, the Multichannel Analysis of Surface Waves (MASW) technique has shown to provide accurate non-destructive estimates of the in-situ asphalt concrete dynamic modulus, which may complement the FWD backcalculation process, however the values only constitute the upper two thirds of the master curve, while FWD determined moduli values generally constitute the lower portion of the curve. Therefore, it is a requirement to correct surface wave measured moduli to a standard design frequency using the master curve. To date, the master curves utilized in correcting seismic measured moduli have been constructed using conventional methods and have not incorporated the seismic data into the construction process. There is currently no in-situ non-destructive test method available to measure the dynamic moduli at the range of frequencies required to construct the master curve and researchers have not attempted to construct the master curve in-situ ultimately making the master curve more accessible for asphalt concrete characterization.

This research demonstrates the construction of an in-situ non-destructive master curve using a combination of MASW and FWD data collected over a range of temperatures, which then provides a technique to correct the MASW data for enhancing the FWD backcalculation process or to seed the AC modulus directly. Additionally, for MASW moduli correction, the addition of the surface wave data into the master curve construction process is extremely important for providing the most accurate results when used in design.



## LIST OF SYMBOLS USED

|                      |  |
|----------------------|--|
| A                    | Intercept of linear regression model of viscosity temperature susceptibility |
| a                    | Coefficient of quadratic relationship between shift factor and temperature   |
| a                    | Fitting parameter (Section 4.5.2)  |
| a <sub>1</sub>       | Coefficient to establish damage parameter (Section 5.4)                      |
| a <sub>2</sub>       | Coefficient to establish damage parameter (Section 5.4)                      |
| a <sub>3</sub>       | Coefficient to establish damage parameter (Section 5.4)                      |
| a <sub>5</sub>       | Coefficient to establish damage parameter (Section 5.4)                      |
| a(T)                 | Shift factor at temperature T  |
| b                    | Coefficient of quadratic relationship between shift factor and temperature   |
| b <sub>1</sub>       | Coefficient of polynomial function (Section 5.5)                             |
| b <sub>2</sub>       | Coefficient of polynomial function (Section 5.5)                             |
| b <sub>3</sub>       | Coefficient of polynomial function (Section 5.5)                             |
| b <sub>4</sub>       | Coefficient of polynomial function (Section 5.5)                             |
| C                    | Laboratory to field adjustment factor (Section 4.7)                          |
| C1                   | Fitting parameter (Section 4.5.3)  |
| C2                   | Fitting parameter (Section 4.5.3)  |
| c                    | Coefficient of quadratic relationship between shift factor and temperature   |
| c                    | Speed of light in free space (Section 3.4)                                   |
| c                    | Fitting parameter (Section 4.5.1)  |
| d                    | Distance between the transmitter and the receiver units within the antenna   |
| d <sub>j</sub>       | Damage estimate (Section 5.4)  |
| E                    | Elastic modulus  |
| E <sub>i</sub>       | Backcalculated modulus at a given temperature recorded in the field          |
| E <sub>Seismic</sub> | Elastic modulus at seismic frequency   |
| E <sub>FWD</sub>     | Elastic modulus at FWD frequency   |
| E*                   | Complex dynamic modulus (used as dynamic modulus for simplicity)             |
| E*                   | Dynamic modulus  |
| E* <sub>M</sub>      | Laboratory measured dynamic  |
| E* <sub>P</sub>      | Predicted dynamic modulus values   |

|               |   |
|---------------|---|
| $E'$          | Storage modulus   |
| $E''$         | Loss modulus  |
| $f$           | Frequency   |
| $h$           | Layer thickness   |
| $h_{ac}$      | Asphalt concrete thickness  |
| $h_i$         | Thickness of the $i^{\text{th}}$ layer  |
| $k'_1$        | Correction parameter (Section 4.7)  |
| $N$           | Number of observations  |
| $N_f$         | Number of repetitions to fatigue cracking   |
| $R^2$         | Coefficient of determination  |
| $S_e$         | Standard error  |
| $S_y$         | Standard deviation  |
| $t$           | Total recorded travel time (Section 3.4)  |
| $t$           | Time  |
| $t_i$         | Electromagnetic wave two way travel time through the $i^{\text{th}}$ layer                                    |
| $T$           | Temperature   |
| $T_i$         | Selected temperature of interest  |
| $T_R$         | Temperature (Rankine)   |
| $T_{ref}$     | Reference temperature   |
| $V$           | Electromagnetic wave velocity   |
| $V_R$         | Rayleigh wave velocity  |
| $V_S$         | Shear wave velocity   |
| $VTS$         | Slope of linear regression model of viscosity temperature susceptibility                                      |
| $\alpha$      | Difference between maximum and minimum modulus values (master curve sigmoidal function)                       |
| $\alpha'$     | Difference between maximum and minimum modulus values (damaged master curve sigmoidal function) (Section 5.4) |
| $\beta$       | Shape parameter in master curve sigmoidal function  |
| $\delta$      | Minimum modulus value (master curve sigmoidal function)   |
| $\Delta t$    | FWD loading time difference obtained from time history data   |
| $\varepsilon$ | Compressive strain  |

|              |   |
|--------------|---|
| $\epsilon_i$ | Dielectric constant of the $i^{\text{th}}$ layer                        |
| $\epsilon_t$ | Tensile strain at the critical location                                 |
| $\epsilon_0$ | Maximum strain amplitude  |
| $\eta$       | Bitumen viscosity at the age and temperature of interest                |
| $\eta_{Tr}$  | Viscosity at temperature and RTFO aging                                 |
| $\gamma$     | Shape parameter in master curve sigmoidal function                      |
| $\nu$        | Poisson's Ratio   |
| $\omega$     | Angular frequency   |
| $\delta$     | Phase lag separating stress from strain                                 |
| $\rho$       | Density   |
| $\rho_4$     | Cumulative percent retained on the number 4 sieve                       |
| $\rho_{3/4}$ | Cumulative percent retained on the $3/4$ inch sieve                     |
| $\rho_{3/8}$ | Cumulative percent retained on the $3/8$ inch sieve                     |
| $\rho_{200}$ | Percent passing the number 200 sieve                                    |
| $\sigma$     | Compressive stress  |
| $\sigma_0$   | Maximum stress amplitude  |
| $\theta$     | Parameter used in damaged master curve sigmoidal function (Section 5.4) |
| $\xi$        | Reduced frequency   |

## **ACKNOWLEDGEMENTS**

The author would like to sincerely thank his current supervisors Dr. Nouman Ali and Dr. Christopher Barnes, in addition to his former supervisor Dr. Jean-François Trottier for their supervision, guidance, friendship and support both professionally and personally throughout the thesis project.

The following persons also contributed significantly to the success of this project:

Dr. Dean Forgeron and Dr. George Jarjoura of the guidance committee for direction, evaluation and support. The civil engineering technical staff, faculty members and students who contributed their technical services, friendship and assistance.

This research was funded by the Natural Sciences and Engineering Research Council of Canada through their support of Dr. Jean-François Trottier, who was Canada Research Chair for Structural Health Monitoring and Innovative Materials during that period; Industry Canada, through the Atlantic Innovative Fund; Stantec, formerly Jacques Whitford; Canada Foundation for Innovation; Nova Scotia Research and Innovative Trust; Dalhousie University; University of New Brunswick; Nova Scotia Department of Transportation and Infrastructure Renewal; New Brunswick Department of Transportation; Prince Edward Island Department of Transportation and Public Works; and, Newfoundland and Labrador Department of Transportation and Works.

An additional thank you to Nova Scotia Department of Transportation and Infrastructure Renewal and New Brunswick Department of Transportation for the additional funding contributed to the development of the instrumented test sections and traffic control.

The author would especially like to thank his wife, Denise, and sons Gavin and Owen for their love, emotional support, and understanding throughout the thesis, and to his mom, for her continued support and motivation during the thesis and always.

# CHAPTER 1 INTRODUCTION

## 1.1 BACKGROUND

With the current state of declining transportation infrastructure throughout North America, many highway agencies are in the process of adapting the Guide for the Mechanistic-Empirical Design of New and Rehabilitated Pavement Structures (MEPDG). In the Canadian Maritime Provinces a similar trend is developing where the application of purely empirical designs from the 1950's are slowly transforming to a mechanistic-empirical methodology with expectations of improving current pavement performance. The mechanistic-empirical design framework requires detailed information on four key inputs, which include climate, material properties, traffic, and the pavement structure, used to predict the pavement response and ultimately the expected performance (NCHRP, 2004). The pavement response is employed to estimate cumulative damage for different distress types by means of transfer functions calibrated using historical performance data collected on pavement sections throughout North America. Regardless of the pavement type to be designed, the element considered to be the most influential in determining the performance of a pavement structure are the materials used in the various structural layers. As a result it is extremely important to characterize the materials in question using the properties that are required to predict the levels of stress, strain and displacement in the pavement structure.

For flexible pavements, the dynamic modulus ( $|E^*|$ , or  $E^*$  for simplicity) of the asphalt concrete layer is a mandatory input at all three hierarchical levels described in the MEPDG (NCHRP, 2004). Due to the viscoelastic nature of asphalt concrete, the asphalt master curve is also required to characterize the dynamic modulus over a wide range of frequencies at a given reference temperature and allows for the comparison of modulus values when testing has been performed at multiple loading frequencies and test temperatures for use in design. Depending on the design scenario (new or rehabilitated) and level of engineering effort required, the asphalt concrete dynamic modulus is generally measured through

laboratory or in-situ testing at the highest degree of complexity, or predictive stiffness models are used for lower levels of design. To compute the dynamic modulus from a predictive model, construction records or laboratory testing on asphalt concrete samples is required to determine binder viscosity data, gradation information, and volumetric parameters. To measure the dynamic modulus and construct an in-situ master curve coinciding with the highest level of rehabilitation design, the MEPDG recommends performing Falling Weight Deflectometer (FWD) testing to backcalculate the asphalt concrete modulus and the use of field cores to establish mixture volumetric parameters to input into the MEPDG predictive equation. FWD testing and the backcalculation procedure are described in Chapter 3, while the MEPDG predictive equation is detailed in Chapter 4. For new pavements, the highest level of design requires laboratory dynamic modulus testing (AASHTO TP 62, detailed in Chapter 3), however in practice if the asphalt concrete layer is sufficiently thick, extracted cores can be used to conduct AASHTO TP 62 testing to determine the dynamic modulus and characterize the master curve.

Non-destructive deflection testing by means of the FWD has become a fundamental tool for many transportation agencies when evaluating the structural adequacy of in-service pavements. In circumstances where a pavement evaluation is performed as part of an overall rehabilitation strategy, the MEPDG also requires the construction of the asphalt concrete master curve by means of AASHTO TP 62 or the predictive equation, which both necessitate extracted core samples. However, many transportation agencies are hesitant to perform destructive core extraction, especially on newer roadways considering that when not correctly repaired can result in cracking, potholes and moisture infiltration, and therefore may not attempt to construct the master curve. Furthermore, AASHTO TP 62 testing requires sophisticated and expensive testing equipment which is not available to all transportation agencies and has been recognised as prohibitive for routine master curve development (Dogan et al., 2003)(Bonaquist and Christensen, 2005)(Kweon and Kim, 2006). In regards to FWD testing, the recorded global structural response is influenced by the entire pavement structure and does not specifically target the asphalt concrete layer. In addition, several factors including variation in layer thicknesses, the presence of bedrock or a highly non-linear subgrade, thin asphalt layers, edge restraint, and seasonal

characteristics can influence and complicate the backcalculation process and alter the results obtained (Irwin, 2002)(Hakim and Brown, 2006).

In addition to FWD, seismic test methods including surface wave testing (Ryden, 2004) (Nazarian et al., 2005)(Celaya and Nazarian, 2006)(Barnes, 2008), and resonance frequency measurements (Kweon and Kim, 2006)(Lacroix et al., 2009)(Ryden, 2011, Van Velsor et al., 2011, Gudmarsson et al., 2012a) have been used successfully to determine the asphalt concrete modulus over a broad frequency range. The portable seismic pavement analyzer (PSPA) (Oh et al., 2012) and multichannel analysis of surface waves (MASW) (Barnes and Trottier, 2010) have been used successfully to determine the asphalt concrete modulus in-situ, whereas resonant frequency testing is generally performed on samples in the laboratory (Ryden 2011, Gudmarsson et al., 2012a).

Seismic test methods have the ability to complement FWD testing to fully characterize the entire pavement structure, however the moduli values obtained using seismic methods are determined at much higher frequencies (5 – 90 kHz) than is generated by vehicular traffic and the FWD (10 – 25 Hz). The MEPDG does provide a brief description of seismic testing of pavement systems but does not describe the testing procedure or correction procedure required to implement in-situ measured seismic moduli in pavement design.

The master curve constructed using conventional test methods (AASHTO TP 62) has proven to be a valuable tool for correcting higher frequency surface wave moduli down to a lower frequency design value (Celaya and Nazarian, 2006)(Barnes and Trottier, 2009)(Oh et al., 2012) but there remains the requirement to perform destructive core testing. In addition, the dynamic modulus values determined using AASHTO TP 62 are generally measured at frequencies ranging from 0.1 Hz to 25 Hz which are considerably less than the frequencies achieved using seismic testing.

One aspect that has not been examined regarding master curve development for correcting seismic moduli is the influence of including the higher frequency seismic modulus data with the conventional dynamic modulus data. Gudmarsson et al. (2012b) suggested that

additional research was required to evaluate the validity of the time-temperature superposition principle for moduli values obtained from high frequency seismic test methods.

One of the primary concerns that many highway agencies share is the capability to adequately characterize their pavement materials. In many cases, the asphalt concrete mixture parameters required in the MEPDG are unknown since the pavement structures that are currently in service were constructed several years prior to making the decision to adapt the newer pavement design methodology. In Nova Scotia for example, the PG binder grade is generally consistent throughout the province, however there is an abundance of quality aggregates used throughout the province, therefore constructing the master curve for one particular mixture may not be valid for another since aggregate type influences the dynamic modulus (Ping and Xiao, 2007). Consequently, to characterize the in service pavements throughout the province would require the extraction of numerous core samples and a tremendous amount of AASHTO TP 62 laboratory testing or volumetric parameter verification. However, the Nova Scotia Department of Transportation and Infrastructure Renewal (NSTIR), similarly to many transportation agencies throughout North America, does not have direct access to the equipment required to perform AASHTO TP 62 testing and no study has been performed to validate the predictive equation for the local materials.

There is currently no non-destructive in-situ test method available that can provide similar results to conventional laboratory dynamic modulus testing for constructing the asphalt concrete master curve (Gudmarsson et al., 2012b). The ability to characterize the asphalt master curve in-situ would be extremely useful as it would eliminate the requirement for destructive core extraction, eliminate the requirement for expensive and time consuming laboratory testing, provide a method of directly establishing the damaged master curve, and provide a method for correcting seismic moduli to a design frequency and ultimately enhance the FWD backcalculation process by seeding the asphalt concrete modulus so that the underlying materials can be of direct focus. To fully depict the range of reduced frequencies required to construct a functional master curve, dynamic moduli values must be measured at a multitude of frequencies and temperatures (Ryden, 2011). Constructing



a master curve solely using seismic determined dynamic modulus data has been challenging (Kweon and Kim, 2006, Lacroix et al., 2009)(Ryden, 2011)(Gudmarsson et al., 2012a) as the lower frequency content required to fully characterize the curve is unavailable. Using resonant frequency testing to determine the dynamic modulus at fundamental modes of vibration, Kwon and Kim (2006) and Lacroix et al., (2009) attempted to construct a master curve solely from the seismic data, however due to the absence of low frequency content, the predictive equation was applied to determine dynamic modulus values at higher temperatures. The use of resonant acoustic spectroscopy (RAS), where additional modes of vibration can be observed, was implemented by Ryden (2011) on cylindrical asphalt concrete disks and by Gudmarsson et al. (2012a) on asphalt beam samples with similar results. Ryden (2011) concluded that resonant frequency testing could not be used to establish dynamic modulus values corresponding to the lower frequency range of the master curve. Gudmarsson et al. (2012b) fitted theoretical frequency response functions (FRFs) with measured FRFs using the finite element method to characterize the asphalt concrete properties at a wider range of frequencies with success, however the results were not compared to conventional testing methods and heavy computer simulation was required for analysis. This technique required laboratory testing of asphalt concrete beam samples and therefore could not be performed in-situ.

In contrast to the high frequency seismic data, FWD moduli are measured at frequencies similar to conventional AASHTO TP 62 testing and may provide the low frequency content required to construct a master curve in combination with the seismic moduli. Therefore, the main focus of this thesis is to combine in-situ FWD and seismic surface wave testing to determine the dynamic modulus over a full range of frequencies and temperatures and then attempt to construct a master curve based solely on the non-destructive data. As part of their testing protocol, many highway agencies, including NSTIR, perform seasonal FWD testing on several roadways to characterize the seasonal variations in the pavement structure. Supplementing current FWD test programs with relatively inexpensive seismic testing could conceivably provide the data necessary to construct an in-situ master curve offering the benefits described above.

## **1.2 THESIS OBJECTIVES**

The objectives of this thesis, addressed by the three papers included in Chapters 3, Chapter 4, and Chapter 5, are as follows:

- 1) To evaluate and validate the importance of using GPR testing for determining layer thicknesses when performing FWD testing for pavement design and evaluation.
- 2) To evaluate the capability of multichannel surface wave testing to complement FWD testing and the backcalculation procedure.
- 3) To evaluate some of the FWD temperature correction models relative to constructed master curves using data collected from the Canadian Maritime Provinces.
- 4) To evaluate the influence of shift factor model and the inclusion of surface wave derived moduli on the ability of the master curve to correct seismic data for design.
- 5) To evaluate the dynamic modulus predictive equation for use in the Canadian Maritime Provinces.
- 6) To demonstrate the importance of evaluating the ability of the constructed master curve to correct seismic moduli through design examples.
- 7) To develop a master curve solely from in-situ nondestructive testing for correcting high frequency seismic moduli to a standard design value.
- 8) To develop an alternative method to the procedure described in the MEPDG for constructing the damaged master curve.

## **CHAPTER 2      SUMMARY OF PAPER OBJECTIVES**

The dynamic modulus values used in the construction of asphalt concrete master curves are generally measured using the conventional techniques described in the MEPDG, AASHTO TP 62 and the predictive equation. These methods require expensive testing equipment not accessible to all transportation agencies. When assessing in-situ pavements, destructive core testing is required and leads to moisture infiltration and cracking when not correctly repaired. Barnes (2008) suggested that the construction of a master curve based on non-destructive test methods would make construction of master curves more accessible to agencies that do not have the sophisticated laboratory equipment. In addition, master curves constructed using conventional techniques are generally constructed using relatively undamaged extracted specimens, which may not adequately characterize the in-situ asphalt concrete condition and ultimately skew seismic moduli corrected values.

The research objectives of this thesis include constructing an in-situ master curve non-destructively and optimizing some of the current tools utilized in pavement evaluation by combining several non-destructive testing techniques. The following papers address these objectives in addition to evaluating some of the current design parameters for the Canadian Maritime environment. Some of the key elements addressed in the papers are summarized below:

- 1) Construction of roadways can be highly variable in regards to consistent layer thicknesses, both for bound and unbound materials. Thickness is a key input when performing pavement design and evaluation, however many transportation agencies still rely on destructive coring and boring methods to determine pavement layer thicknesses. These methods are time consuming and do not provide continuous thickness data. In addition to thickness variations along the length of a highway section, there may be considerable differences across the width of a section which is not identified using destructive methods and ultimately severely influencing the pavement design.

- 2) FWD backcalculated moduli are used in assessing in-situ pavement structures and in the construction of the master curve for the asphalt concrete layer. There are several factors including variation in layer thicknesses, the presence of bedrock or a highly non-linear subgrade, thin asphalt layers, edge restraint, and seasonal characteristics that can influence and complicate the backcalculation process and alter the results obtained. Surface wave testing has been used to compute in-situ asphalt concrete moduli, however an assessment of the usefulness of the seismic moduli in complementing the FWD testing has not been provided until recently.
- 3) Temperature correction of FWD backcalculated moduli to a standard design temperature has been a focal point for many researchers, equipment manufacturers and highway agencies. Several correction models have been developed for agencies throughout the United States, however these models have not been validated for the materials currently used in the Canadian Maritime Provinces.
- 4) With the emergence of seismic surface wave methods to measure the in-situ dynamic modulus, the asphalt concrete master curve has become an increasingly valuable tool in correcting the higher frequency seismic moduli to a standard design value. The master curves currently used in correcting seismic moduli to standard temperatures and frequencies are constructed using conventional dynamic modulus data (AASHTO TP 62, predictive equation), however including the in-situ determined seismic moduli into the master curve construction process has not been examined. In addition, the impact of the shift factor model used in generating the asphalt concrete master curve on seismic moduli correction has not been examined.
- 5) When evaluating the various methods of measuring the dynamic modulus and master curve construction techniques, validation is generally limited to a statistical investigation. Small deviations that might be overlooked in the statistical analysis may not adequately represent the variations in design parameters. Additionally, there must be emphasis on calibrating developed models for local conditions.

- 6) Many highway agencies conduct seasonal FWD testing on test sections located throughout their jurisdiction, however seismic testing has not been added to their test program since they have no method of correcting the data to a standard frequency. Researchers have attempted to construct master curves using seismic data measured in a laboratory, but have had little success. Consequently, there is a requirement to develop an in-situ master curve so that seismic testing becomes more attractive to highway agencies and the benefits of combining multiple non-destructive test methods can be examined.
  
- 7) Literature has shown that seismic moduli may be sensitive to damage in the asphalt concrete, however the current approach to construct the field damaged dynamic modulus master curve requires FWD testing in tandem with core extraction for determining the mixture volumetric parameters for use in the predictive equation. Due to the variability of the predictive equation and the factors influencing the backcalculated moduli, determining a damaged master curve in-situ would be valuable.

## **CHAPTER 3      PAPER 1: USE OF GPR AND MASW TO COMPLEMENT BACKCALCULATED MODULI AND DESIGN LIFE CALCULATIONS**

Edmund Surette, Christopher Barnes, Nouman Ali

Based on: Paper prepared for presentation at the  
“Pavement Evaluation, Performance and Management” Poster Session  
2010 Annual Conference of the  
Transportation Association of Canada  
Halifax, Nova Scotia

### **3.1 ABSTRACT**

Non-destructive deflection testing by means of the falling weight deflectometer is one of the most reliable and established methods for evaluating the structural capacity of pavements. However, there are several factors that can influence the moduli values obtained through the backcalculation process and the resulting calculated design life or required overlay thickness. Some of the difficulties associated with backcalculation include constructing a suitable pavement model due to the as-built variations in layer thicknesses in addition to determining the modulus for thin asphalt layers. Many researchers have reported success when using Ground Penetrating Radar (GPR) to determine flexible pavement layer thicknesses. Recently, the Multi-Channel Analysis of Surface Waves (MASW) technique has been shown to provide accurate non-destructive estimates of the in-situ asphalt concrete modulus. In this study, nondestructive deflection testing in addition to GPR and MASW testing was performed along a 200 m test section and across the transverse width of the traffic lane to establish variations in thickness and moduli. Backcalculation was performed with and without GPR thickness data resulting in a 40% variation in modulus. The modulus obtained via GPR data provided a significantly better estimate to the recorded MASW modulus. Using the 1993 AASHTO Guide for Design of Pavement Structures, the difference in modulus and thickness between GPR and

non GPR data resulted in nearly a two inch difference in required overlay thickness. The results obtained using the new Mechanistic-Empirical Pavement Design Guide (MEPDG) identified considerable differences in rutting performance, but only minute differences in asphalt fatigue.

### **3.2 INTRODUCTION**

With the release of the new Mechanistic-Empirical Pavement Design Guide (MEPDG), pavement design technology is currently undergoing a major upgrade. The MEPDG which is intended to supersede the 1993 AASHTO Guide for Design of Pavement Structures uses key material characterization inputs such as the dynamic modulus for asphalt concrete layers and the resilient modulus for granular layers to design suitable overlays that will extend the service life of the pavement system. Non-destructive testing such as deflection testing by means of the falling weight deflectometer (FWD), ground penetrating radar (GPR), and seismic methods, is also highly recommended for the evaluation of existing pavements for rehabilitation. A large number of highway agencies are now in the process of implementing or are developing studies to prepare adoption of the new MEPDG.

The traditional method used to determine the dynamic modulus of asphalt concrete involves subjecting cylindrical samples to sinusoidal loading at various frequencies and temperatures. This method requires sophisticated and expensive testing equipment which may not be available to all transportation agencies and involves extracting core samples from in-situ pavements. Accordingly, FWD testing has become the primary means of characterizing the in-situ properties of flexible pavements (Park et al., 2001). Using a process known as backcalculation, layer moduli can be determined for a particular pavement using the recorded deflection values. However, literature has shown (Ullidtz and Stubstad, 1985)( Irwin, 2002) that there are several factors that can influence the results obtained through the backcalculation process. Two of these factors include variations in pavement layer thicknesses and the insensitivity in computing the modulus of thin asphalt

layers. Consequently, the errors in the backcalculated moduli will modify the requirements for an appropriate pavement design.

Conventionally, pavement layer thicknesses have been established using destructive techniques such as coring or drilling bore holes which are time consuming and do not provide continuous thickness data. In recent years, GPR has been shown to be a valuable non-destructive tool in assessing pavement layer thickness (Maser et al., 2006). As a result, some agencies now specify the use of GPR when performing deflection testing.

Seismic surface wave propagation methods which include the steady state Rayleigh wave method (Jones, 1955) and Spectral Analysis of Surface Waves (SASW) (Heisey et al., 1982)(Nazarian et al., 1983) have been utilized in determining layer moduli for pavement and geotechnical engineering purposes for over 50 years. More recently, Multi-channel Simulation with One Receiver (MSOR) (Ryden et al., 2003) and the Multi-Channel Analysis of Surface Waves (MASW) (Park et al., 1999)(Barnes and Trottier, 2009) technique have shown to provide accurate non-destructive estimates for computing the in-situ asphalt concrete modulus of the top surface layer.

An experimental study was conducted to compare pavement layer thicknesses determined from GPR and conventional destructive techniques and to establish the effect on the backcalculated moduli and resultant design requirements. Moduli values computed from the MASW test were compared to traditional dynamic modulus testing and were used to validate the backcalculated moduli values.

### **3.3 FALLING WEIGHT DEFLECTOMETER**

One of the most reliable methods used to evaluate the structural capacity and remaining serviceable life of in-situ pavements is to use nondestructive deflection testing. The impulse devices, particularly the falling weight deflectometer (FWD), are recently developed and are currently the most used by highway and airport agencies (Shahin, 1994).



The FWD consists of a drop-mass system where a weight can be lifted to various heights and then dropped to produce the desired impulse force. A load cell and several velocity transducers or geophones measure the magnitude of the load in addition to the deflections at different offset positions from the load center. One important characteristic of the FWD is that the load applied to the pavement structure is comparable to highway traffic loading with regards to both frequency and magnitude.

From the measured deflections and load magnitude, in addition to other input parameters such as pavement layer thickness, the analyzer is capable of computing the various layer moduli using a process known as backcalculation. Backcalculation is an iterative process that takes the measured surface deflection and attempts to match it with a theoretical surface deflection generated from an identical pavement structure using assumed layer moduli. The assumed layer moduli in the theoretical model are adjusted until they produce a surface deflection that closely matches the measured one, within a specified tolerance. The backcalculation process is normally completed using computer software.

Several factors can influence the assumed moduli values which can lead to erroneous results (Hasim et al., 1994)(Irwin, 2002). First, it is extremely important to create a closely matching theoretical pavement model to the in-situ conditions. In many situations this can be a difficult task as layer thicknesses are often not known or may vary substantially throughout a pavement section and subsurface layers may be overlooked. In addition, some pavement layers are too thin to be backcalculated in the pavement model. This phenomenon is termed sensitivity and can occur if a layer is too thin for its modulus to have an influence on the surface deflections. If the deflection is insensitive to the layer modulus, then any backcalculated value for that layer may suffice. To overcome some of these concerns, additional destructive or nondestructive testing may be implemented in conjunction with the FWD.

### **3.4 GROUND PENETRATING RADAR**

Many researchers (Al-Qadi et al., 2004)(Willett et al., 2006) have reported success when using ground penetrating radar (GPR) technology to measure flexible pavement layer thickness. In pavement design, GPR is generally used to determine pavement layer thickness as a complement or replacement to coring and test pits. In many instances, GPR is considered to be a better alternative to coring as it is a quick nondestructive method which provides continuous thickness data collected near or at highway speeds (Maser et al., 2006).

The primary components of a GPR system include a control unit with associated software for data collection and processing and one or several radar antennas for emitting and receiving electromagnetic waves. Depending on the type of antenna that is used for pavement evaluation, GPR systems are classified as either air coupled or ground coupled. In the air-coupled systems, the “horn” antennas are typically suspended 150 – 500 mm above the surface for operation at highway speeds (up to 80km/h). These systems provide a clean radar signal, although the depth of penetration is limited because part of the electromagnetic energy sent by the antenna is reflected back by the pavement surface. Conversely, the antennas used in the ground coupled systems are in full contact with the ground surface providing a higher depth of penetration at the same frequency, but limiting the survey speed.

The short electromagnetic waves travel through the pavement’s layers and reflect off surfaces or objects that exhibit discontinuities in electrical properties, for example different materials, changes in moisture content, or changes in density (Loizos et al., 2007). The intensity of the reflected pulses is directly proportional to the contrast in dielectric constant between adjacent materials. The reflected pulses are received by the antenna and are recorded as waveforms which are digitized and interpreted by computing the amplitude and arrival times from each main reflection (Maser et al., 2006). In order to calculate the thickness, the dielectric constant of the material must be known. The dielectric value can either be calibrated based on measured thicknesses (cores, test pits etc.) or can be estimated

nondestructively. Using the horn antenna, the dielectric constant of hot mix asphalt is estimated by using the amplitude of the reflected signal from a metallic plate placed on the pavement surface and the amplitude of the reflected signal from the surface.

For the horn antenna method, the pavement thickness can be computed from the amplitudes and arrival times using Equation (1) (Al Qadi et al., 2004)(Loizos et al., 2007).

$$h_i = \frac{ct_i}{2\sqrt{\epsilon_i}} \quad (1)$$

Where,  $h_i$  = the thickness of the  $i^{\text{th}}$  layer,  $t_i$  = the electromagnetic wave two way travel time through the  $i^{\text{th}}$  layer,  $c$  = the speed of light in free space, and  $\epsilon_i$  = the dielectric constant of the  $i^{\text{th}}$  layer.

For the ground coupled systems which are in direct contact with the pavement surface, the equations displayed for the horn antenna method cannot be used because the radar wave does not travel through air. Consequently, the dielectric constant cannot be calculated directly from the data and needs to be calibrated from core samples. Based on the Pythagorean Theorem, Equation (2) can be constructed for layer thickness.

$$h = 0.5\sqrt{(Vt)^2 - d^2} \quad (2)$$

Where  $h$  = the layer thickness,  $V$  = the electromagnetic wave velocity,  $t$  = the total recorded travel time, and  $d$  = distance between the transmitter and the receiver units within the antenna.

### **3.5 SEISMIC SURFACE WAVE PROPAGATION METHODS**

Surface waves are stress waves that propagate along the free surface of a material. The velocity of wave propagation is dependent on the elastic properties of the material and consequently can be used to estimate the elastic modulus. Several techniques including Spectral Analysis of Surface Waves (SASW), Multi-Channel Simulation with One Receiver (MSOR) and Multi-channel Analysis of Surface Waves (MASW) have been used in determining the asphalt concrete modulus in a pavement system (Nazarian et al., 1983)( Ryden et al., 2004)(Barnes and Trottier, 2010).

When the surface of an elastic medium is impacted, two types of stress waves will be generated, body waves and surface waves. Body waves consist of compression waves (P wave) and shear waves (S wave) which propagate radially outward from the load point along a hemispherical wave front within the elastic medium. The surface wave, also called Rayleigh wave, does not propagate into the body of the elastic medium, but rather travels along the surface of the half space. Surface wave testing uses the dispersive nature of Rayleigh waves in a layered medium to evaluate the elastic stiffness properties of the different layers (Ryden et al., 2004). Dispersion is defined as the variation of Rayleigh wave velocity with frequency (wavelength) where the stiffness changes with depth.

In recent years, a new approach to surface wave testing has been introduced to avoid some of the problems encountered with SASW (Ryden et al., 2004)(Barnes and Trottier, 2009). This new approach, which was used in this research, is based on the MASW data processing technique and the MSOR method of data acquisition. In the MSOR method a multichannel record is obtained with only one receiver which is fixed at a surface point and receives signals from impacts at incremental offsets (Ryden et al., 2001). It has been shown (Ryden et al., 2003) that the fundamental symmetric and anti-symmetric free plate Lamb wave modes dominate for wavelengths within plates that are supported by significantly less stiff material. MASW has proven (Park et al., 1998, 1999) to be an effective technique of developing Rayleigh dispersion curves by identifying and tracking the approximate fundamental Lamb wave modes which asymptotically approach the fundamental Rayleigh

wave mode. Once the phase velocities have been determined the shear wave velocity may be estimated using Equation (3) (Nazarian et al., 1999)(Ryden and Park, 2006) and the modulus is calculated by means of Equation (4) (Ryden and Park, 2006).

$$V_s = V_R(1.13 - 0.16\nu) \quad (3)$$

$$E = 2(\rho V_s^2)(1 + \nu) \quad (4)$$

The modulus that is determined using surface wave methods is considered to be a high frequency modulus, with velocity data obtained at frequencies ranging between 5 and up to 90 kHz. In general, the traffic and FWD frequency used in design is in the range of 10 to 25 Hz. As a result, the asphalt concrete master curve defined in the next section may be used to shift the high frequency moduli to a design value (Barnes and Trottier, 2009).

### **3.6 DYNAMIC MODULUS MASTER CURVE**

Dynamic modulus testing is typically conducted on a servo-controlled hydraulic machine using cylindrical specimens subjected to a compressive haversine or sine wave load at a given temperature and loading frequency. Strain gauges or LVDTs are positioned on opposite sides of the specimen to measure the vertical deflections. During the test, the axial strain on the specimen is maintained between 50 and 150 microstrain to ensure linear elastic behavior. For linear viscoelastic materials such as hot mix asphalt (HMA) mixtures, the stress-strain relationship under a continuous sinusoidal load is defined by its complex dynamic modulus ( $E^*$ ) (Witczack et al., 2004). The complex modulus is defined as the ratio of the amplitude of the sinusoidal stress ( $\sigma$ ) at any given time ( $t$ ) and the angular load frequency ( $\omega$ ) to the corresponding sinusoidal strain ( $\epsilon$ ) at the same time. Due to the viscoelasticity, a phase lag ( $\theta$ ) separates the stress from the strain. The sinusoidal stress and strain are defined by Equation (5) and Equation (6) respectively.

$$\sigma = \sigma_0 \cdot \sin(\omega t) \quad (5)$$

$$\varepsilon = \varepsilon_0 \cdot \sin(\omega t - \phi) \quad (6)$$

Where,  $\sigma_0$  = stress amplitude and  $\varepsilon_0$  = strain amplitude. The complex dynamic modulus consists of two components, the storage modulus ( $E'$ ) (real part) that describes the elastic component and the loss modulus ( $E''$ ) (imaginary part) which describes the viscous component. These are determined based on Equation (7) and Equation (8).

$$E' = \frac{\sigma_0}{\varepsilon_0} \cos \phi \quad (7)$$

$$E'' = \frac{\sigma_0}{\varepsilon_0} \sin \phi \quad (8)$$

The dynamic modulus ( $|E^*|$ ) is defined as the absolute value of the complex modulus, which is the sum of the storage and loss moduli as shown in Equation (9) and can be computed by dividing the maximum load by the maximum strain. For simplicity, the dynamic modulus is generally denoted as  $E^*$  in literature and not  $|E^*|$ . Both  $|E^*|$  and  $E^*$  are used to describe the dynamic modulus throughout this thesis.

$$|E^*| = |E' + iE''| = \frac{\sigma_0}{\varepsilon_0} \quad (9)$$

Due to the viscoelastic properties of asphalt concrete, the computed dynamic modulus varies with load frequency and temperature. Typically, it increases with increasing loading frequency and with decreasing temperature. The relationship between the modulus, frequency and temperature can be expressed by a master curve which is usually constructed at a reference temperature, generally 21°C. The master curve enables the prediction of the moduli at any loading frequency or temperature and assists in the comparison of data on an equal basis. The master curve of asphalt concrete can be mathematically modeled by a sigmoidal function described by Equation (10) proposed by Pellinen et al. (2004).

$$\text{Log}(E^*) = \delta + \frac{\alpha}{1 + e^{\beta - \gamma(\log \xi)}} \quad (10)$$

Where  $E^*$  = dynamic modulus,  $\xi$  = reduced frequency,  $\delta$  = minimum modulus value,  $\alpha$  = span of modulus values, and  $\beta, \gamma$  = shape parameters. The master curve is constructed using the principle of time-temperature superposition. The tested dynamic modulus results at various temperatures and frequencies are shifted to a reduced frequency at an arbitrarily selected reference temperature,  $T_0$ , as shown in Equation (11).

$$\log(\xi) = \log(f) + \log[a(T)] \quad (11)$$

Where,  $a(T)$  = shift factor,  $a(T_0) = 0$ ,  $f$  = frequency, and  $\xi$  = reduced frequency. The shift factor  $a(T)$  can be represented as a second order polynomial function of the temperature,  $T$  (Witczak et al., 2004) as shown in Equation (12).

$$\text{Log}[a(T)] = aT^2 + bT + c \quad (12)$$

Where  $a(T)$  = shift factor at temperature  $T$ , and  $a, b$  and  $c$  = coefficients of the second order polynomial. The master curve is constructed by simultaneously solving the four coefficients of the sigmoidal function ( $\delta, \alpha, \beta, \gamma$ ) and the three coefficients of the second order polynomial ( $a, b, c$ ). This is completed by optimizing the theoretical model to fit the experimental data by adjusting the coefficients using the “Solver” function in Excel until the least square error is minimized.

## **3.7 EXPERIMENTAL TESTING AND RESULTS**

### **3.7.1 Site Description**

As part of a multiyear research project between Dalhousie University and the Nova Scotia Department of Transportation and Infrastructure Renewal (NSTIR), three 200 meter test

sites throughout the province of Nova Scotia were selected for non-destructive testing evaluation (NDT). The non-destructive testing conducted included FWD, GPR, and MASW testing. In addition to the non-destructive tests, the sections were cored for calibration purposes and during construction instrumentation was placed within the pavement structure.

For this particular study, the test section selected was located on Highway 103, near Barrington, Nova Scotia. The highway was constructed in 2006 and is a two-lane controlled access arterial highway. The pavement section, shown in Figure 1, was designed as per the highway design standards utilized by NSTIR. This type of cross section is commonly seen in the majority of Nova Scotia arterial highways. The pavement structure is composed of two asphalt type B-HF lifts approximately 50 mm in thickness, and a 50 mm thick asphalt type C-HF lift. The granular base is considered to be a type I granular material with a maximum size of  $\frac{3}{4}$  inch while the subbase is a type II granular material with maximum size of 1  $\frac{1}{2}$  inches.

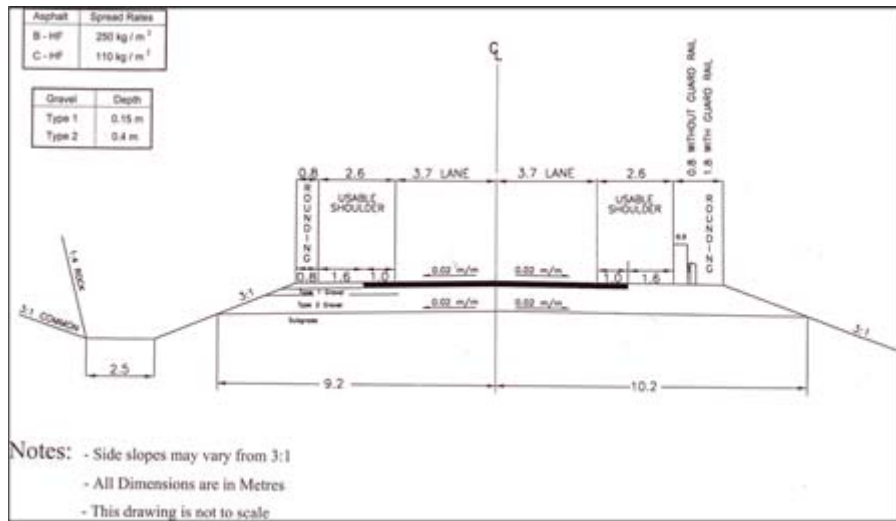


Figure 1 Typical pavement cross section.



### 3.7.2 Coring and Trenching

During highway construction, instrumentation was placed at the top of the subgrade and throughout the granular layers located at the midpoint of the 200 meter section. This was completed by trenching a section of the roadway, installing the sensors and then backfilling and compacting with a plate tamper. During this process, the subbase and base thicknesses were measured to be 550 mm and 150 mm respectively, for a total of 700 mm.

Once paving was completed, core samples were extracted from the outer wheel path at various stations along the 200 meter section. The cores were then used to determine the asphalt thickness, calibrate the GPR data, and also to perform dynamic modulus testing. The thickness measurements are displayed in Table 1.

Table 1 Asphalt core thicknesses.

| <b>Station (m)</b> | <b>Thickness (mm)</b> |
|--------------------|-----------------------|
| 15                 | 133                   |
| 55                 | 156                   |
| 85                 | 174                   |
| 135                | 162                   |
| 175                | 163                   |

### 3.7.3 Dynamic Modulus and Master Curve

The cores extracted for thickness determination were also used for dynamic modulus test specimens. The cores ranged from 136 mm to 175 mm in thickness and were tested with a servo-hydraulic testing system according to AASHTO TP 62-03 and ASTM D3497. The samples were tested at frequencies of 0.1, 1, 5, 10, and 25 Hz and at temperatures of -15, 0, 10, 21, and 40°C using a controlled environmental chamber. The resultant master curve, sigmoidal curve fitting parameters, and shift factor coefficients are displayed in Figure 2. The master curve was used to shift high frequency moduli values from surface wave testing

to a 10Hz FWD value in addition to shifting moduli values collected at various temperatures to a standard 21°C value. The dynamic modulus at 21°C and 10Hz frequency was determined to be 3469 MPa.

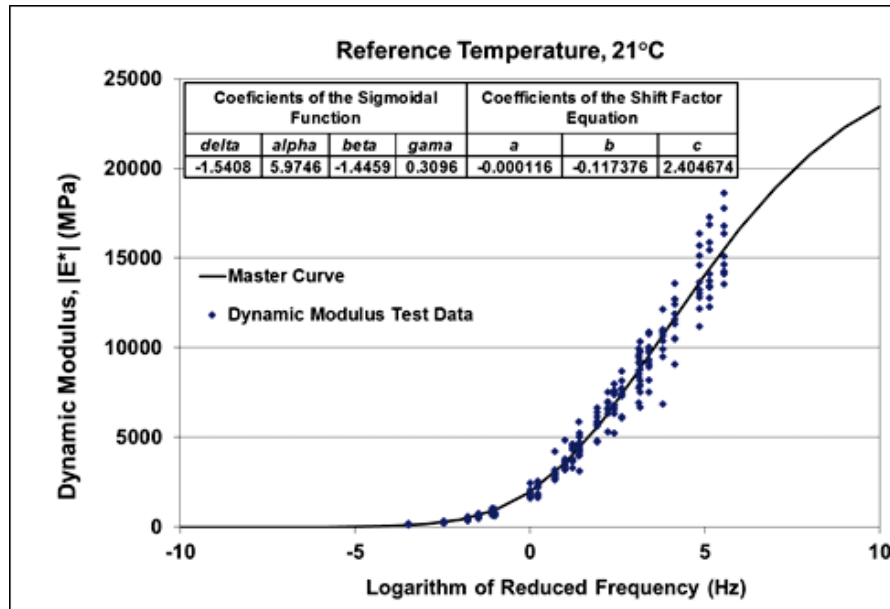


Figure 2 Dynamic modulus master curve.

### 3.7.4 Temperature Measurement

The pavement response under an applied load is temperature dependent and therefore pavement temperature must be recorded for each test station. During all non-destructive testing, the temperature at mid-depth of the asphalt concrete layer was measured and used as the average temperature for moduli backcalculation and MASW analysis. All calculated moduli values were then shifted from the corresponding measured temperature value to a standard 21°C value using the constructed master curve.

### 3.7.5 Ground Penetrating Radar

Ground penetrating radar (GPR) testing was conducted along the entire 200 meter test section in the outer wheel path to determine the longitudinal variation in pavement thickness. In addition, GPR was used to determine the transverse variation in thickness at both Station 10 and Station 180. The GPR system used in this research was the SIRveyor SIR-20 manufactured by Geophysical Survey Systems, Inc. (GSSI). Two ground coupled antennas were implemented in the analysis. A 1.6 GHz antenna was employed to detect the thickness of the asphalt concrete layer, while a 900 MHz antenna clearly identified the base layers. The antennas were mounted in a plastic sled and towed behind the test vehicle as shown in Figure 3. Radan 6.5 analysis software manufactured by GSSI was implemented in the analysis and the cores extracted from the site were used to calibrate the GPR data. The results of the longitudinal asphalt concrete survey and transverse survey are displayed in Figures 4 and 5 respectively. The granular thicknesses are displayed in Figure 6.



Figure 3 GPR antenna sled.

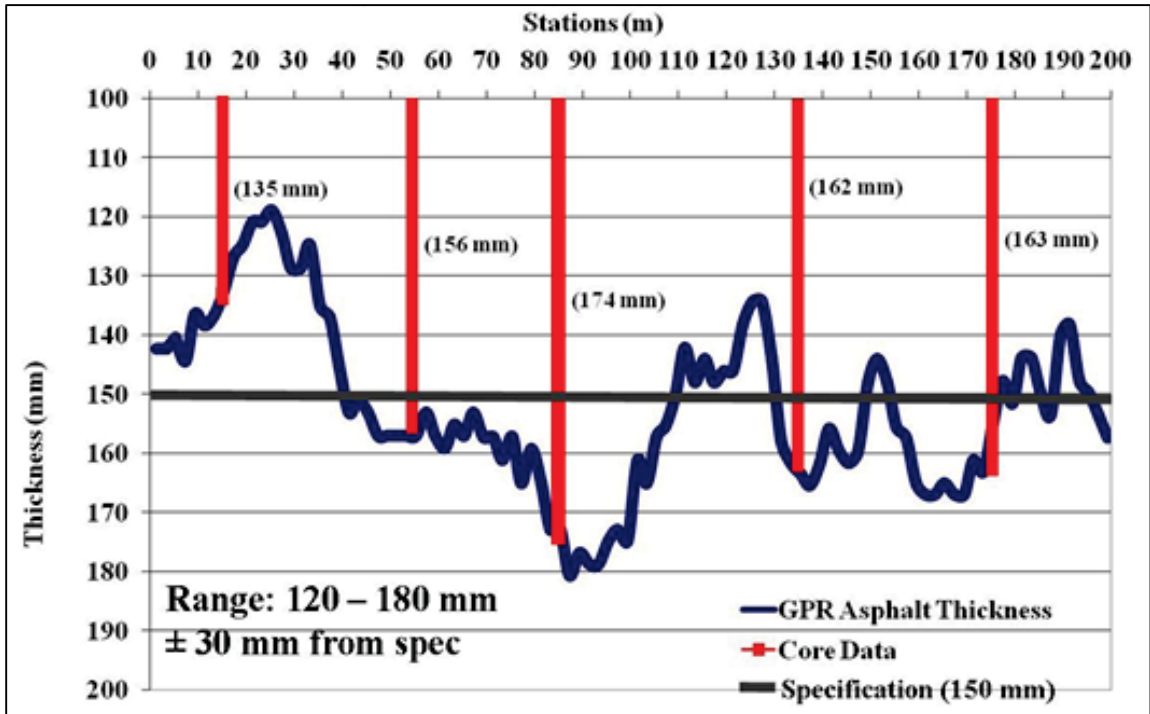


Figure 4 Longitudinal GPR results.

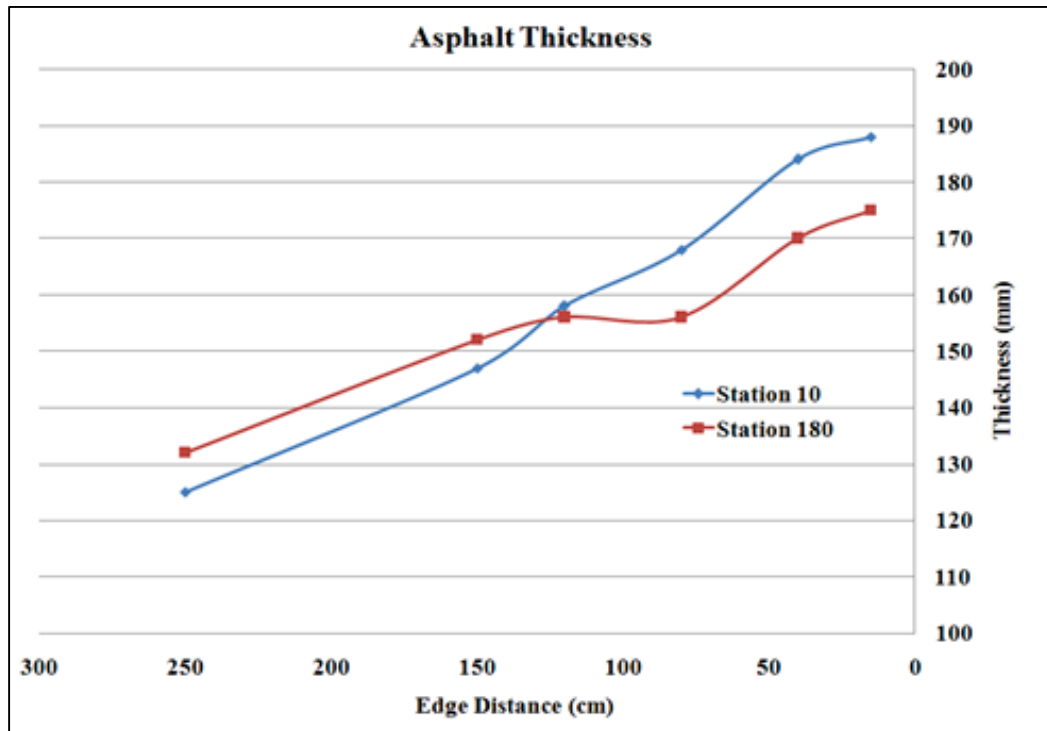


Figure 5 Transverse GPR results.

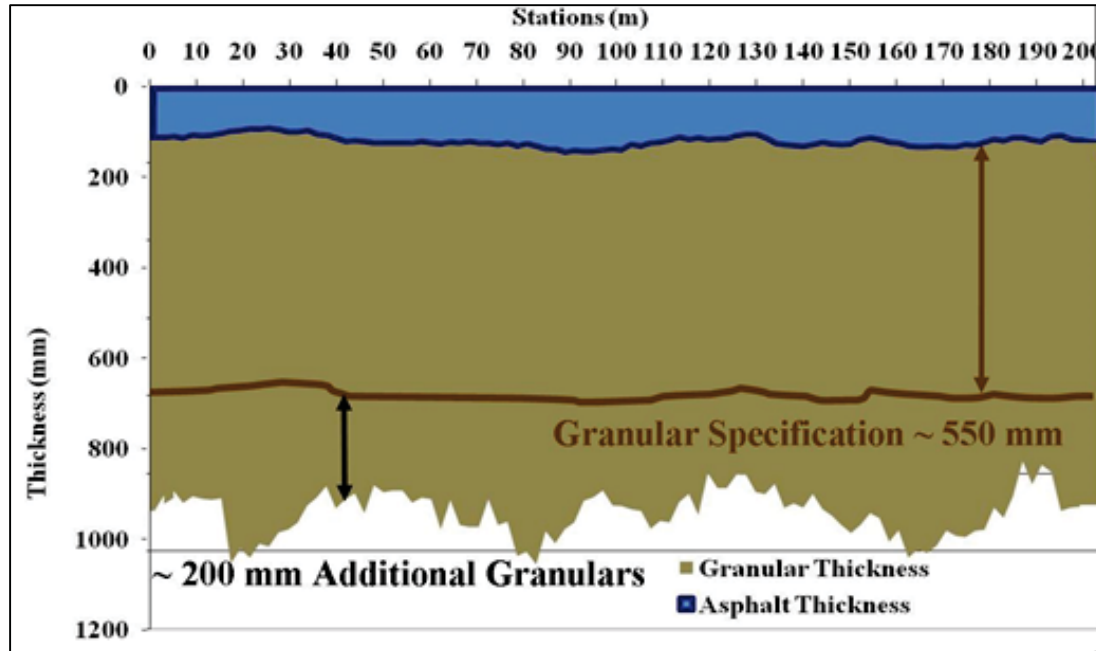


Figure 6 GPR granular material thickness.

The GPR results indicate a longitudinal variation in asphalt concrete thickness of 55 mm and a transverse variation of approximately 65 mm. The total granular material thickness which was specified to be 550 mm and measured to be 700 mm at the trench location ranged from 700 mm to 945 mm. Therefore 150 to 400 mm of additional granular material was found along the 200 m section. Since destructive techniques only provide data at random locations, GPR results seem to offer a substantial improvement to characterizing the entire pavement structure along a continuous profile.

### 3.7.6 Surface Wave Testing

The MASW data processing technique and MSOR data recording procedure previously described were implemented for this research. The data collection procedure used was based on Barnes and Trottier (2009). The data was collected using an Olsen Instruments Freedom Data PC using a 1 MHz National Instruments data acquisition board with an Impact Echo test head consisting of a 100 kHz displacement transducer as the receiver.

The impact was generated using a high frequency impactor consisting of a stainless steel A-6 autoharp string housed in an aluminum block with a rubber membrane lining the bottom. A one cm wide 24 gauge sheet metal strip was bonded to the asphalt surface with an epoxy to overcome some of the source generating difficulties related to the heterogeneous nature of the asphalt concrete. A magnetically mounted 15 kHz accelerometer was placed at each impact location to trigger data collection. Data was recorded at 20 offset positions from the receiver, ranging from three to 22 cm. The test setup is shown in Figure 7. Using a Matlab analysis, the phase velocity dispersion curves were constructed. The high frequency moduli were then shifted to a 10 Hz value for comparison with the FWD backcalculated moduli. A typical phase velocity dispersion curve is shown in Figure 8 while the moduli values calculated for Station 10 and Station 180 are displayed in Table 2 and Table 3 respectively. Due to the high frequency content generated by the high frequency impactor, the phase velocities at 80-90 kHz correspond to wavelengths near 16-16.5 mm. Therefore, the moduli values displayed are the average moduli values determined from the phase velocities corresponding to wavelengths ranging from the bottom of the asphalt layer up to approximately 20 mm from the surface.



Figure 7 MSOR test setup.

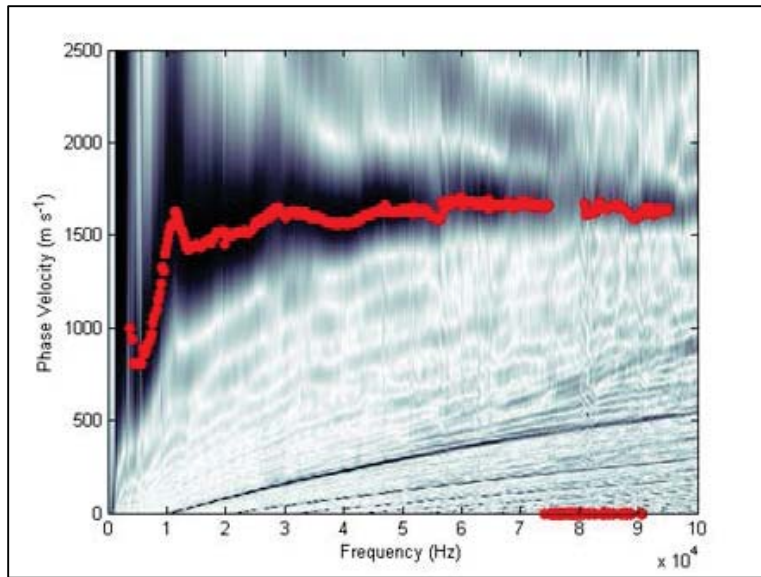


Figure 8 Phase velocity dispersion curve for Station 10 center lane.

Reviewing the calculated surface wave values for both Station 10 and Station 180, there is a decreasing trend in asphalt concrete modulus from the center lane to the pavement edge. This reduction in modulus may be related to construction flaws such as compaction or could be caused by traffic or temperature induced damage. There were no visible surface cracks at the test point locations however there may have been slight amounts of damage in underlying lifts. The moduli values determined from the center lane locations match extremely well with the dynamic modulus values determined at 21°C and 10 Hz. Consequently, since the dynamic modulus values were computed when the pavement was relatively new, it can be assumed that the center lane surface wave modulus represents a relatively undamaged pavement.

### 3.7.7 Falling Weight Deflectometer

Non-destructive deflection testing was conducted using a Dynatest model 8082 Heavy weight deflectometer (HWD) as shown in Figure 9. The HWD is equipped with a 300 mm diameter segmented loading plate and geophones mounted at off-set distances from the

load center of 0, 200, 300, 450, 600, 900, 1200, 1500, and 1800 mm. The loading sequence included three seating drops of approximately 30 kN (425 kPa) and four 40 kN (570 kPa) drops representing the standard axle load of 80kN (18 kips)). By performing multiple drops at each load, replicates were obtained for the measured data, reducing possible errors. The 40 kN load was used in the backcalculation analysis.



Figure 9 Dynatest 8082 HWD.

The backcalculation was conducted using ELMOD 5 software with two separate analyses performed. The first scenario incorporated the GPR determined thicknesses while the second used thickness data obtained from the closest core and trench location. Similarly to the surface wave determined asphalt concrete moduli, the backcalculated moduli values were also shifted to a 21°C value using the constructed master curve. The complete backcalculation results for all the pavement layers in addition to the asphalt concrete moduli determined with the surface wave and dynamic modulus methods are shown in Table 2 and Table 3 for Station 10 and Station 180 respectively. The backcalculated moduli for the entire 200 m section are provided in Figure 10.



Table 2 Moduli results from Station 10.

| Station          | Edge Dist (cm) | Asphalt (6.7°C) | Asphalt (21°C) | Granular       | Subgrade | MASW (21°C) 10Hz | Dynamic Modulus |
|------------------|----------------|-----------------|----------------|----------------|----------|------------------|-----------------|
|                  |                |                 |                | Base + Subbase |          |                  |                 |
| CL               | 250            | 6096            | 2964           | 264            | 89       | 3360             | 3469            |
| CL No GPR        | 250            | 4725            | 2297           | 277            | 91       |                  |                 |
| OWP              | 150            | 4396            | 2137           | 270            | 84       | 2992             |                 |
| OWP No GPR       | 150            | 5294            | 2574           | 289            | 85       |                  |                 |
| Mid Outer        | 120            | 3451            | 1678           | 257            | 90       | NA               |                 |
| Mid Outer No GPR | 120            | 4878            | 2371           | 286            | 81       |                  |                 |
| WL               | 80             | 4635            | 2253           | 232            | 71       | 2970             |                 |
| WL No GPR        | 80             | 7664            | 3726           | 268            | 67       |                  |                 |
| Mid Edge         | 40             | 3837            | 1865           | 182            | 52       | NA               |                 |
| Mid Edge No GPR  | 40             | 7765            | 3775           | 217            | 47       |                  |                 |
| Edge             | 15             | 1805            | 878            | 137            | 43       | 2119             |                 |
| Edge No GPR      | 15             | 3777            | 1836           | 156            | 40       |                  |                 |

Table 3 Moduli results from Station 180.

| Station          | Edge Dist (cm) | Asphalt (9.9°C) | Asphalt (21°C) | Granular       | Subgrade | MASW (21°C) 10Hz | Dynamic Modulus |
|------------------|----------------|-----------------|----------------|----------------|----------|------------------|-----------------|
|                  |                |                 |                | Base + Subbase |          |                  |                 |
| CL               | 250            | 5817            | 3274           | 253            | 75       | 3343             | 3469            |
| CL No GPR        | 250            | 3594            | 2023           | 273            | 69       |                  |                 |
| OWP              | 150            | 3500            | 1970           | 255            | 81       | 2495             |                 |
| OWP No GPR       | 150            | 2918            | 1642           | 286            | 74       |                  |                 |
| Mid Outer        | 120            | 3519            | 1981           | 255            | 89       | 2766             |                 |
| Mid Outer No GPR | 120            | 3153            | 1775           | 276            | 83       |                  |                 |
| WL               | 80             | 4263            | 2400           | 228            | 66       | 2659             |                 |
| WL No GPR        | 80             | 3858            | 2172           | 257            | 59       |                  |                 |
| Mid Edge         | 40             | 3697            | 2081           | 159            | 51       | 2707             |                 |
| Mid Edge No GPR  | 40             | 3896            | 2193           | 185            | 45       |                  |                 |
| Edge             | 15             | 2174            | 1224           | 135            | 36       | 2557             |                 |
| Edge No GPR      | 15             | 2398            | 1350           | 161            | 31       |                  |                 |

Examining the results, it is important to note that there are substantial differences in the moduli values across the transverse orientation of the lane. The asphalt concrete moduli backcalculated in the center of the lane correspond with both the MASW and dynamic modulus results. However, as you approach the pavement edge, the moduli values for the asphalt concrete as well as the granular materials and subgrade drop significantly. This may be attributed to edge effects caused by the lack of shoulder support. Figure 11 present the raw deflection data obtained at Station 10. From this graph, it is observed that the deflections recorded from all nine geophones remain relatively constant from the center of the lane up to approximately 120 cm from the edge. From the 120 cm mark to the edge, the deflections increase significantly which signifies the lack of shoulder support.

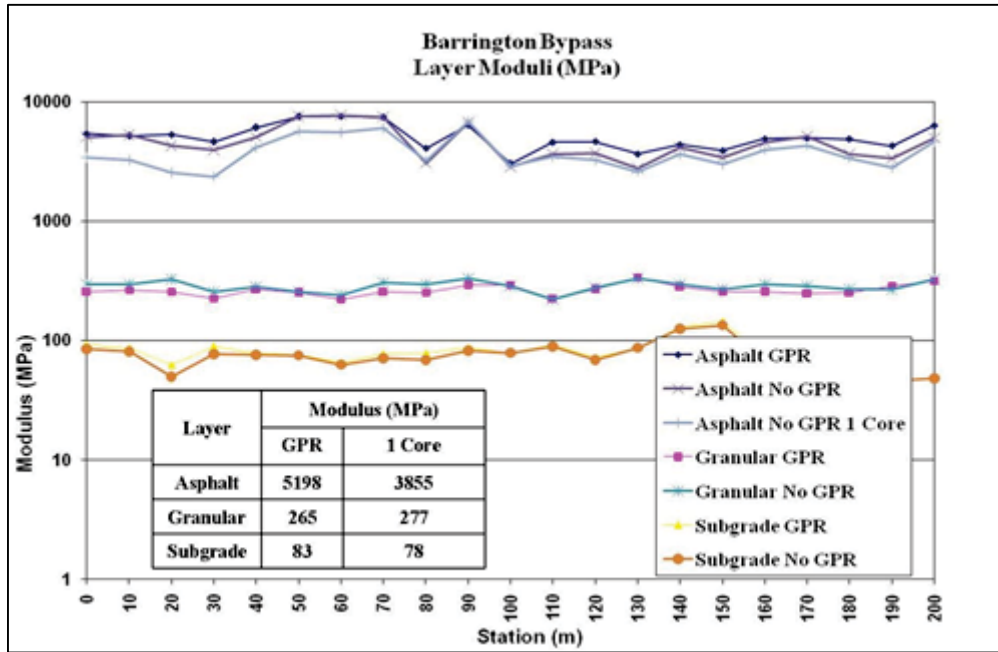


Figure 10 Backcalculated moduli results for 200 m section.

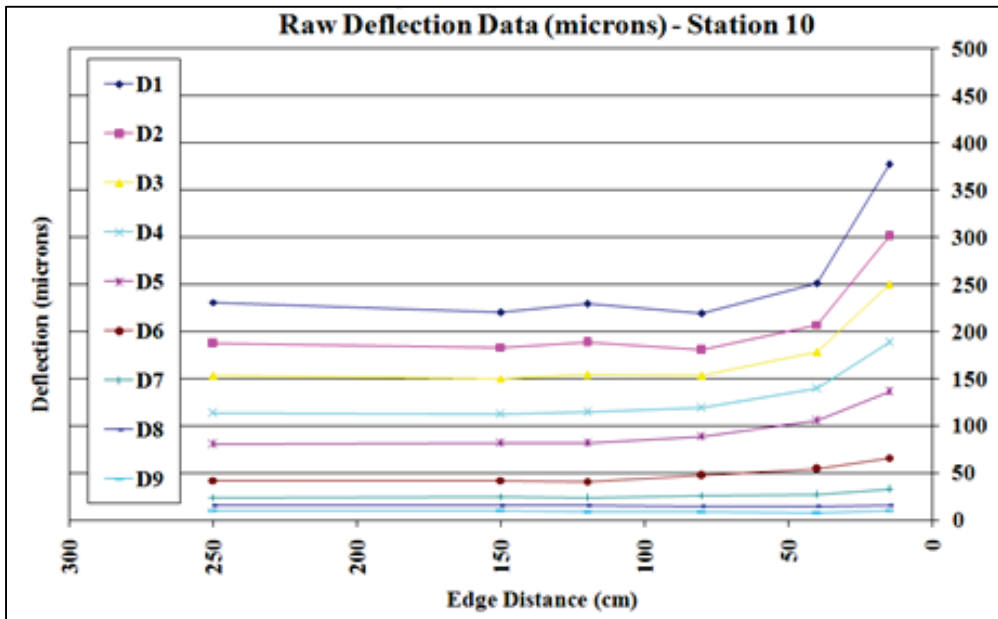


Figure 11 Raw deflection data Station 10.

The MASW asphalt modulus only decreases slightly across the lane which could indicate slight amounts of damage in the wheel path, or perhaps construction flaws as you approach the edge (lack of compaction). Consequently, the difference in backcalculated moduli to MASW moduli generally increases near the edge of the lane. The backcalculated moduli are not only influenced by the damage across the traffic lane, but also by the lack of shoulder support. The MASW results are not influenced by the lack of shoulder support as the test focuses solely within the asphalt layer. Therefore the results represent the actual material modulus and not necessarily the modulus required to fit the pavement system. As a result, the MASW modulus may be used to differentiate between edge effects and actual pavement distress.

In addition to the variations caused by the edge effects, there are also significant differences between the backcalculated moduli results obtained with and without GPR thicknesses. The results indicate up to a 40 percent difference in asphalt concrete moduli. Reviewing the data, it should also be noted that the asphalt moduli values incorporating GPR data correspond significantly better with the MASW results, especially at the center lane (no damage or edge effects).

### 3.7.8 Design Parameters

To demonstrate the importance of incorporating GPR data into the backcalculation procedure, the modulus and thickness values calculated with and without GPR were used to calculate the effective structural number ( $SN_{eff}$ ) based on the 1993 AASHTO Guide for Design of Pavement Structures and remaining service life based on the MEPDG.

The AASHTO designs were computed based on equations and methodology provided in the AASHTO Guide. To compute  $SN_{eff}$  the 1993 guide specifies two methods. The first method is based on non-destructive deflection data, while the second uses a visual condition survey assessment and the resultant layer coefficients. However, there are equations and charts found in the guide that enable the computation of layer coefficients

based on the existing modulus of the various pavement layers above the subgrade. Utilizing the NDT and condition survey methods,  $SN_{eff}$  was calculated for both thickness scenarios for Station 10 and Station 180 as shown in Table 4. The condition survey method was implemented for analyzing the entire 200 m section as shown in Table 5. The difference in  $SN_{eff}$  caused by the thickness variation translates into considerable differences in the required overlay thickness.

Table 4  $SN_{eff}$  with and without GPR thickness data for Station 10 and Station 180.

| Station | $SN_{eff}$ |        |                  |        | Difference in Overlay Thickness (mm) Based on $SN_{eff}$ |                  |
|---------|------------|--------|------------------|--------|--|------------------|
|         | NDT Method |        | Condition Survey |        | NDT Method   | Condition Survey |
|         | GPR        | No GPR | GPR              | No GPR |  |                  |
| 10 OWP  | 7.39       | 6.46   | 7.53             | 6.97   | 53.7   | 32.3             |
| 180 OWP | 7.54       | 6.57   | 7.54             | 7.03   | 56.0   | 29.2             |
| 10 CL   | 7.09       | 6.39   | 7.19             | 6.72   | 40.4   | 27.1             |
| 180 CL  | 7.47       | 6.70   | 7.73             | 7.10   | 44.5   | 36.3             |

Table 5  $SN_{eff}$  with and without GPR thickness data for entire 200 m section.

| Station | $SN_{eff}$ |        | Difference in Overlay Thickness (mm) |
|---------|------------|--------|--------------------------------------|
|         | NDT Method |        |                                      |
|         | GPR        | No GPR |                                      |
| Average | 7.61       | 7.19   | 24.3                                 |

The MEPDG also provides detailed methods to compute remaining service life. These methods are based on asphalt fatigue and subgrade rutting models. The models selected in this research were established by the Asphalt Institute. The number of load repetitions required to cause failure are related to the strain located at critical areas of the pavement structure (bottom of AC layer, top of subgrade). Using moduli values determined from backcalculation and the related thickness values, the strains at these critical areas were determined for both scenarios. An ELSYM 5 spreadsheet was implemented to compute

the strains at the bottom of the AC layer and at the top of the subgrade. The results are provided in Table 6.

Table 6 Remaining service life.

| Location           | ESAL  | Strain in Asphalt |          | Strain in Subgrade |          | $N_f$ (Fatigue) |          | $N_f$ (Rutting) |          | Design Life (Yrs) |        |
|--------------------|-------|-------------------|----------|--------------------|----------|-----------------|----------|-----------------|----------|-------------------|--------|
|                    |       | GPR               | No GPR   | GPR                | No GPR   | GPR             | No GPR   | GPR             | No GPR   | GPR               | No GPR |
| <b>Station 10</b>  |       |                   |          |                    |          |                 |          |                 |          |                   |        |
| CL                 | 23456 | 2.22E-04          | 2.31E-04 | 1.30E-04           | 1.55E-04 | 1.22E+05        | 1.35E+05 | 3.43E+08        | 1.58E+08 | 5.2               | 5.7    |
| OWP (Center)       | 23456 | 2.18E-04          | 2.07E-04 | 1.30E-04           | 1.59E-04 | 1.72E+05        | 1.74E+05 | 3.39E+08        | 1.41E+08 | 7.3               | 7.4    |
| OWP (Edge)         | 23456 | 2.35E-04          | 2.16E-04 | 1.27E-04           | 1.65E-04 | 1.65E+05        | 1.52E+05 | 3.73E+08        | 1.19E+08 | 7.0               | 6.5    |
| Average            | 23456 | 2.25E-04          | 2.18E-04 | 1.29E-04           | 1.59E-04 | 1.53E+05        | 1.53E+05 | 3.52E+08        | 1.39E+08 | 6.5               | 6.5    |
| <b>Station 180</b> |       |                   |          |                    |          |                 |          |                 |          |                   |        |
| CL                 | 23456 | 2.03E-04          | 2.04E-04 | 1.28E-04           | 1.60E-04 | 1.52E+05        | 2.25E+05 | 3.69E+08        | 1.36E+08 | 6.5               | 9.6    |
| OWP (Center)       | 23456 | 2.27E-04          | 2.16E-04 | 1.22E-04           | 1.89E-04 | 1.62E+05        | 2.23E+05 | 4.53E+08        | 6.43E+07 | 6.9               | 9.5    |
| OWP (Edge)         | 23456 | 2.22E-04          | 2.14E-04 | 1.15E-04           | 1.79E-04 | 1.74E+05        | 2.14E+05 | 5.91E+08        | 8.08E+07 | 7.4               | 9.1    |
| Average            | 23456 | 2.17E-04          | 2.11E-04 | 1.22E-04           | 1.76E-04 | 1.63E+05        | 2.21E+05 | 4.71E+08        | 9.38E+07 | 6.9               | 9.4    |

The design life provided in Table 6 is calculated based on the fatigue life. From the results, there does not seem to be considerable differences in the design life when considering asphalt fatigue, as the variation in thickness seem to offset the changes in moduli. However, the rutting performance for the GPR data is nearly half of the value from the non GPR results. Because of the low traffic volume, rutting is generally not a concern for this particular section. Consequently, if the thicknesses were smaller and traffic volumes increased, the rutting performance would have a significant effect on the design life.

### 3.8 CONCLUSIONS

Non-destructive deflection testing by means of the FWD in addition to GPR and MASW testing were performed along a 200 meter test section and across the transverse width of the traffic lane to establish variations in thickness and moduli. Cores were also extracted along the test section to calibrate GPR data and to perform dynamic modulus testing for master curve construction. Using GPR, it was determined that a 65 mm variation existed between the center of the lane and the pavement edge. As a result there were also

significant differences between the nearest measured core thickness and the actual thickness measured with GPR. Since cores can only be extracted at certain points along a pavement section, GPR results provide a much better estimate to the continuous thickness profile. Consequently, this thickness data can also be used to complement the backcalculation process. It was found that the backcalculated moduli determined with GPR provided a better estimate to the MASW calculated moduli and measured dynamic moduli from conventional methods. In terms of design life and required overlay thickness, there can be significant error if improper thickness and moduli values are incorporated into the analysis. Using the AASHTO 1993 Pavement Guide, the difference in modulus and thickness between GPR and non-GPR data in this study resulted in nearly a 50 mm difference in overlay thickness.

It was determined that MASW may be used to differentiate between asphalt moduli reductions related to pavement edge effects and actual pavement distress. The MASW results are not influenced by the lack of shoulder support as compared to the backcalculated results. The MASW reduction in modulus across the lane width coincides with actual damage or flaws within the asphalt layer. The backcalculated moduli values show a reduction due to a combination of damage and lack of shoulder support. In addition, the MASW calculated moduli which may be determined to within approximately 20 mm from the surface correspond to the measured dynamic modulus. Consequently, using the MASW determined in-situ moduli values may complement the FWD for thin layer asphalts.

### **3.9 REFERENCES**

Al-Qadi, I.L., and Lahouar, S. (2004). "Ground Penetrating Radar: State of the Practice for Pavement Assessment", *Materials Evaluation*, American Society for Nondestructive Testing, Vol. 62, No. 7, pp. 759-763.

American Association of State Highway and Transportation Officials. (1993). "AASHTO Guide for Design of Pavement Structures", Washington, D.C.

Barnes, C.L., Trottier, J.-F. (2009). "Evaluating High-Frequency Visco-Elastic Moduli in Asphalt Concrete", Research in Nondestructive Evaluation, Volume 20, Issue 2, pp.116-130.

Barnes, C.L., Trottier, J.-F. (2010). "Evaluating in-service asphalt concrete damage using surface waves", International Journal of Pavement Engineering, Volume 11, Number 6, pp. 449-458.

Hasim, M.S., Hameed, A.M., Mustaffa, M.S. (1994). "The effect of edge restraint on FWD deflection values tested on asphalt road pavement", 4th International Conference, Bearing Capacity of Roads and Airfields, Minnesota Department of Transportation, Minneapolis, MN, pp. 259-272.

Heisey, J.S., Stokoe II, K.H., and Meyer, A.H. (1982). "Moduli of pavement systems from spectral analysis of surface waves", Transportation Research Record 852, Transportation Research Board, National Research Council, Washington, D.C. pp. 22-31.

Irwin, L.H. (2002). "Backcalculation: An Overview and Perspective", <http://pms.nevadadot.com/2002presentations/11.pdf>

Jones, R. (1955). "A vibration method for measuring the thickness of concrete road slabs in situ", Magazine of Concrete Research, Vol 7, No. 20., pp.97-102.

Loizos, A., and Plati, C. (2007). "Accuracy of pavement thickness estimation using different ground penetrating radar analysis approaches", NDT & E International, Elsevier Science, Vol. 40, No. 2, pp. 147-157.

Maser, K.R., Holland, T.J., Roberts, R., and Popovics, J. (2006). “NDE methods for quality assurance of new pavement thickness”, *The International Journal of Pavement Engineering*, Vol. 7, No. 1, pp. 1-10.

National Cooperative Highway Research Program (NCHRP) (2004). “Guide for mechanistic-empirical design of new and rehabilitated pavement structures” NCHRP 1-37A Design Guide, Washington, D.C., <http://www.trb.org/mepdg/guide.htm> [Accessed 25 January 2010].

Nazarian, S., Stokoe II, K. H., Hudson, W.R. (1983). “Use of Spectral Analysis of Surface Waves Method for Determination of Moduli and Thicknesses of Pavement Systems”, *Transportation Research Record 930*, Transportation Research Board, National Research Council, Washington, D.C. pp. 38-45.

Park, C.B., Miller, R.D., and Xia, J. (1998). “Imaging dispersion curves of surface waves on multi-channel record”, *Kansas Geological Survey, 68<sup>th</sup> Annual International Meeting of the Society of Exploration Geophysicists, Expanded Abstracts*, p. 1377-1380.

Park, C.B., Miller, R.D., and Xia, J. (1999). “Multimodal analysis of high frequency surface waves”, *Proceedings of the Symposium of Applied Geophysics in Engineering and Environmental Problems (SAGEEP 1999)*, Oakland, CA, p.115-121.

Park, D., Buch, N., Chatti, K. (2001). “Effective Layer Temperature Prediction Model and Temperature Correction via Falling Weight Deflectometer Deflections”, *Transportation Research Record 1764*, Transportation Research Board, National Research Council, Washington, D.C. pp. 97-111.



Pellinen, T.K., Witzak, M.W., and Bonaquist, R.A. (2004). "Asphalt mix master curve construction using sigmoidal fitting function with non-linear least squares optimization", Recent Advances in Materials Characterization and Modeling of Pavement Systems, American Society of Civil Engineers Geotechnical Special Publication No. 123. pp. 83-101.

Ryden, N., Ulriksen, P., Park, C.B., Miller, R.D., Xia, J., and Ivanov, J. (2001). "High frequency MASW for non-destructive testing of pavements-accelerometer approach", Proceedings of the Symposium on the Application of Geophysics to Engineering and Environmental Problems (SAGEEP 2001), Environmental and Engineering Geophysical Society, Annual Meeting, Denver, RBA-5.

Ryden, N., Park, C.B., Ulriksen, P., and Miller R.D. (2003). "Lamb wave analysis for non-destructive testing of concrete plate structures ", Proceedings of the Symposium on the Application of Geophysics to Engineering and Environmental Problems (SAGEEP 2003), San Antonio, TX April 6-10,INF03.

Ryden, N., Park, C.B., Ulriksen, P., and Miller, R.D. (2004). "Multimodal Approach to Seismic Pavement Testing", Journal of Geotechnical and Geoenvironmental Engineering., Vol. 130, No. 6, pp. 636-645.

Ryden, N., Park, C.B. (2006). "Fast simulated annealing inversion of surface waves on pavement using phase-velocity spectra", Geophysics, Vol. 71, No. 4, pp. R49-R58.

Shahin, M. (1994). "Pavement Management for Airports, Roads, and Parking Lots, 2<sup>nd</sup> Edition", Springer, New York, N.Y.

Ullidtz, P., and Stubstad, R.N. (1985). Analytical Empirical Pavement Evaluation Using the Falling Weight Deflectometer", Transportation Research Record 1022, Transportation Research Board, National Research Council, Washington, D.C. pp. 36-44.

Willett, D.A., Mahboub, K., and Rister, B. (2006). "Accuracy of Ground-Penetrating Radar for Pavement Layer Thickness Analysis", Journal of Transportation Engineering, ASCE, Vol. 132, No. 1, pp. 96-103.

Witczak, M.W., and Bari, J. (2004). "Development of a E\* master curve database for lime Modified Asphaltic Mixtures", <http://www.lime.org/Publications/MstrCurve.pdf>

## **CHAPTER 4      PAPER 2: ROBUST MASTER CURVE DETERMINATION USING COMPLIMENTARY MASW TECHNIQUES**

Edmund Surette, Christopher Barnes, Nouman Ali

Based on: Paper to be submitted to International Journal of Pavement Engineering

### **4.1 ABSTRACT**

Recently, the Multi-Channel Analysis of Surface Waves (MASW) technique has been shown to provide accurate non-destructive estimates of the in-situ asphalt concrete modulus. However these moduli are measured at high frequencies and need to be shifted using the master curve to a design frequency that corresponds to traffic loading. Master curves were constructed using several shift factor models fitted to dynamic moduli as measured from laboratory testing, as modelled using predictive equations, and as determined via a combination of MASW and laboratory methods. The majority of the master curves constructed provided reasonable predictions of the measured dynamic moduli. Master curves constructed using the combination of conventional and MASW data provided significantly more consistent and accurate results when high frequency moduli were shifted to a lower design frequency. Master curves developed using both surface wave and complex dynamic modulus tests should be developed for utilizing surface wave test results in pavement condition evaluation and mechanistic empirical design under traffic loading.

### **4.2 KEYWORDS**

Keywords: asphalt concrete; dynamic modulus; surface waves; master curve.

### 4.3 INTRODUCTION

With the release of the Mechanistic-Empirical Pavement Design Guide (MEPDG), the time and temperature dependent dynamic modulus  $E^*$  has become the primary design input for asphalt concrete layers influencing the structural response of new or rehabilitated pavements. Due to the viscoelastic nature of asphalt concrete the dynamic modulus is a function of both temperature and rate of loading. Other parameters including age and mixture characteristics such as binder stiffness, aggregate gradation, binder content and air voids also influence the modulus properties of asphalt concrete (NCHRP, 2004). The asphalt master curve is used to characterize the dynamic modulus over a wide frequency range at a given reference temperature and allows for the comparison of moduli measured at different loading frequencies and test temperatures.

The dynamic modulus  $E^*$  can be measured using laboratory or in situ testing methods, or through the use of predictive models depending on the desired reliability level (NCHRP, 2004)(Biswas and Pellinen, 2007). Currently, the most common laboratory testing method used is AASHTO TP 62 which involves subjecting either laboratory compacted cylindrical specimens or drilled cores to sinusoidal axial loading at various frequencies and temperatures. This test requires sophisticated and expensive testing equipment that may not be available to all transportation agencies. In addition to cost restrictions, the time required for AASHTO TP 62 sample conditioning and testing has proven prohibitive to many researchers for master curve development (Dougan et al., 2003)(Kweon and Kim, 2006). For rehabilitation design, the MEPDG recommends the use of nondestructive testing equipment such as the Falling Weight Deflectometer (FWD) or seismic surface wave propagation methods. Some of the seismic techniques that have shown to provide accurate non-destructive estimates for computing the in-situ asphalt concrete layer moduli for pavement design include the Spectral Analysis of Surface Waves method (SASW) (Heisey et al. 1982)(Nazarian et al. 1983)(Roesset et al., 1990), the Seismic Pavement Analyzer (Yuan et al., 1998)(Celaya and Nazarian, 2006), Multichannel Simulation with One Receiver (MSOR) (Ryden et al., 2003) and the Multichannel Analysis of Surface Waves (MASW) method (Park et al., 1999)(Barnes et al., 2010). If laboratory or non-

destructive testing equipment is not available, the dynamic modulus may be determined using the predictive equation described in the MEPDG (NCHRP, 2004). This equation is based on the Witczak predictive model and has shown to provide reasonable predictions of the dynamic modulus for hot-mix asphalt mixtures (Bari and Witczak, 2005)(Dongre et al., 2005). Depending on the hierarchical level required for design, the predictive equation requires parameters that include the asphalt binder viscosity, air void content, effective bitumen content, and aggregate gradation which may not be easily determined for existing pavements.

When considering an existing roadway,  $E^*$  is commonly determined via in-situ nondestructive testing, however,  $E^*$  values determined from FWD or seismic surface wave propagation methods should be corrected based on temperature to a common design value in order to provide a consistent measure of the pavement response or to simply compare results regardless of the temperature (Hadidi et al., 2006)(Hakim and Brown, 2006). The difference between FWD and seismic surface wave methods exist in the loading frequency and the dependence of the results on the structural system. Moduli values obtained using seismic methods are low-magnitude high-strain rate values (high frequency, 5 to 90 kHz), compared to vehicular traffic and FWD which cause higher magnitude deformation at low-strain rates (low frequency, 10 to 25 Hz).

Unlike deflection methods, which measure the global deflection response of the pavement system, seismic wave methods can provide an independent estimate of the uppermost asphalt concrete layer modulus. There has been considerable research conducted to determine temperature prediction models and correction factors for FWD data (Park et al., 2001). Nonetheless, due to the high frequency content of the seismic methods, the measured moduli values need to be corrected for both temperature and frequency if they are to be used in pavement analysis and design, therefore the correction factors developed for FWD are ineffective for seismic data. The MEPDG recommends using the master curve for temperature correction, however the master curve has also proven to be a valuable tool for shifting higher frequency surface wave moduli down to lower frequency design values (Bai, 2004)(Celaya and Nazarian, 2006)(Barnes and Trottier, 2009).

The dynamic modulus master curve is constructed using the principal of time-temperature superposition. The master curve is constructed at a selected reference temperature, usually 21 °C, and the moduli data collected at the various temperatures is shifted relative to loading frequency, or the inverse of load duration, until all data merges to form a single smooth function, or master curve. The amount of shifting required to form the master curve is described by the shift factors for various temperatures, determined using one of the following equations or models, the MEPDG Model (NCHRP, 2004)(Pellinen et al., 2004)(Bonaquist and Christensen, 2005), the Arrhenius Equation (Pellinen et al., 2004)(Rowe and Sharrrock, 2011)(Walubita et al., 2011), the Williams-Landel-Ferry (WLF) Equation (Pellinen et al., 2004)(Rowe and Sharrock, 2011)(Ryden, 2011)(Walubita et al., 2011), and the Second Order Polynomial Equation (Bari and Witeczak, 2005).

With the emergence of seismic surface wave methods to measure the in-situ dynamic modulus, the asphalt concrete master curve has become an increasingly valuable tool in pavement evaluation and design. Recognizing the importance of the master curve, this paper evaluates several master curve construction techniques and describes the benefits of introducing MASW data into the analysis to adequately depict a broader range of reduced frequencies. This paper also demonstrates the importance of validating the constructed master curve by implementing shifted moduli into design examples, as opposed to simply limiting validation to a statistical investigation. The scope of work involved constructing master curves utilizing the shift factor models listed above with dynamic moduli values obtained from: 1) AASHTO TP 62 results; 2) predictive models; and, 3) a combination of AASHTO TP 62 and MASW testing. The fatigue life and the design period for a typical pavement structure were computed based on measured seismic moduli that were shifted to a design value using the different master curve models. These were compared to the laboratory determined dynamic moduli to characterize the accuracy of the master curves and the resulting temperature/frequency shifted dynamic modulus values in regards to pavement design.

## 4.4 DETERMINATION OF DYNAMIC MODULUS

The MEPDG recommends laboratory testing using cylindrical specimens of new asphalt concrete manufactured in the laboratory to determine the dynamic modulus according to the AASHTO TP 62 method, for the design of new or reconstructed pavements. In contrast, the existing asphalt layer dynamic modulus for rehabilitation design is measured in the field using non-destructive testing equipment, or core samples may be extracted from the roadway to perform AASHTO TP 62 testing if there is sufficient thickness to provide the required height to diameter ratio.

### 4.4.1 Laboratory Testing AASHTO TP 62

AASHTO TP 62 testing is conducted on a servo hydraulic testing machine using cylindrical specimens subjected to a sinusoidal axial compressive load at a given temperature and loading frequency. Strain gauges or LVDTs are positioned on opposite sides of the specimen to measure the vertical deflections and the axial strain on the specimen is maintained between 50 and 150 microstrain to ensure linear elastic behavior. For linear viscoelastic materials such as Hot Mix Asphalt (HMA), the stress-strain relationship when subjected to a continuous sinusoidal load is characterized by its complex dynamic modulus according to Equation (13), which is defined as the ratio of the amplitude of the sinusoidal stress,  $\sigma$ , at any given time,  $t$ , and the angular load frequency,  $\omega$ , to the corresponding sinusoidal strain,  $\varepsilon$ , at the same time, separated by a phase lag,  $\phi$ , due to the viscoelasticity (Witczack and Bari, 2004).

$$E^* = \frac{\sigma}{\varepsilon} = \frac{\sigma_0 \cdot \sin(\omega t)}{\varepsilon_0 \cdot \sin(\omega t - \phi)} \quad (13)$$

Where,  $\sigma_0$  = maximum stress amplitude, and  $\varepsilon_0$  = maximum strain amplitude. The dynamic modulus is defined as the absolute value of the complex dynamic modulus and can be computed by dividing the maximum (peak-to-peak) stress by the recoverable (peak-to-

peak) axial strain as shown in Equation (9). For simplicity, the dynamic modulus is generally denoted as  $E^*$  and not  $|E^*|$  as is the case in this thesis.

#### 4.4.2 Multichannel Analysis of Surface Waves

Rayleigh waves are stress waves that propagate along the free surface of a semi-infinite half-space, where the velocity of wave propagation is dependent on the elastic properties of the half-space material and consequently can be used to estimate the elastic and shear moduli. It has been shown for asphalt concrete pavement layers of finite thickness that at wavelengths less than or equal to the asphalt concrete thickness, the dominant wave modes tend to follow the fundamental anti symmetric Lamb wave mode that occurs in a free plate (Jones, 1955)(Ryden et al., 2004). MASW has proven to be an effective technique for identifying and tracking the fundamental Lamb wave modes which asymptotically approach the fundamental Rayleigh wave providing a singular velocity for each sampled frequency (Park et al. 1998)(Park et al., 1999). A dispersion curve of approximate Rayleigh wave velocity versus wavelength can provide an estimate of the HMA moduli for all wavelengths contained within the layer thickness (Barnes and Trottier, 2009). If the properties of the asphalt concrete layer (density ( $\rho$ ), Poisson's Ratio ( $\nu$ )) are assumed to be uniform, Rayleigh wave theory (Equation (14)) provides a simple method of converting the measured velocity dispersion curve into a multitude of seismic elastic moduli relating to a particular set of frequencies (Achenbach, 1973)(Nazarian et al., 1999)(Ryden and Park, 2006)(Barnes and Trottier, 2009).

$$E_{Seismic} = 2\rho[(1.13 - 0.16\nu)V_R]^2(1 + \nu) \quad (14)$$

The dynamic modulus determined using a surface wave method is considered to be a high frequency modulus, with velocity data obtained at frequencies ranging between 5 and up to 90 kHz. As a result, MASW testing may be quite useful for evaluating thin overlays since it can provide modulus estimates at depths as shallow as 15-20 mm, however the



moduli must be frequency shifted using a master curve to conventional traffic and FWD frequencies (10-25 Hz) for use in design.

#### 4.4.3 MEPDG Dynamic Modulus Predictive Equation

The MEPDG has adopted a hierarchical input system composed of three levels for determining the required design inputs for materials. AASHTO TP 62 laboratory testing or non-destructive in-situ testing is required for Level 1 dynamic modulus measurements, while a predictive equation is applied for Level 2 and Level 3 analyses. The MEPDG dynamic modulus predictive equation, which is based on the Witczak model (Bari and Witczak, 2005), has the ability to predict dynamic modulus values over a range of frequencies, temperatures, and aging conditions using information from material specifications or the volumetric design of the mixture. The dynamic modulus for Level 2 input is determined directly from the predictive equation using specific laboratory binder test and mix data. Level 3 input is developed using the predictive equation and typical properties of the binder and mix. The current MEPDG version (NCHRP, 2004) of the Witczak Predictive Equation is shown in Equation (15):

$$\log E^* = 3.750063 + 0.02932\rho_{200} - 0.001767(\rho_{200})^2 - 0.002841\rho_4 - 0.058097V_a - 0.802208\left(\frac{V_{beff}}{V_{beff} + V_a}\right) + \left(\frac{3.871977 - 0.0021\rho_4 + 0.003958\rho_{38} - 0.000017(\rho_{38})^2 + 0.005470\rho_{34}}{1 + e^{(-0.603313 - 0.313351\log(f) - 0.393532\log(\eta))}}\right) \quad (15)$$

Where  $E^*$  is the dynamic modulus (psi);  $\eta$  is the bitumen viscosity ( $10^6$  Poise);  $f$  is the loading frequency (Hz);  $V_a$  is the air void content (%);  $V_{beff}$  is the effective bitumen content (% by volume);  $\rho_{34}$  is the cumulative percent retained on the  $3/4$  inch sieve;  $\rho_{38}$  is the cumulative percent retained on the  $3/8$  inch sieve;  $\rho_4$  is the cumulative percent retained on the number 4 sieve; and  $\rho_{200}$  is the percent passing the number 200 sieve.

## 4.5 DYNAMIC MODULUS MASTER CURVE CONSTRUCTION

Dynamic modulus values measured at multiple temperatures and frequencies can be used to construct the master curve for a particular asphalt concrete mixture using the principle of time-temperature superposition. The master curve can be mathematically modeled by a sigmoidal function described by Equation (10) proposed by Pellinen et al. (2004).

The measured dynamic modulus results at various temperatures and frequencies are shifted to a reduced frequency at an arbitrarily selected reference temperature,  $T_0$ , generally selected to be 21°C, as shown in Equation (16).

$$\log(\xi) = \log(f) + \log[a(T)] \quad (16)$$

Where,  $a(T)$  is the shift factor,  $a(T_0) = 0$ ,  $f$  is the frequency, and  $\xi$  is the reduced frequency. Various models describing shift factors used for asphalt material analysis include the MEPDG, Arrhenius, and WLF models, or it can be represented as a second order polynomial function.

### 4.5.1 Log-Log Viscosity Relationship (MEPDG)

In the MEPDG model, the shift factors are expressed as a function of binder viscosity according to Equation (17), which considers aging effects over the pavement life using the model developed by Mirza and Witzak (1995).

$$\log[a(T)] = c[\log(\eta) - \log(\eta_{Tr})] \quad (17)$$

Where  $a(T)$  is the shift factor as a function of temperature and age,  $c$  is fitting parameter,  $\eta$  is viscosity at the age and temperature of interest (cP),  $\eta_{Tr}$  is viscosity at temperature and

RTFO aging (cP). The viscosity of the asphalt binder as a function of temperature can be determined from the ASTM viscosity-temperature relationship defined by Equation (18).

$$\log(\log \eta) = A + VTS \log T_R \quad (18)$$

Where  $\eta$  is viscosity (cP),  $T_R$  is temperature (Rankine), A and VTS are the intercept and slope of a linear regression model of the viscosity temperature susceptibility.

#### 4.5.2 Arrhenius

The Arrhenius shift factor as applied to asphalt materials generally takes the form as described in Equation (19) (Rowe and Sharrock, 2011).

$$\log[a(T)] = a \left( \frac{1}{T} - \frac{1}{T_{ref}} \right) \quad (19)$$

Where  $a(T)$  is the shift factor,  $a$  is fitting parameter,  $T$  is test temperature of interest (K), and  $T_{ref}$  is the reference temperature (K).

#### 4.5.3 WLF

The WLF model for computing the shift factor is shown in Equation (20) (Ryden, 2011).

$$\log[a(T)] = \frac{-C_1(T_i - T_{ref})}{C_2 + T_i - T_{ref}} \quad (20)$$

Where  $C_1$  and  $C_2$  are fitting parameters,  $T_i$  is the selected temperature of interest ( $^{\circ}\text{C}$ ), and  $T_{ref}$  is the reference temperature ( $^{\circ}\text{C}$ ).

#### 4.5.4 Second Order Polynomial

The shift factor  $a(T)$  can also be represented as a second order polynomial function of the temperature,  $T$  (Witczak and Bari, 2004) as shown in Equation (21).

$$\text{Log}[a(T)] = aT^2 + bT + c \quad (21)$$

Where  $a$ ,  $b$  and  $c$  are coefficients of the second order polynomial, and  $T$  is the temperature of interest ( $^{\circ}\text{C}$ ).

### 4.6 EXPERIMENTAL TESTING AND RESULTS

MASW testing was conducted on 70 x 250 x 450 mm field produced asphalt concrete plate specimens that were later cored and used to perform AASHTO TP 62 testing. The plate specimens were extracted from a pavement section constructed solely for research purposes following Nova Scotia Department of Transportation and Infrastructure Renewal specifications for a Type C, 14 mm maximum aggregate size asphalt mixture produced with 6.0% PG58-28 asphalt binder. The hot mix asphalt was produced with an Astec double drum six-pack asphalt plant, placed with a Cedarapids asphalt paver, and compacted with both a steel drum vibratory and rubber tired pneumatic roller. The compaction effort varied throughout the mat to obtain locations of varying air void content, however for this particular study, plates with 4.0% air voids were selected. To obtain additional mixture data for the MEPDG equations, two plates were used to determine the maximum theoretical density, gradation, and asphalt content for the particular test location.

The plate samples were stored and tested using surface waves in a temperature controlled environmental room at temperatures of -19.3, -0.3, 9.4, 19.5, and 39.5 $^{\circ}\text{C}$ . Surface wave data was collected using the multichannel simulation with one receiver (MSOR) approach as described by Ryden et al. (2001) and Barnes and Trottier (2009) and evaluated using the MASW data processing technique (Park et al., 1999). The data was collected using a 100

kHz displacement transducer as the receiver and an Olsen Instruments Freedom NDT Data PC having a 1 MHz National Instruments data acquisition board to sample the surface wave data. The impact was generated using a high frequency impactor consisting of a stainless steel A-6 autoharp string housed in an aluminum block with a rubber membrane lining the bottom. A one cm wide 24 gauge sheet metal strip was bonded to the asphalt surface with an epoxy to overcome some of the source generating difficulties related to the heterogeneous nature of the asphalt concrete. Barnes and Trottier (2009) demonstrated that surface waves up to 80-90 kHz could be measured in asphalt concrete plates using this impactor. A magnetically mounted 15 kHz accelerometer was placed at each impact location to trigger data collection. Data was recorded at 20 different offsets from the receiver, ranging from three to 22 centimetres. Using a Matlab program, the phase velocity dispersion curves were constructed by tracing the convergent fundamental Lamb wave modes imaged using the MASW technique described by Park et al. (1999) as shown in Figure 12. The phase velocity dispersion curve was used to compute the viscoelastic moduli at different frequencies according to the measured density of 2250 kg/m<sup>3</sup> and assumed values of Poisson's ratio at each test temperature as described in Table 2.2.14 of the MEPDG as shown in Table 7 (NCHRP, 2004).

Table 7 Typical values of Poisson's ratio versus temperature (NCHRP, 2004).

| <b>Temperature (°F)</b> | <b>Poisson's Ratio</b> |
|-------------------------|------------------------|
| < 0                     | < 0.15                 |
| 0 - 40                  | 0.15 – 0.20            |
| 40 - 70                 | 0.20 – 0.30            |
| 70 - 100                | 0.30 – 0.40            |
| 100 - 130               | 0.40 – 0.48            |
| > 130                   | 0.45 – 0.48            |

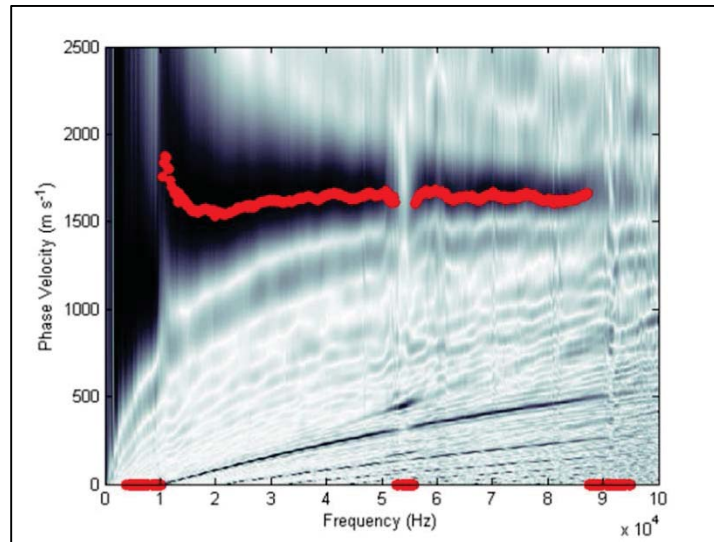


Figure 12 Phase velocity dispersion curve from plate sample.

Once the surface wave testing was complete, 100 mm diameter samples were cored from the plate samples. To achieve the recommended height to diameter ratio, two cores samples were glued together using a thin layer of high strength epoxy ( $E = 30$  GPa). The epoxy layer was less than half of a millimetre in thickness and likely did not influence the results. The cores were tested with a servo-hydraulic testing system according to AASHTO TP 62-03 and ASTM D3497. The samples were tested at frequencies of 0.1, 1, 5, 10, and 25 Hz at temperatures of -18, 0, 10, 21, and 40°C using a controlled environmental chamber.

Master curves were constructed for data sets consisting of the AASHTO TP 62 dynamic moduli, and a combination of the AASHTO TP 62 data with surface wave based moduli, using the different shift factor models described above. The master curves were constructed by simultaneously solving the four coefficients of the sigmoidal function ( $\delta$ ,  $\alpha$ ,  $\beta$ ,  $\gamma$ ) and the coefficients of the shift factor model equations. This was completed by fitting the theoretical model to the experimental data using a least square error approach by adjusting the coefficients using the “Solver” function in Microsoft Excel™. In addition to constructing master curves with measured dynamic modulus data, master curves were developed using the MEPDG predictive equation at input Level 2 and Level 3, where at

Level 2 the asphalt binder viscosity is measured and the A and VTS values are determined as opposed to Level 3 which uses default values provided in the MEPDG. The resulting coefficients of the master curve sigmoidal function and shift parameters for each construction technique are listed in Table 8, and the fitted master curves are shown in Figure 13.

Table 8 Master curve and shift parameters.

| Construction Technique    |                            | Master Curve Parameters |          |         |          |            |          |        |
|---------------------------|----------------------------|-------------------------|----------|---------|----------|------------|----------|--------|
| MEPDG                     |                            | $\delta$                | $\alpha$ | $\beta$ | $\gamma$ | $c$        |          |        |
|                           | TP62                       | -1.3166                 | 5.7459   | -1.3338 | 0.3619   | 1.4066     |          |        |
|                           | TP62 & MASW                | 0.6303                  | 3.7622   | -0.8051 | 0.4137   | 1.4636     |          |        |
|                           | TP62 (No Binder Viscosity) | 2.2120                  | 18.8880  | 2.7616  | 0.0506   | 3.6893     |          |        |
| Polynomial                |                            | $\delta$                | $\alpha$ | $\beta$ | $\gamma$ | $a$        | $b$      | $c$    |
|                           | TP62                       | 0.5294                  | 3.9268   | -0.7996 | 0.3522   | 0.0005     | -0.1593  | 3.1348 |
|                           | TP62 & MASW                | 0.5819                  | 3.8116   | -0.8771 | 0.4125   | 0.0006     | -0.1521  | 2.9194 |
| WLF                       |                            | $\delta$                | $\alpha$ | $\beta$ | $\gamma$ | $C1$       | $C2$     |        |
|                           | TP62                       | 0.5321                  | 3.9251   | -0.7984 | 0.3515   | 49.5195    | 352.5831 |        |
|                           | TP62 & MASW                | 0.6813                  | 3.7074   | -0.7808 | 0.4306   | 19.9816    | 163.9698 |        |
| Arrhenius                 |                            | $\delta$                | $\alpha$ | $\beta$ | $\gamma$ | $C$        |          |        |
|                           | TP62                       | 0.3481                  | 4.1050   | -0.8666 | 0.3527   | 11842.7667 |          |        |
|                           | TP62 & MASW                | -0.3908                 | 4.7883   | -1.2016 | 0.3933   | 10967.7134 |          |        |
| MEPDG Predictive Equation |                            | $\delta$                | $\alpha$ | $\beta$ | $\gamma$ |            |          |        |
|                           | Binder Viscosity           | 2.8881                  | 3.8492   | -0.6291 | 0.3134   |            |          |        |
|                           | No Binder Viscosity        | 2.8881                  | 3.8492   | -1.0234 | 0.3134   |            |          |        |

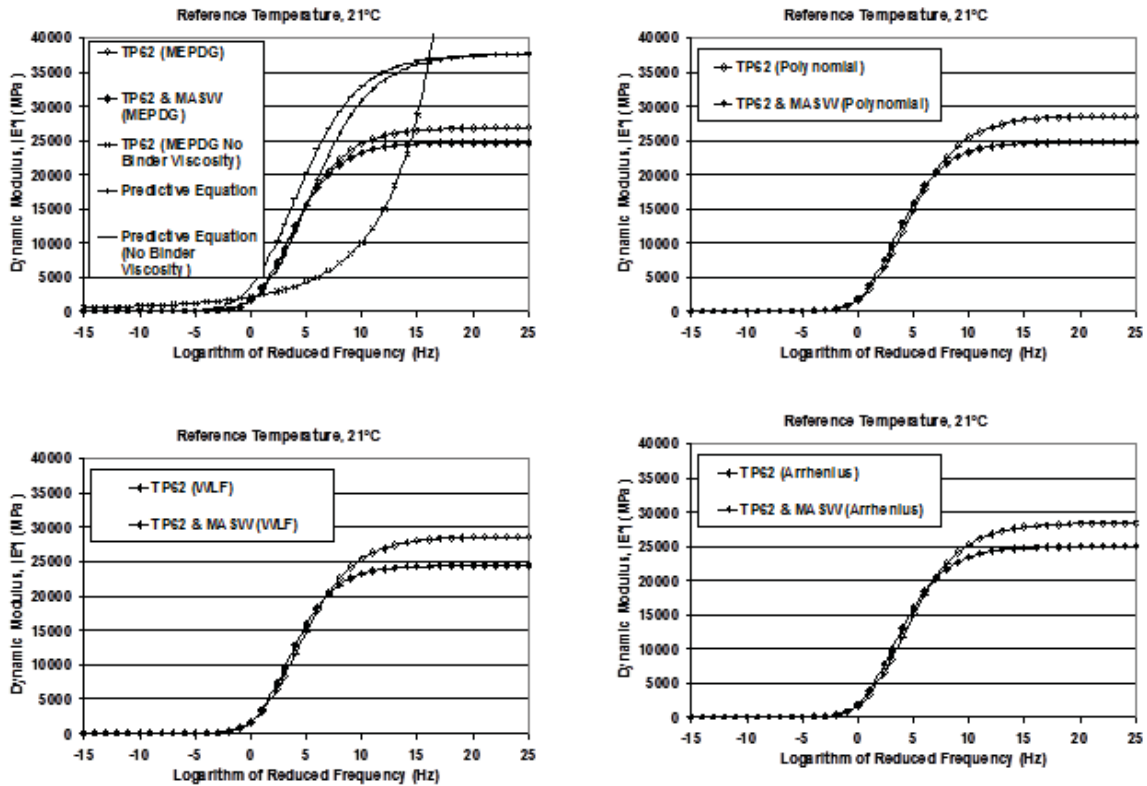


Figure 13 Combinations of dynamic modulus data sets and master curve models.

To compare the master curve construction techniques, the predicted dynamic modulus values ( $E^*_p$ ) were plotted against the laboratory measured values ( $E^*_M$ ) for each shift factor model and data set evaluated, as shown in Figure 14. Two goodness of fit statistics were computed: the coefficient of determination,  $R^2$  and the ratio of standard error to the standard deviation,  $S_e/S_y$ . In general, a high  $R^2$  ( $>0.9$ ) and low  $S_e/S_y$  ( $<0.35$ ) indicate excellent fitting of the master curve to the measured data (Zhu et al., 2011). As a result, the only master curve technique that did not provide excellent results was the Level 3 predictive equation without binder data.

To better assess each master curve construction technique and the impact of combining AASHTO TP 62 and MASW data for shifting high frequency dynamic modulus values collected at different temperatures, the individual master curves were used to shift high frequency MASW data at multiple test temperatures to a reference frequency of 10 Hz and temperature of 21°C as listed in Table 9. The master curve shifted dynamic modulus values



were then compared to the measured AASHTO TP 62 dynamic modulus at the proposed reference temperature and frequency by calculating the percentage Average Relative Error (ARE) using Equation (22) according to Singh et al. (2012).

$$ARE = \frac{\sum_{i=1}^N \frac{(E^*_P - E^*_M)}{E^*_M}}{N} \times 100 \quad (22)$$

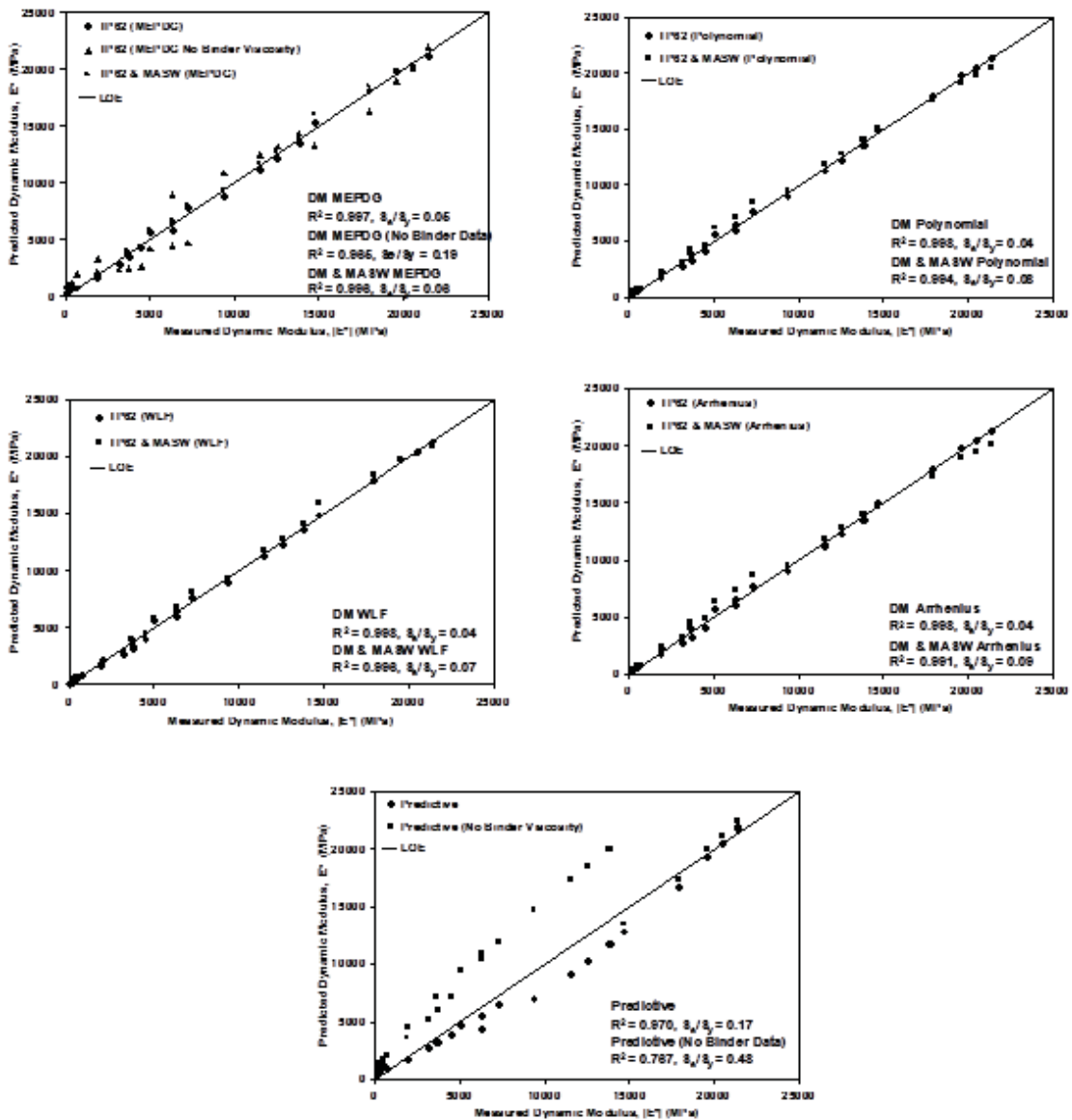


Figure 14 Plot of master curve versus laboratory  $E^*$ .

Table 9 Frequency and temperature corrected dynamic modulus.

| Test Temperature (°C)  |   | -19.3          | -0.3           | 9.4            | 19.5            | 39.5             | Average        |
|--|---|----------------|----------------|----------------|-----------------|------------------|----------------|
| Frequency and Temperature Shifted Dynamic Modulus,  E*  to 21°C and 10 Hz, MPa (Relative Error, %) | TP62 (MEPDG)                                    | 3280<br>(12.7) | 3367<br>(10.4) | 3501<br>(6.8)  | 3580<br>(4.7)   | 3409<br>(9.2)    | 3428<br>(8.8)  |
|  | TP62 (MEPDG No Binder Viscosity)                | 1193<br>(68.2) | 1734<br>(53.8) | 4666<br>(23.9) | 8513<br>(126.6) | 11371<br>(202.7) | 5494<br>(95.1) |
|  | TP62 (Polynomial)                               | 2943<br>(21.7) | 3089<br>(18.3) | 3254<br>(13.4) | 3499<br>(6.9)   | 4308<br>(14.7)   | 3415<br>(15.0) |
|  | TP62 (WLF)                                      | 2939<br>(21.8) | 3067<br>(18.4) | 3252<br>(13.5) | 3499<br>(6.9)   | 4427<br>(17.8)   | 3437<br>(15.7) |
|  | TP62 (Arrhenius)                                | 2984<br>(20.6) | 3110<br>(17.2) | 3288<br>(12.5) | 3510<br>(6.6)   | 4239<br>(12.8)   | 3426<br>(13.9) |
|  | TP62 & MASW (MEPDG)                             | 3435<br>(8.6)  | 3412<br>(9.2)  | 3490<br>(7.1)  | 3539<br>(5.8)   | 3475<br>(7.5)    | 3470<br>(7.6)  |
|  | TP62 & MASW (Polynomial)                        | 3737<br>(0.5)  | 3689<br>(1.8)  | 3733<br>(0.6)  | 3745<br>(0.3)   | 3747<br>(0.3)    | 3731<br>(0.7)  |
|  | TP62 & MASW (WLF)                               | 3469<br>(7.7)  | 3423<br>(8.9)  | 3471<br>(7.6)  | 3486<br>(7.2)   | 3450<br>(8.2)    | 3460<br>(7.9)  |
|  | TP62 & MASW (Arrhenius)                         | 3902<br>(3.9)  | 3866<br>(2.9)  | 3903<br>(3.9)  | 3893<br>(3.6)   | 3947<br>(5.1)    | 3902<br>(3.9)  |
|  | MEPDG Predictive Equation                       | 2391<br>(36.3) | 2751<br>(26.8) | 3051<br>(18.8) | 3304<br>(12.1)  | 3200<br>(14.8)   | 2939<br>(21.8) |
|  | MEPDG Predictive Equation (No Binder Viscosity) | 4541<br>(20.9) | 4215<br>(12.2) | 4474<br>(19.1) | 4692<br>(24.9)  | 4612<br>(22.8)   | 4507<br>(20.0) |
| AASHTO TP62-03 Determined Dynamic Modulus at 21°C and 10 Hz, MPa                                   |   | 3757           |                |                |                 |                  |                |
| 95% Confidence Interval, MPa   |   | 3532 - 3982    |                |                |                 |                  |                |

Where  $E^*_p$  is the predicted or shifted dynamic modulus,  $E^*_M$  is the laboratory measured dynamic modulus, and  $N$  is the number of observations. Figure 15 shows the plot of ARE for the frequency and temperature shifted dynamic modulus for each master curve construction technique. It can be seen from Figure 15 that the master curve constructed using the combination of AASHTO TP 62 and MASW data with the polynomial shift factor equation provided the smallest overall ARE of 0.7% and the smallest ARE at each test temperature. The results also show that the master curves constructed with the combination of AASHTO TP 62 and MASW data provide the smallest relative error no matter what shift factor model is used. The predictive equation at Level 2 and Level 3 and the AASHTO TP 62 using the MEPDG model with no binder data (Level 3) displayed the highest ARE values. It is also important to note that the master curves constructed with the combination

of dynamic modulus data provided the most consistent results across the range of test temperatures. By combining both test methods, dynamic modulus data is available at a wider range of reduced frequencies since the MASW test provides data at much higher frequencies than the AASHTO TP 62 testing as shown in Figure 16. Regarding the shift factor models, the MEPDG model provided the best ARE with AASHTO TP 62 data only, while the polynomial equation followed by the Arrhenius equation resulted in the lowest ARE when the combination of data was implemented. Therefore it is difficult to conclude which model generates the best overall master curve, however it can be stated that using a combination of dynamic modulus data no matter what model is applied provides for significantly better results.

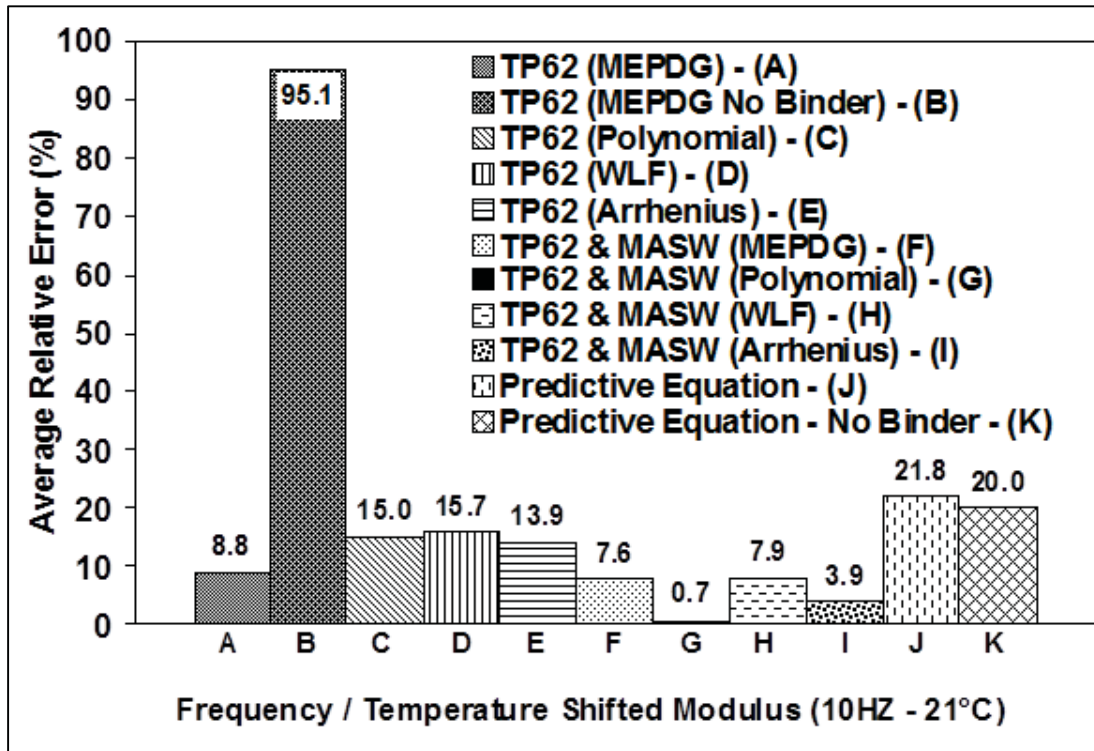


Figure 15 Average relative error for the frequency and temperature shifted E\*.

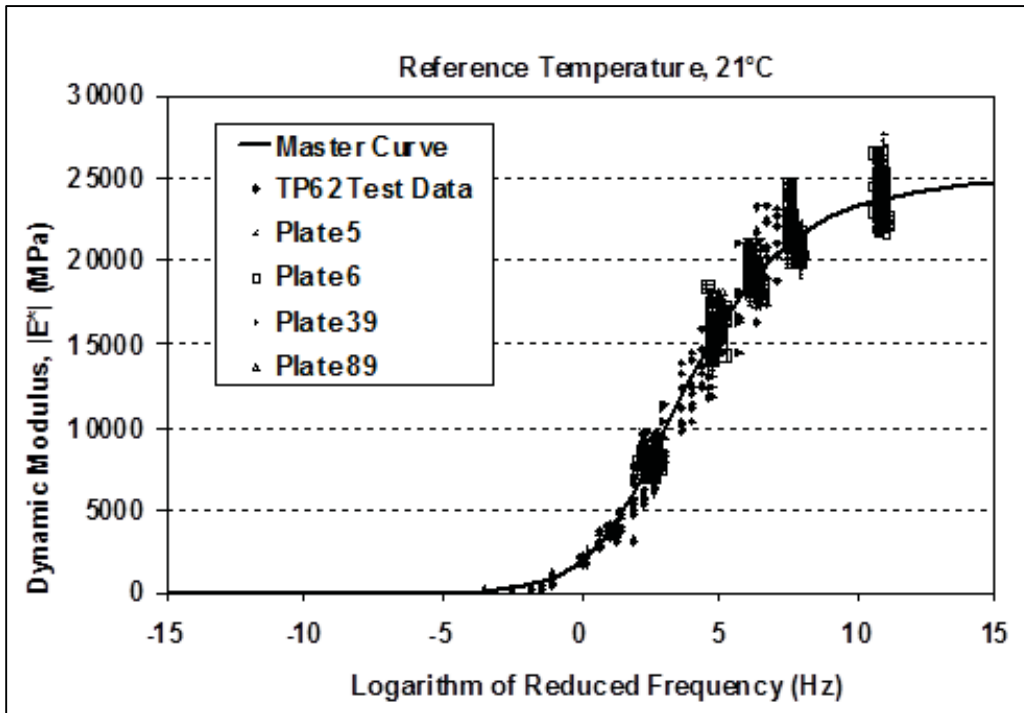


Figure 16 Master curve constructed using a combination of AASHTO TP 62 and MASW data and the polynomial equation.

#### 4.7 IMPACT ON PAVEMENT DESIGN

One measure by which pavement engineers calculate the life expectancy or design period of asphalt concrete pavements is based on the number of load repetitions to cause fatigue cracking, which is a function of tensile strain and mix stiffness or modulus. The MEPDG recommends the use of Equation (23) (NCHRP, 2004) to predict the number of load applications to fatigue failure and differentiates between bottom-up and top-down cracking by implementing Equations (26) and (27) (NCHRP, 2004).

$$N_f = 0.00432 * k_1' * C \left( \frac{1}{\varepsilon_t} \right)^{3.9492} \left( \frac{1}{E} \right)^{1.281} \quad (23)$$

$$C = 10^M \quad (24)$$

$$M = 4.84 \left( \frac{V_b}{V_a + V_b} - 0.69 \right) \quad (25)$$

Where,  $N_f$  is the number of repetitions to fatigue cracking,  $\varepsilon_t$  is the tensile strain at the critical location (bottom of asphalt concrete layer for bottom-up cracking and asphalt concrete surface for top-down cracking),  $E$  is the asphalt concrete stiffness,  $C$  is the laboratory to field adjustment factor,  $V_b$  is the effective binder content (%),  $V_a$  is the air voids (%), and  $k'_1$  is a parameter introduced to provide a correction for different asphalt thicknesses ( $h_{ac}$ ) and is defined by Equation (26) for bottom-up cracking and Equation (27) for top-down cracking.

$$k'_1 = \frac{1}{0.000398 + \frac{0.003602}{1 + e^{(11.02 - 3.49 * h_{ac})}}} \quad (26)$$

$$k'_1 = \frac{1}{0.01 + \frac{12.00}{1 + e^{(15.676 - 2.8186 * h_{ac})}}} \quad (27)$$

To further characterize the importance of correctly shifting the MASW measured dynamic modulus in relation to pavement design, the corrected dynamic modulus values determined in Table 9 were used to predict the repetitions to fatigue failure and corresponding design period in comparison to the laboratory measured dynamic modulus as displayed in Table 10. Table 10 lists the modulus, tensile strain at the surface and bottom of the asphalt concrete layer and the load repetitions to failure and the design period for both bottom-up and top-down cracking. The tensile strain was computed using linear elastic layered theory based on a total asphalt thickness of 150 mm, supported by a 150 mm thick 200 MPa granular base, and a 300 mm thick 150 MPa granular subbase on a 60 MPa subgrade. The shifted modulus values used in the analysis were the average shifted modulus values calculated from the range of test temperatures and varied from 2910 MPa to 5465 MPa for all master curve models with the laboratory design value measured to be 3757 MPa (21°C

and 10Hz). The reference design periods, based on the measured modulus, were calculated to be 24.4 years for bottom-up cracking and 5.7 years for top-down cracking, in comparison to the calculated design periods for the shifted moduli which ranged from 20.5 to 32 years for bottom-up cracking and 3.3 to 12.4 years for top-down cracking. The design periods based on the modulus values shifted with the master curve constructed using the combination of AASHTO TP 62 and MASW data and the polynomial equation provided close approximations to the results based on the reference values, 24.2 versus 24.4 years for bottom-up cracking and 5.9 versus 5.7 years for top-down cracking. It is evident from the results displayed in Table 3 that the master curve utilized to shift the higher frequency seismic moduli to a reference design value has a considerable influence on pavement design and therefore should be constructed with the largest number of test points which fully depict the reduced frequency range for that particular asphalt concrete.

Table 10 Predicted fatigue design period.

| Parameter   | Master Curve Construction Technique |  |                                 |                                 |   | AASHTO TP62-03<br>Determined Dynamic<br>Modulus at 21°C and<br>10 Hz, MPa |
|---|-------------------------------------|--|---------------------------------|---------------------------------|---|---|
|   | TP62<br>(MEPDG)                     | TP62 - MEPDG<br>(No Binder<br>Viscosity) | TP 62 &<br>MASW -<br>Polynomial | MEPDG<br>Predictive<br>Equation | MEPDG Predictive<br>Equation (No<br>Binder Viscosity) |   |
| Average<br>Frequency/Temperature Shifted<br>Modulus 21°C and 10 Hz, MPa | 3428                                | 5494                                     | 3731                            | 2939                            | 4507  | 3757  |
| Tensile Strain ( $\epsilon_t$ ) Bottom HMA                              | 226.6                               | 169.0                                    | 215.5                           | 247.9                           | 191.9   | 213.6   |
| Tensile Strain ( $\epsilon_t$ ) Top HMA                                 | 46.9                                | 50.3                                     | 48.5                            | 42.1                            | 50.4  | 48.8  |
| $N_f$ ( $10^6$ ESAL) Bottom-Up<br>Cracking                              | 3.760                               | 6.522                                    | 4.115                           | 3.220                           | 5.099   | 4.184   |
| Design Period (Years) - Bottom-<br>Up Cracking                          | 22.8                                | 32.0                                     | 24.2                            | 20.5                            | 27.7  | 24.4  |
| $N_f$ ( $10^6$ ESAL) Top-Down<br>Cracking                               | 0.869                               | 0.359                                    | 0.683                           | 1.625                           | 0.460   | 0.654   |
| Design Period (Years) - Top<br>Down Cracking                            | 7.3                                 | 3.3                                      | 5.9                             | 12.4                            | 4.2   | 5.7   |

## 4.8 CONCLUSIONS

In this study four methods of modelling the shift factor used in generating the asphalt concrete master curve (the MEPDG Model, the Arrhenius Equation, the WLF Equation, and the Second Order Polynomial Equation) were used in conjunction with three different methods of obtaining the dynamic modulus. Eleven different master curves were evaluated to determine which would best shift high frequency MASW data collected at multiple temperatures to a reference design temperature and frequency (21°C and 10Hz).

The master curves were first evaluated by plotting the master curve predicted  $E^*$  versus the laboratory measured  $E^*$  values and calculating goodness of fit statistics. The coefficient of determination,  $R^2$  and the ratio of standard error to the standard deviation,  $S_e/S_y$  were computed for each master curve. The results indicated that the only master curve that did not provide acceptable results was the Level 3 MEPDG predictive equation without binder data. Consequently, to assess the impact of subtle differences among the various master curves on pavement evaluation, actual MASW data were shifted to reference design values and compared to the measured laboratory values. The percentage relative error was significantly less in all cases for the master curves constructed with a combination of data, regardless of shift factor equation. Therefore using a combination of dynamic modulus data appears to be significantly more important than the selection of shift factor equation. The MEPDG and polynomial equations seemed to provide the best results, regardless of the dynamic modulus collection technique. This analysis demonstrated the importance of implementing a combination of MASW and AASHTO TP 62 dynamic modulus data to construct master curves to be used in shifting MASW field data to reference temperatures and frequencies.

If MASW data is to be used in pavement analysis and design, the ability of a master curve to properly shift data to a reference design value becomes extremely important as demonstrated by the fatigue analysis. It is important to validate master curves statistically,

but small deviations that might be overlooked in the statistical analysis may not adequately represent the variations in design parameters.

Future research should explore the influence of asphalt concrete mixtures (different aggregate size, binder type, binder content, air voids etc.) on the observed results from this study and should attempt to identify whether MASW data alone may be used to develop a master curve.

#### **4.9 REFERENCES**

AASHTO TP 62-03 (2005). “Standard method of test for determining dynamic modulus of hot-mix asphalt concrete mixtures”, American Association of State Highway and Transportation Officials, Washington, D.C.

Achenbach, J.D. (1973). *Wave Propagation in Elastic Solids*, North Holland Publishing Company, Amsterdam/New York.

ASTM C 215 (2008). “Standard test method for fundamental transverse, longitudinal, and torsional frequencies of concrete specimens”, ASTM International, West Conshohocken, PA. [www.astm.org](http://www.astm.org).

ASTM D3497-79 (2003). “Standard Test Method for Dynamic Modulus of Asphalt Mixtures”, ASTM International, West Conshohocken, PA. [www.astm.org](http://www.astm.org).

Bai, X. (2004). “Assessment of relationship between dynamic and seismic moduli of asphalt concrete mixtures”, M.Sc. thesis, The University of Texas at El Paso.

Bari, J., Witczak, M.W. (2005). “Evaluation of the effect of lime modification on the dynamic modulus stiffness of hot-mix asphalt”, Transportation Research Record 1929, Transportation Research Board, National Research Council, Washington, D.C., pp. 10-19.



Barnes, C.L. (2008). "Evaluating moisture damage in asphalt concrete using surface waves", Ph.D. thesis, Dalhousie University.

Barnes, C.L., Trottier, J.-F. (2009). "Evaluating High-Frequency Visco-Elastic Moduli in Asphalt Concrete", *Research in Nondestructive Evaluation*, Volume 20, Issue 2, pp.116-130.

Barnes, C.L., Trottier, J.-F. (2010). "Evaluating in-service asphalt concrete damage using surface waves", *International Journal of Pavement Engineering*, Volume 11, Number 6, pp. 449-458.

Biswas, K.G., Pellinen, T.K. (2007). "Practical methodology of determining the in situ dynamic (complex) moduli for engineering analysis", *ASCE Journal of Materials in Civil Engineering*, Vol. 19, No. 6, pp.508-514.

Bonaquist, R., Christensen, D.W. (2005). "Practical procedure for developing dynamic modulus master curves for pavement structural design", *Transportation Research Record 1929*, Transportation Research Board, National Research Council, Washington, D.C., pp. 208-217.

Celaya, M., Nazarian, S. (2006). "Seismic testing to determine quality of hot-mix asphalt", *Transportation Research Record 1946*, Transportation Research Board, National Research Council, Washington, D.C., pp. 113-122.

Dongre, R., Myers, L., D'Angelo, J., Paugh, C., Gudimettla, J. (2005). "Field evaluation of Witczak and Hirsch models for predicting dynamic modulus of hot-mix asphalt", *Journal of the Association of Asphalt Paving Technologists from the Proceedings of the Technical Sessions*, Vol. 74, 2005.

Dougan, C.E., Stephens, J.E., Mahoney, J., Hansen, G. (2003). "E\* dynamic modulus – test protocol – problems and solutions", Report No. CT-SPR-0003084-F-03-3, Connecticut Transportation Institute, University of Connecticut, Storrs, Connecticut.

Hadidi, R., Gucunski, N., Zaghoul, S., Vitillo, N., Shoukouhi, P. (2006). "Development of paving layer moduli temperature correction models for seismic pavement analyzer (SPA) in New Jersey", The 85<sup>th</sup> Transportation Research Board Annual Meeting, Washington, D.C., January 22-26.

Hakim, B., Brown, S.F. (2006). "Pavement analysis using the FWD: Practical difficulties and proposed simplifications", 10<sup>th</sup> International Conference on Asphalt Pavement, International Society of Asphalt Pavements, Quebec, Canada, August 12-17.

Heisey, J.S., Stokoe II, K.H., and Meyer, A.H. (1982). "Moduli of pavement systems from spectral analysis of surface waves", Transportation Research Record 852, Transportation Research Board, National Research Council, Washington, D.C., pp. 22-31.

Jones, R. (1955). "A vibration method for measuring the thickness of concrete road slabs in situ", Magazine of Concrete Research, Vol 7, No. 20, pp.97-102.

Kweon, G., Kim, Y.R. (2006). "Determination of asphalt concrete complex modulus with impact resonance test", Transportation Research Record 1970, Transportation Research Board, National Research Council, Washington, D.C., pp. 151-160.

Mirza, M.W., Witczak, M.W. (1995). "Development of a global aging system for short and long term aging of asphalt cements", Annual Meeting of the Association of Asphalt Paving Technologists, The Association of Asphalt Paving Technologists, March, pp. 393-430.

National Cooperative Highway Research Program (NCHRP) (2004). "Guide for mechanistic-empirical design of new and rehabilitated pavement structures" NCHRP 1-37A Design Guide, Washington, D.C., <http://www.trb.org/mepdg/guide.htm> [Accessed 25 January 2010].

Nazarian, S., Stokoe II, K. H., Hudson, W.R. (1983). "Use of Spectral Analysis of Surface Waves Method for Determination of Moduli and Thicknesses of Pavement Systems", Transportation Research Record 930, Transportation Research Board, National Research Council, Washington, D.C., pp. 38-45.

Nazarian, S., Yuan, D., Tandon, V. (1999). "Structural field testing of flexible pavement layers with seismic methods for quality control", Transportation Research Record 1654, Transportation Research Board, National Research Council, Washington, D.C., pp. 50-60.

Park, C.B., Miller, R.D., and Xia, J. (1998). "Imaging dispersion curves of surface waves on multi-channel record", Kansas Geological Survey, 68<sup>th</sup> Annual International Meeting of the Society of Exploration Geophysicists, Expanded Abstracts, pp. 1377-1380.

Park, C.B., Miller, R.D., and Xia, J. (1999). "Multimodal analysis of high frequency surface waves", Proceedings of the Symposium of Applied Geophysics in Engineering and Environmental Problems (SAGEEP 1999), Oakland, CA, pp.115-121.

Park, D., Buch, N., Chatti, K. (2001). "Effective Layer Temperature Prediction Model and Temperature Correction via Falling Weight Deflectometer Deflections", Transportation Research Record 1764, Transportation Research Board, National Research Council, Washington, D.C., pp. 97-111.

Pellinen, T.K., Witzak, M.W., and Bonaquist, R.A. (2004). "Asphalt mix master curve construction using sigmoidal fitting function with non-linear least squares optimization", *Recent Advances in Materials Characterization and Modeling of Pavement Systems*, American Society of Civil Engineers Geotechnical Special Publication No. 123, pp. 83-101.

Roesset, J.M., Chang, D.W., Stokoe II, K.H., Aouad, M. (1990). "Modulus and thickness of the pavement surface layer from SASW tests", *Transportation Research Record 1260*, Transportation Research Board, National Research Council, Washington, D.C., pp. 53-63.

Rowe, G.M., Sharrock, M.J. (2011). "Alternate shift factor relationship for describing temperature dependency of viscoelastic behavior of asphalt materials", *Transportation Research Record 2207*, Transportation Research Board, National Research Council, Washington, D.C., pp. 125-135.

Ryden, N., Park, C.B., Ulriksen, P., and Miller R.D. (2003). "Lamb wave analysis for non-destructive testing of concrete plate structures ", *Proceedings of the Symposium on the Application of Geophysics to Engineering and Environmental Problems (SAGEEP 2003)*, San Antonio, TX, April 6-10, INF03.

Ryden, N., Park, C.B., Ulriksen, P., and Miller, R.D. (2004). "Multimodal Approach to Seismic Pavement Testing", *Journal of Geotechnical and Geoenvironmental Engineering*, Vol. 130, No. 6, pp. 636-645.

Ryden, N., Park, C.B. (2006). "Fast simulated annealing inversion of surface waves on pavement using phase-velocity spectra", *Geophysics*, Vol. 71, No. 4, pp. R49-R58.

Ryden, N. (2011). "Resonant frequency testing of cylindrical asphalt samples", *European Journal of Environmental and Civil Engineering*, Vol. 15, No. 4, pp. 587-600.

Singh, D., Zaman, M., Commuri, S. (2012). "Evaluation of dynamic modulus of modified and unmodified asphalt mixes for different input levels of the MEPDG", International Journal of Pavement Research and Technology, Chinese Society of Pavement Engineering, Vol. 5, No.1, pp. 1-11.

Walubita, L.F., Alvarez, A.E., Simate, G.S. (2011). "Evaluating and comparing different methods and models for generating relaxation modulus master-curves for asphalt mixes", Construction and Building Materials, Vol. 25, pp. 2619-2626.

Witczak, M.W., and Bari, J. (2004). "Development of a E\* master curve database for lime Modified Asphaltic Mixtures", <http://www.lime.org/Publications/MstrCurve.pdf>

Yuan, D., Nazarian, S., Chen, D.-H., Hugo, F. (1998). "Use of seismic pavement analyzer to monitor degradation of flexible pavements under Texas mobile load simulator", Transportation Research Record 1615, Transportation Research Board, National Research Council, Washington, D.C., pp. 3-10.

Zhu, H., Sun, L., Yang, J., Chen, Z., Gu, W. (2011). "Developing master curves and predicting dynamic modulus of polymer-modified asphalt mixtures", ASCE Journal of Materials in Civil Engineering, Vol. 23, No. 2, pp. 131-137.

## **CHAPTER 5      PAPER 3: IN-SITU ASPHALT MASER CURVE CONSTRUCTION USING NON-DESTRUCTIVE TESTING TECHNIQUES**

Edmund Surette, Christopher Barnes, Nouman Ali

Based on : Paper to be submitted to NDT&E International

### **5.1 ABSTRACT**

The MEDPG recommends falling weight deflectometer (FWD) testing in combination with construction of the complex modulus master curve using the predictive equation for in-situ asphalt concrete characterization. If there is adequate asphalt concrete thickness, asphalt cores may be tested using AASHTO TP 62 to determine the dynamic modulus and construct the master curve. Both the predictive equation and AASHTO TP62 require destructive core extraction and can be too costly for many agencies. Recently, the Multi-Channel Analysis of Surface Waves (MASW) technique has provided accurate non-destructive estimates of the in-situ asphalt concrete modulus, however the measured moduli need to be corrected to a conventional design frequency using the master curve. MASW data provides dynamic modulus values at much higher reduced frequencies than conventional testing, generally constituting only the upper two thirds of the master curve, while FWD determined moduli values generally constitute the lower portion of the curve. It was shown in this research that when MASW and FWD testing are performed in tandem over a range of temperatures it is possible to construct an in-situ non-destructive master curve that may then be used to correct the MASW data for enhancing the FWD backcalculation process or to seed the asphalt concrete modulus directly. In circumstances where FWD test data may not be available, i.e. thin pavements, and a non-destructive process to shift MASW data is required, a standard equation was established, however as with the master curve it is heavily influenced by material type.

## **5.2 KEYWORDS**

Keywords: asphalt concrete; dynamic modulus; master curve; non-destructive testing, damage.

## **5.3 INTRODUCTION**

Many highway agencies are in the process of implementing the Guide for the Mechanistic-Empirical Design of New and Rehabilitated Pavement Structures (MEPDG). The implementation of the guide is expected to improve on current pavement analysis and design procedures and to ultimately improve pavement performance. Some of the key components of the MEPDG design approach include the necessity to fully characterize the materials encompassing the pavement structure and the use of a hierarchical system to select or determine a particular design input. For flexible pavements, the dynamic modulus ( $E^*$ ) of the asphalt concrete layer is a mandatory input at all three hierarchical levels due to its influence on the prediction of the strains and displacements under loading required for analysis. Due to the viscoelastic nature of asphalt concrete, the asphalt master curve is also required to characterize the dynamic modulus over a wide range of frequencies at a given reference temperature and allows for the translation of modulus values when testing has been performed at multiple loading frequencies and test temperatures. There are three basic ways to obtain the asphalt concrete dynamic modulus, laboratory, in-situ testing, or the use of predictive stiffness models. To characterize the asphalt concrete in-situ, Hierarchical Level 1 requires falling weight deflectometer (FWD) testing to backcalculate the asphalt concrete modulus and the use of field cores to establish mix volumetric parameters to input into the predictive equation. In practice, if the asphalt concrete layer is thick enough, cores can be used to conduct the dynamic modulus test (AASHTO TP 62) to determine the dynamic modulus and characterize the master curve.

For many agencies, the use of the FWD has become an integral part in evaluating the structural adequacy of pavements. However, cores need to be extracted either to perform AASHTO TP 62 testing or to determine mixture volumetric parameters for the predictive equation to successfully characterize the asphalt concrete using the master curve. FWD testing records a global structural response that is influenced by the entire pavement structure and does not specifically target the asphalt concrete layer. As a result, FWD deflections are commonly utilized for computing the moduli of all the pavement layers. In addition, there are several factors including variation in layer thicknesses, the presence of bedrock or a highly non-linear subgrade, thin asphalt layers, edge restraint, and seasonal characteristics that can influence and complicate the backcalculation process and alter the results obtained (Ullidtz and Stubstad, 1985)(Chang et al., 1992)(Hasim et al., 1994)(Irwin, 2002)(Hakim and Brown, 2006) . For design, the FWD backcalculated moduli values computed at a measured temperature must be corrected to a typical reference temperature. Consequently there has been considerable research conducted to determine temperature prediction models and correction factors for the FWD (Park et al., 2001), but the MEPDG recommends using the master curve for temperature correction.

To construct the master curve by means of AASHTO TP 62 or by using the predictive equation, asphalt cores need to be extracted from the roadway which is a destructive process that can result in cracking, potholes and moisture infiltration when repaired incorrectly. Both AASHTO TP 62 and the testing involved in determining the mixture volumetric parameters for the predictive equation are time consuming and can yield a significant expense to transportation agencies. AASHTO TP 62 testing requires sophisticated and expensive testing equipment which may not be available to all transportation agencies and has been recognised therefore as being too prohibitive for routine master curve development (Dougan et al., 2003)(Bonaquist and Christensen, 2005)(Kweon and Kim, 2006).

Besides FWD, there are a number of seismic tests including Multichannel Analysis of Surface Waves (MASW) (Barnes and Trottier, 2009), the portable seismic pavement analyzer (PSPA) (Nazarian et al., 2005)(Celaya and Nazarian, 2006)(Oh et al., 2012), and



resonance frequency measurements (Kweon and Kim, 2006)(Ryden, 2011)(Van Velsor et al., 2011)(Gudmarsson et al., 2012a) that can be used to determine the asphalt concrete modulus over a broad frequency range. The PSPA (Oh et al., 2012) and MASW (Barnes and Trottier, 2010) have been used successfully to determine the asphalt concrete modulus in-situ. MASW has proven (Park et al., 1999) to be an effective technique of developing Lamb wave dispersion curves, where phase velocity is plotted vs. frequency and used to highlight various wave modes within the measured wave field. Literature has shown (Ryden et al., 2004)(Barnes and Trottier, 2009) that at wavelengths less than the asphalt concrete thickness, the dominant wave modes tend to follow the fundamental anti symmetric Lamb wave mode that occurs in a free plate, and therefore by identifying and tracking the approximate fundamental Lamb wave modes which asymptotically approach the fundamental Rayleigh wave mode, the velocity dispersion curve can provide a singular velocity for each sampled frequency. Basic Rayleigh wave theory relates this phase velocity to the asphalt concrete modulus, density and Poisson's ratio as described in Equation (14). Once the phase velocities have been determined they may be converted to modulus values to form a plot of modulus versus frequency or wavelength.

The difference between moduli as determined via FWD and seismic methods exist in the loading frequency. Moduli values obtained using seismic methods are based on high-rate, low-magnitude strain values (high frequency, 5 to 90 kHz), compared to vehicular traffic and FWD which cause higher magnitude deformation at low-strain rates (low frequency, 10 to 25 Hz). Measured seismic moduli require temperature and frequency correction if they are to be used in pavement analysis and design. There has been considerable research conducted to determine temperature prediction models and correction factors for the FWD (Park et al., 2001), but due to the high frequency content of the seismic methods, the correction factors developed for FWD are ineffective. The MEPDG recommends using the master curve for temperature correction, however the master curve has also proven to be a valuable tool for shifting higher frequency surface wave moduli down to lower frequency design values (Bai, 2004)(Celaya and Nazarian, 2006)(Barnes and Trottier, 2009)(Oh et al., 2012). As shown (Ryden, 2011)(Van Velsor et al., 2011) seismic testing performed at a multitude of test temperatures provides dynamic modulus values at a wide

range of reduced frequencies, predominantly at higher reduced frequencies that can be produced by traditional test methods. As described in Chapter 4, constructing the master curve by incorporating seismic data provides a broader range of reduced frequencies that enhances the overall master curve and is extremely important when correcting seismic moduli for use in design. However, to construct a master curve solely using seismic determined dynamic modulus data could be challenging as the lower frequency content required to fully characterize the curve is unavailable (Kweon and Kim, 2006, Lacroix et al., 2009)(Ryden, 2011)(Gudmarsson et al., 2012b).

One of the primary concerns that highway agencies share is the capability to adequately characterize their pavement materials. In many cases, the asphalt concrete mixture parameters required in the MEPDG are unknown since the pavement structures that are currently in service were constructed several years prior to making the decision to adapt a newer pavement design system. The ability to characterize the asphalt master curve in-situ would be extremely useful and therefore this paper focuses on combining in-situ FWD and MASW testing to determine the dynamic modulus over a full range of frequencies and temperatures needed to construct a master curve. As part of their testing protocol, many highway agencies, such as the Nova Scotia Department of Transportation and Infrastructure Renewal (NSTIR) perform seasonal FWD testing on some of the roadways to characterize the seasonal variations in the pavement structure. NSTIR currently has 18 test sites, one in each county, where they have been conducting seasonal FWD testing. One of the concerns is that there is no historical data for the asphalt concrete, however cores could be used to establish volumetric parameters. Implementing MASW testing in tandem with FWD testing would provide the data necessary to construct an in-situ master curve for shifting the higher frequency MASW modulus data to a lower frequency value for use in design directly or for enhancing the FWD backcalculation process. In the case of pavements with thin asphalt concrete layers, it could also provide a seed modulus so that the underlying materials can be of direct focus. In addition, if data is routinely collected over the life of the pavement, having the capability to construct the master curve using in-situ data provides the opportunity to establish an in-situ “damaged” master curve as was observed during the course of testing for this particular project.

For cases where FWD data may not be available to provide lower frequency asphalt concrete modulus values for the master curve construction, the predictive equation may be required in tandem with MASW (Lacroix et al., 2009). However, if the materials are indeed similar and the agency wants to establish the master curve non-destructively (no core extraction), the data collected from a calibration site located near the vicinity of the actual test location may be used to establish a master curve for shifting data. In an effort to simplify the correction procedure, a standard equation was established based on the master curve. The concern with a standard equation, as with traditional master curve construction, is that the local materials such as aggregate type (Ping and Xiao, 2007) and pavement age can play a significant role in the master curve parameters. In Nova Scotia for example, the PG binder grade is generally consistent throughout the province, however there is an abundance of quality aggregate sources routinely used in construction yet may vary widely in modulus values.

#### **5.4 FIELD AND LABORATORY TESTING**

As part of a multiyear research effort between Dalhousie University, provincial governments and local industry, four 200 metre in-service highway test sections were selected throughout Nova Scotia and New Brunswick, Canada; Highway 103 near Barrington, Nova Scotia; Highway 103 near Tantallon, Nova Scotia; Trunk 2 near Bass River, Nova Scotia; and, Route 8 near Miramichi, New Brunswick. The Barrington and Miramichi test sites were utilized for the majority of the work described in this study. Both highway sections were newly constructed in the fall of 2006 and were instrumented with moisture and temperature sensors during construction. The asphalt concrete mixtures used at the Barrington test site were designed using the Marshall Method and specified to meet the Nova Scotia Department of Transportation and Infrastructure Renewal Specification which required a type B-HF asphalt at a spread rate of 250 kg/m<sup>3</sup> and a type C-HF at a rate of 110 kg/m<sup>3</sup>. The B-HF asphalt concrete mixture design contained 5.1% PG58-28 asphalt binder and exhibited 4.0% air voids at 75 blows compactive effort, while the C-HF was

designed with 5.3% PG58-28 asphalt binder and 4.0% voids. The Miramichi test section was designed using the Superpave mix design method as per the New Brunswick Department of Transportation Specification having two lifts of Type B asphalt using 4.7% PG58-34 asphalt binder at a spread rate of 115 kg/m<sup>3</sup>, and one lift of Type D with 5.8% PG58-34 at 85 kg/m<sup>3</sup>, both designed to have 4.0% air voids at 100 gyrations.

The binder specifications and the volumetric design of the asphalt mixture established during design and construction of both test sites were implemented into the MEPDG dynamic modulus predictive equation (NCHRP, 2004), which is based on the Witczak predictive equation (Bari and Witczak, 2005) and was used to predict dynamic modulus values over a range of frequencies, temperatures, and aging to construct the predictive master curve. The dynamic modulus for Hierarchical Level 2 input is determined directly from the predictive equation using specific laboratory binder test and mix data. The MEPDG version (NCHRP, 2004) of the Witczak Predictive Equation is shown in Equation (15).

Approximately one month after the roadways were open to traffic, drilled asphalt concrete core specimens were obtained from both test sites to confirm the asphalt concrete thickness and to perform laboratory dynamic modulus testing as per AASHTO TP 62. AASHTO TP 62 testing was conducted on a servo hydraulic testing machine using the cylindrical core specimens and subjected to a sinusoidal axial compressive load at a range of temperatures (~ -18, 0, 10, 21, 40 C) and loading frequencies (0.1, 1, 5, 10, 25 Hz). Using the principle of time-temperature superposition, the dynamic modulus values were then used to construct the E\* master curve using the sigmoidal function, Equation (10) as described in the MEPDG (NCHRP, 2004). The measured dynamic modulus results at various temperatures and frequencies were shifted to a reduced frequency at an arbitrarily selected reference temperature of 21°C, as shown in Equation (16). For this study, the shift factors were represented as a second order polynomial function of the temperature, T (Witczak and Bari, 2004) as shown in Equation (12).

During construction, temperature probes were installed at the top of the subgrade, and in the middle of the base and subbase granular layers, in addition to a time-domain reflectometry (TDR) probe used to measure moisture at the top of the subgrade. The instrumentation installation permitted an accurate measurement of the granular pavement layer thicknesses at each test location. Once construction was complete, Ground Penetrating Radar (GPR) was also used to determine the pavement layer thicknesses over the entire 200 metre pavement sections to provide a continuous thickness profile for supplementing the FWD backcalculation (Maser et al., 2006)(Willett et al., 2006).

Field testing which incorporated FWD and MASW methods began once construction was complete and continued periodically for several years as shown in Table 11. FWD testing was performed in the outer wheel path at ten-meter increments along the 200-meter test section, while MASW testing was generally performed at two of the FWD test locations. It was observed that during certain periods within the yearly cycle there was a significant reduction in asphalt concrete modulus, as determined via both MASW and FWD testing. The reduction in modulus generally occurred during the fall, winter, and early spring (October – April). Consequently, once observed, testing was also performed along the center lane in addition to the outer wheel path for comparison purposes.

MASW data was collected using the multichannel simulation with one receiver (MSOR) approach described by Barnes and Trottier (2009) using an Olsen Instruments Freedom Data PC incorporating a 1 MHz National Instruments data acquisition board with an Impact Echo test head consisting of a 100 kHz displacement transducer as the receiver. The impact was generated using a high frequency impactor (80 – 90 kHz) consisting of a stainless steel A-6 autoharp string housed in an aluminum block with a rubber membrane lining the bottom. A one cm wide 24-gauge sheet metal strip was bonded to the asphalt surface with an epoxy to provide consistent spectral content in the impact generated surface waves. A magnetically mounted 15 kHz accelerometer was placed at each impact location to trigger data collection and data was recorded at 20 offset positions from the receiver, ranging from three to 22 centimetres. Due to the viscoelastic nature of the asphalt concrete, testing at lower temperatures produced higher ranges of maximum coherent frequency (10

– 90 kHz), while at higher temperatures it was difficult to achieve maximum coherent frequencies above 50 kHz (10 – 40 kHz). Using a Matlab analysis program developed by Barnes (2008), the phase velocity dispersion curves were constructed by tracking the fundamental anti symmetric Lamb wave mode. The phase velocities were then used to compute the moduli values at different frequencies using Equation (14) and by incorporating the measured density and the Poisson’s ratio, which varied with the test temperature as described in Table 2.2.14 of the MEPDG (NCHRP, 2004).

Table 11 Field testing dates.

| Barrington     |      | Miramichi     |      |
|----------------|------|---------------|------|
| FWD            | MASW | FWD           | MASW |
| December 2006  | -    | February 2007 |      |
| February 2007  |      | April 2007    | -    |
| April 2007     |      | May 2007      |      |
| June 2007      |      | June 2007     |      |
| September 2007 |      | August 2007   |      |
| November 2007  |      | October 2007  | -    |
| January 2008   |      | April 2008    | -    |
| April 2008     |      | December 2008 |      |
| September 2008 |      | November 2009 |      |
| November 2008  | -    |               |      |
| December 2008  |      |               |      |
| March 2009     |      |               |      |

FWD testing was performed using a Dynatest model 8082 Heavy weight deflectometer (HWD). The HWD was equipped with a 300 mm diameter segmented loading plate and geophones mounted at off-set distances from the load center of 0, 200, 300, 450, 600, 900, 1200, 1500, and 1800 mm. The loading sequence generally included three seating drops of approximately 30 kN, four 40 kN drops, a 53.4 kN drop and a 71.2 kN drop. The fourth 40 kN load was used for the backcalculation analysis which was conducted using the deflection basin fit option of ELMOD 5 and incorporated the GPR determined thicknesses for all the pavement layers. During field testing, the temperature at mid-depth (50-60 mm)

of the asphalt concrete layer was measured using a temperature probe inserted into a water-filled hole and used as the average temperature for moduli backcalculation and MASW analysis. Once the field testing data was analyzed, the MASW and FWD analyzed moduli were then used to construct master curves in combination with the AASHTO TP 62 test data, non-destructive data only master curves, and master curves constructed using the predictive equation.

To construct damaged master curves, both the procedure outlined in the MEPDG and by Seo et al. (2012) were implemented. The procedure outlined in the MEPDG to construct an in-situ damaged master curve is described below (NCHRP, 2004):

- 1) Conduct FWD testing in the outer wheel path and backcalculate the asphalt concrete modulus ( $E_i$ ) for the project, combining layers of similar properties and including areas that are both cracked and uncracked.
- 2) Perform field coring to determine the mix volumetric parameters and asphalt viscosity parameters for implementing the predictive equation.
- 3) Develop the undamaged master curve using the predictive equation and the parameters established in Step 2.
- 4) Estimate damage  $d_j$  using Equation (28) below:

$$d_j = \frac{E_i}{E^*} \quad (28)$$

Where,  $E_i$  is the backcalculated modulus at a given temperature recorded in the field, and  $E^*$  is the predicted modulus at the same temperature established from the predictive equation.

- 5) Determine  $\alpha'$  using Equation (29) below:

$$\alpha' = (1 - d_j)\alpha \quad (29)$$

- 6) Determine the damaged master curve implementing  $\alpha'$  instead of  $\alpha$  in the predictive equation.

Recently, Seo et al. (2012) suggested the use of Equation (30) provided below to determine  $\alpha'$  based on FWD data.

$$\alpha' = (\log(E_{FWD}) - \delta) \times (1 + e^{\theta_{FWD}}) \quad (30)$$

Where,

$$\theta_{FWD} = a_1 T^3 + a_2 T^2 + a_3 T + a_5 - 0.4759, \quad (31)$$

T is the temperature, and for a PG58-22 binder,  $a_1 = -6.886E-06$ ,  $a_2 = 2.741E-04$ ,  $a_3 = 4.629E-02$ , and  $a_5 = -1.949E+00$ . There are no coefficients provided for a PG58-28 binder.

## 5.5 DATA ANALYSIS AND DISCUSSION

Dynamic modulus values were computed at a range of loading frequencies and temperatures using the predictive equation, laboratory AASHTO TP 62 testing, and in-situ FWD and MASW testing. AASHTO TP 62 testing was conducted on ten asphalt concrete core samples from the Barrington test site at temperatures of -18.5, -0.5, 10.5, 21, and 40°C and loading frequencies of 0.1, 1, 5, 10, and 25 Hz, while four asphalt concrete cores from the Miramichi test site were tested at temperatures of -19.0, -0.5, 12, 21, and 47°C and loading frequencies of 0.1, 1, 5, 10, and 25 Hz. There were slight variations in the testing temperatures due to fluctuations with the temperature control chamber.

The FWD deflection data collected at multiple temperatures was backcalculated to compute the moduli of all the pavement layers and the FWD testing frequency was determined to be 16.3 Hz using Equation (32) (Lytton et al., 1990),

$$f = \frac{1}{2(\Delta t)} \quad (32)$$

where  $\Delta t$  = FWD loading time difference obtained from time history data. The MASW data collected at multiple temperatures resulted in plots of phase velocity vs. frequency as shown in Figure 17. The phase velocities were later converted to moduli values using Equation (14), providing moduli values at frequencies ranging between 10 and 90 kHz



depending on the test temperature. As expected, the moduli values increased slightly with increased frequency due to the viscoelastic nature of the asphalt concrete.

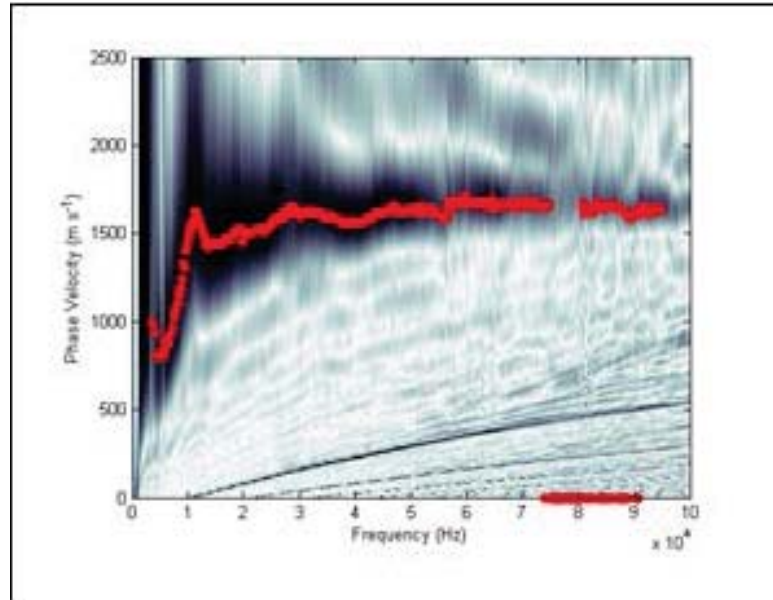


Figure 17 Phase-velocity dispersion curve Barrington site.

Once all of the dynamic modulus values were computed using the various test methods and analysis techniques, undamaged master curves were constructed using the sigmoidal function and shift factor function described above using predictive data, AASHTO TP 62 data, a combination of AASHTO TP 62, FWD and MASW data, solely from FWD and MASW data, and MASW data in combination with predictive data at 40°C. It was observed during data collection and processing that some of the non-destructive test data exhibited signs of damage which is discussed later in the chapter. The predictive equation and AASHTO TP 62 master curves were established as undamaged master curves, therefore for comparison purposes as a viable construction technique, the non-destructive master curves were constructed using data regarded as undamaged.

The master curves were constructed by simultaneously solving the four coefficients of the sigmoidal function ( $\delta$ ,  $\alpha$ ,  $\beta$ ,  $\gamma$ ) and the coefficients of the polynomial function ( $a$ ,  $b$ ,  $c$ ) by optimizing the theoretical model to fit the experimental data by adjusting the coefficients

using the “Solver” function in Excel until the least square error between measured and predicted moduli was minimized. The resulting coefficients of the master curve sigmoidal function and shift parameters for both test sites are listed in Table 12, and the fitted master curves are shown in Figure 18. The master curve using MASW and predictive data for the Miramichi Test Site could not be constructed as the solver function could not converge on a solution. In addition, for the construction of the combined AASHTO TP 62 and non-destructive data master curve, the MASW data incorporated all of the coherent data points from the full range of test frequencies (10 – 90 kHz depending on temperature). However, for computation of the non-destructive only master curve, to allow the “Solver” function to converge on a solution, the number of MASW data points needed to be reduced by averaging the coherent frequency values in 10 kHz segments, i.e., 20 - 30, 30 – 40, 40 – 50 kHz.

Table 12 Master curve parameters.

| Construction Technique     | Master Curve Parameters |          |         |          |         |         |        |
|----------------------------|-------------------------|----------|---------|----------|---------|---------|--------|
|                            | $\delta$                | $\alpha$ | $\beta$ | $\gamma$ | a       | b       | c      |
| <b>Barrington</b>          |                         |          |         |          |         |         |        |
| <b>TP 62</b>               | -1.7428                 | 6.1904   | -1.4679 | 0.3006   | -0.0003 | -0.1060 | 2.3593 |
| <b>TP 62 / MASW / FWD</b>  | 0.5530                  | 3.8625   | -0.8807 | 0.3438   | 0.0000  | -0.1050 | 2.2252 |
| <b>MASW / FWD</b>          | 0.2510                  | 4.1457   | -0.9655 | 0.3605   | -0.0005 | -0.0843 | 2.0124 |
| <b>MASW / Predictive</b>   | 0.2604                  | 4.1459   | -0.8562 | 0.3752   | -0.0005 | -0.0798 | 1.8767 |
| <b>Predictive Equation</b> | 2.8881                  | 3.8492   | -0.6291 | 0.3134   |         |         |        |
| <b>Miramichi</b>           |                         |          |         |          |         |         |        |
| <b>TP 62</b>               | 1.7594                  | 2.6500   | -0.0866 | 0.4907   | -0.0001 | -0.1048 | 2.2388 |
| <b>TP 62 / MASW / FWD</b>  | -0.0239                 | 4.4926   | -0.9608 | 0.3337   | 0.0010  | -0.1258 | 2.1804 |
| <b>MASW / FWD</b>          | -0.0457                 | 4.4672   | -0.9413 | 0.3636   | 0.0017  | -0.1602 | 2.5923 |
| <b>Predictive Equation</b> | 2.8848                  | 3.9088   | -0.2422 | 0.3134   |         |         |        |

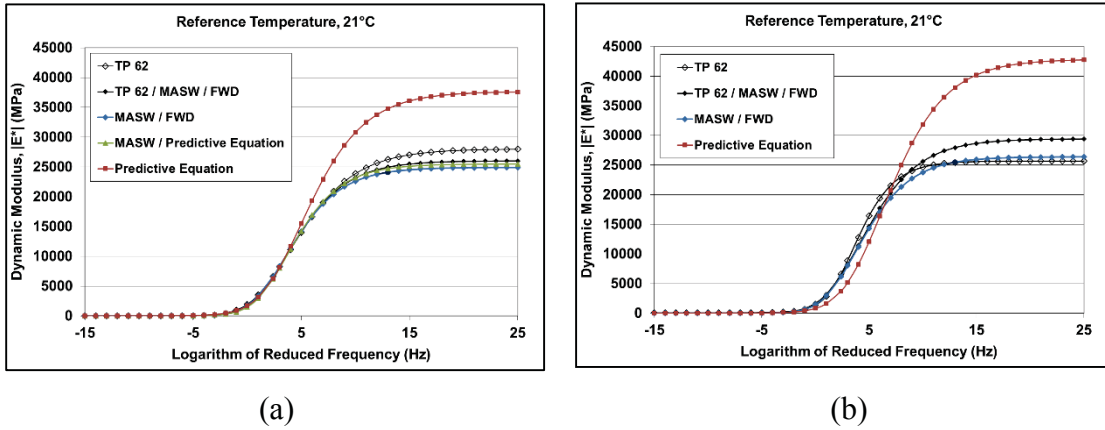


Figure 18 Constructed master curves; (a) Barrington Site, (b) Miramichi Site.

To compare the master curve construction techniques, the master curve obtained  $E^*$  and laboratory measured  $E^*$  values were plotted for each individual method and goodness of fit statistics were computed. Two statistics are provided, the coefficient of determination,  $R^2$  and the ratio of standard error to the standard deviation,  $S_e/S_y$ . In general, a high  $R^2$  ( $>0.9$ ) and low  $S_e/S_y$  ( $<0.35$ ) (Zhu et al., 2011) indicate excellent fitting of the master curve to the measured data. Therefore, reviewing the results provided in Figure 19 and Figure 20, the only master curve technique that does not provide acceptable results is the predictive equation. It was attempted to construct the master curve solely with MASW data given the range of test points, however the Solver Function in Excel could not converge on a solution due to the lack of data points in the lower range of reduced frequency.

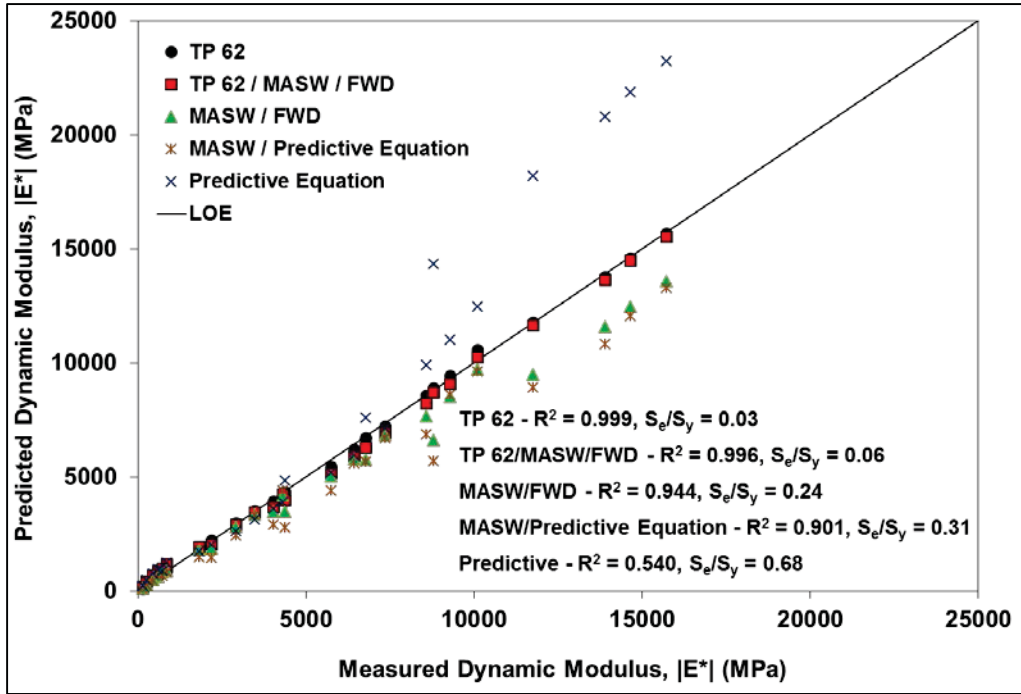


Figure 19 Plot of master curve versus laboratory  $E^*$  for Barrington.

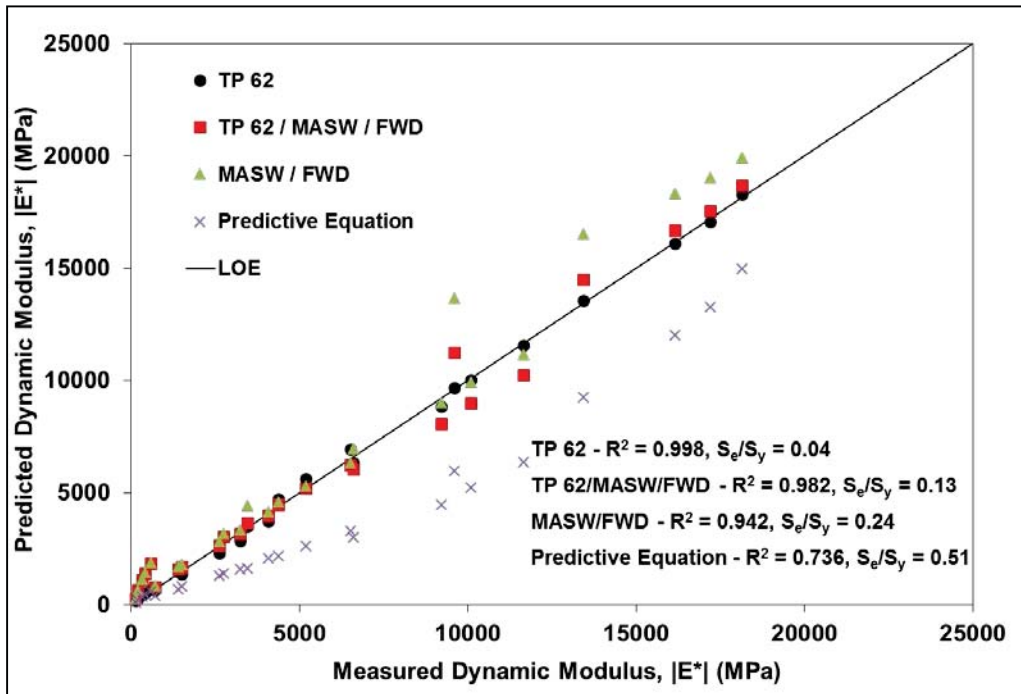


Figure 20 Plot of master curve versus laboratory  $E^*$  for Miramichi.

To better assess the non-destructive master curve construction technique for shifting high frequency dynamic modulus values collected at different temperatures, the individual master curves were used to shift high frequency MASW data at multiple test temperatures to reference frequencies of 10 and 25 Hz and a temperature of 21°C as listed in Table 13 and Table 14. The shifted dynamic modulus values were then compared to the measured AASHTO TP 62 dynamic modulus at the proposed reference temperature and frequencies by calculating the percentage Average Relative Error (ARE) using Equation (22).

Figure 21 and Figure 22 display the ARE for the frequency and temperature shifted dynamic modulus for each master curve construction technique. It can be seen from Figures 21 and 22 that the master curve constructed using the combination of AASHTO TP 62 and non-destructive test data provided the smallest overall ARE. The results also show that the master curves constructed with the non-destructive data provided better results than the AASHTO TP 62 constructed curves, validating the ability to construct master curves using only in-situ non-destructive data. The ARE for the for the Miramichi non-destructive curve was considerably higher than the Barrington non-destructive curve, however it is important to note that more data points were available for the Barrington curve. As one would expect, this indicates that an increased amount of non-destructive data increases the ability of constructing a viable master curve. The master curve constructed using the combination of MASW and predictive data did not provide acceptable results if used for design purposes due to the large ARE. As discussed in Chapter 4, the variability in corrected moduli can significantly influence design parameters.

Table 13 Frequency and temperature shifted dynamic modulus Barrington.

| Test Temperature (°C)   |                                | 4.3         | 5.5         | 7.5         | 9.0         | 21.3        | 22.0        | 28.0        | 31.0        | 32.0        | 34.0        | 39.0        | Average     |
|---|--------------------------------|-------------|-------------|-------------|-------------|-------------|-------------|-------------|-------------|-------------|-------------|-------------|-------------|
| Frequency and Temperature Shifted Dynamic Modulus,  E*  at 21°C and 10 Hz, 25Hz (MPa)<br>(%Error From Mean of Experimental Dynamic Modulus Value) | TP62 (10 Hz)                   | 3394 (2.2)  | 3377 (2.6)  | 3517 (1.4)  | 3380 (2.6)  | 3589 (3.4)  | 3455 (0.4)  | 3612 (4.1)  | 3601 (3.8)  | 3688 (6.3)  | 3658 (5.4)  | 3864 (11.4) | 3558 (4.0)  |
|   | TP62 (25 Hz)                   | 4159 (3.6)  | 4139 (4.1)  | 4310 (0.1)  | 4143 (4.0)  | 4398 (1.9)  | 4235 (1.8)  | 4426 (2.6)  | 4413 (2.3)  | 4519 (4.8)  | 4483 (3.9)  | 4735 (9.8)  | 4360 (3.5)  |
|   | TP62, MASW, FWD (10 Hz)        | 3383 (2.5)  | 3365 (3.0)  | 3500 (0.9)  | 3361 (3.1)  | 3506 (1.1)  | 3369 (2.9)  | 3449 (0.6)  | 3385 (2.4)  | 3446 (0.7)  | 3377 (2.7)  | 3401 (2.0)  | 3413 (2.0)  |
|   | TP62, MASW, FWD (25 Hz)        | 4169 (3.4)  | 4144 (3.9)  | 4309 (0.1)  | 4137 (4.1)  | 4303 (0.3)  | 4135 (4.1)  | 4228 (2.0)  | 4149 (3.8)  | 4224 (2.1)  | 4139 (4.1)  | 4169 (3.3)  | 4192 (2.8)  |
|   | MASW, FWD (10 Hz)              | 3368 (2.9)  | 3338 (3.8)  | 3456 (0.4)  | 3307 (4.7)  | 3378 (2.6)  | 3247 (6.4)  | 3339 (3.7)  | 3309 (4.6)  | 3383 (2.5)  | 3344 (3.6)  | 3532 (1.8)  | 3364 (3.4)  |
|   | MASW, FWD (25 Hz)              | 4186 (3.0)  | 4149 (3.8)  | 4296 (0.4)  | 4111 (4.7)  | 4200 (2.6)  | 4036 (6.4)  | 4151 (3.8)  | 4114 (4.6)  | 4206 (2.5)  | 4158 (3.6)  | 4391 (1.8)  | 4182 (3.4)  |
|   | MASW, Predictive (10 Hz)       | 2947 (15.0) | 2927 (15.6) | 3031 (12.6) | 2901 (16.4) | 2974 (14.3) | 2855 (17.7) | 2938 (15.3) | 2905 (16.3) | 2966 (14.5) | 2913 (16.0) | 3061 (11.8) | 2947 (15.0) |
|   | MASW, Predictive (25 Hz)       | 3743 (13.2) | 3717 (13.8) | 3849 (10.8) | 3685 (14.6) | 3777 (12.4) | 3626 (16.0) | 3731 (13.5) | 3690 (14.5) | 3767 (12.7) | 3700 (14.2) | 3887 (9.9)  | 3743 (13.2) |
|   | ME Predictive Equation (10 Hz) | 2448 (29.4) | 2486 (28.3) | 2628 (24.2) | 2558 (26.3) | 2850 (17.8) | 2854 (17.7) | 3040 (12.4) | 3008 (13.3) | 3063 (11.7) | 2915 (16.0) | 2872 (17.2) | 2793 (19.5) |
|   | ME Predictive Equation (25 Hz) | 3041 (29.5) | 3088 (28.4) | 3264 (24.3) | 3178 (26.3) | 3540 (17.9) | 3544 (17.8) | 3775 (12.5) | 3737 (13.4) | 3805 (11.8) | 3620 (16.1) | 3567 (17.3) | 3469 (19.6) |
| AASHTO TP 62 Determined Dynamic Modulus at 21°C and 10 Hz (MPa)   | 3469                           |             |             |             |             |             |             |             |             |             |             |             |             |
| 95% Confidence Interval (MPa)   | 3312 - 3626                    |             |             |             |             |             |             |             |             |             |             |             |             |
| AASHTO TP 62 Determined Dynamic Modulus at 21°C and 25 Hz (MPa)   | 4314                           |             |             |             |             |             |             |             |             |             |             |             |             |
| 95% Confidence Interval (MPa)   | 3781 - 4846                    |             |             |             |             |             |             |             |             |             |             |             |             |

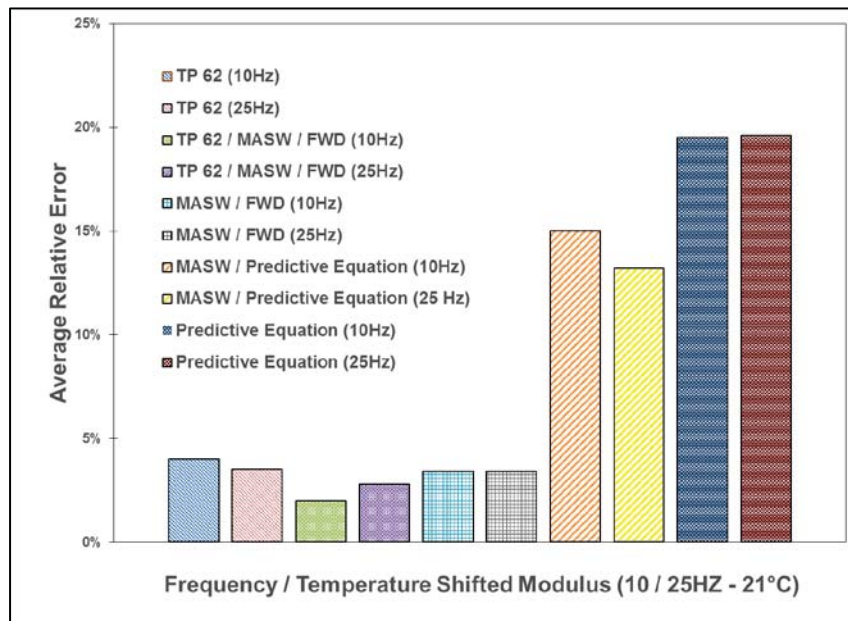


Figure 21 Average relative error for the frequency and temperature shifted E\* Barrington.

Table 14 Frequency and temperature shifted dynamic modulus Miramichi.

| Test Temperature (°C)   |                             | -5.0            | 7.1            | 7.5            | 35.0           | 39.1           | Average        |
|---|-----------------------------|-----------------|----------------|----------------|----------------|----------------|----------------|
| Frequency and Temperature Shifted Dynamic Modulus,  E*  at 21°C and 10 Hz, 25Hz (MPa)<br>(%Error From Mean of Experimental Dynamic Modulus Value) | TP 62 (10 Hz)               | 2783<br>(14.1)  | 2546<br>(24.4) | 2522<br>(22.2) | 3366<br>(3.9)  | 3846<br>(18.7) | 3013<br>(16.1) |
|   | TP 62 (25 Hz)               | 3622<br>(11.1)  | 3322<br>(18.7) | 3291<br>(19.4) | 4393<br>(7.5)  | 5019<br>(22.9) | 3932<br>(15.9) |
|   | TP 62, MASW, FWD (10 Hz)    | 3197<br>(1.3)   | 3145<br>(2.9)  | 3125<br>(3.6)  | 3237<br>(0.1)  | 3158<br>(2.5)  | 3172<br>(2.1)  |
|   | TP 62, MASW, FWD (25 Hz)    | 3997<br>(2.2)   | 3932<br>(3.7)  | 3906<br>(4.4)  | 4046<br>(1.0)  | 3948<br>(3.4)  | 3966<br>(2.9)  |
|   | MASW, FWD (10 Hz)           | 2917<br>(10.0)  | 2859<br>(11.8) | 2910<br>(10.2) | 2982<br>(8.0)  | 2814<br>(13.2) | 2896<br>(10.6) |
|   | MASW, FWD (25 Hz)           | 3707<br>(9.3)   | 3633<br>(11.1) | 3698<br>(9.5)  | 3788<br>(7.3)  | 3576<br>(12.5) | 3680<br>(9.9)  |
|   | Predictive Equation (10 Hz) | 1609<br>(50.3)  | 1754<br>(45.9) | 1753<br>(45.9) | 2573<br>(20.6) | 2668<br>(17.7) | 2071<br>(36.1) |
|   | Predictive Equation (25 Hz) | 20787<br>(49.1) | 2264<br>(44.6) | 2263<br>(44.6) | 3322<br>(18.7) | 3444<br>(15.7) | 2673<br>(34.5) |
| AASHTO TP 62 Determined Dynamic Modulus at 21°C and 10 Hz (MPa)   |                             | 3240            |                |                |                |                |                |
| 95% Confidence Interval (MPa)   |                             | 3073 - 3407     |                |                |                |                |                |
| AASHTO TP 62 Determined Dynamic Modulus at 21°C and 25 Hz (MPa)   |                             | 4085            |                |                |                |                |                |
| 95% Confidence Interval (MPa)   |                             | 3483 - 4687     |                |                |                |                |                |

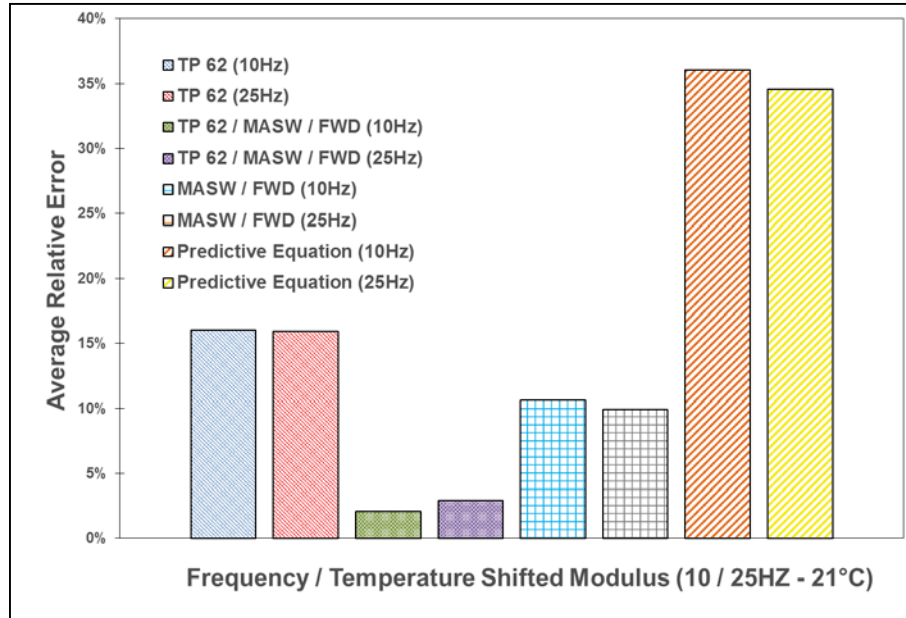


Figure 22 Average relative error for the frequency and temperature shifted E\* Miramichi.

In addition to comparing the capability of the non-destructive master curve for correcting MASW data to a useable design frequency, the master curve was used to correct FWD data for temperature in comparison to some of the standard equations generally used in practice. To compare some of the techniques currently used by local agencies, including the Long Term Pavement Performance (LTPP) Asphalt Temperature Adjustment Factor (ATAF) (Lukanen et al., 2000), and the Dynatest ELMOD 6 Standard SI Curve and Exponential Dependency Function (Dynatest, 2013), with the master curve construction techniques, the dynamic modulus data value at 21°C computed for the Barrington site was corrected using the various techniques to -0.5, 10.5, and 41°C and compared to the actual measured dynamic modulus. Since these functions are limited to FWD correction, the -18.5°C temperature was omitted and only the dynamic modulus values at 10 Hz and 25 Hz were used in the analysis. The results displayed in Figure 23 for the Barrington test site indicate that the moduli values corrected using the AASHTO TP 62 master curve, the combined and non-destructive only master curves, in addition to the LTPP ATAF function provide reasonable data correction. The results indicate that the ELMOD curves need to be calibrated for the local conditions. Equipment manufacturers specify the requirement for calibration and many agencies realize that these curves may need to be calibrated, but rarely take the initiative.

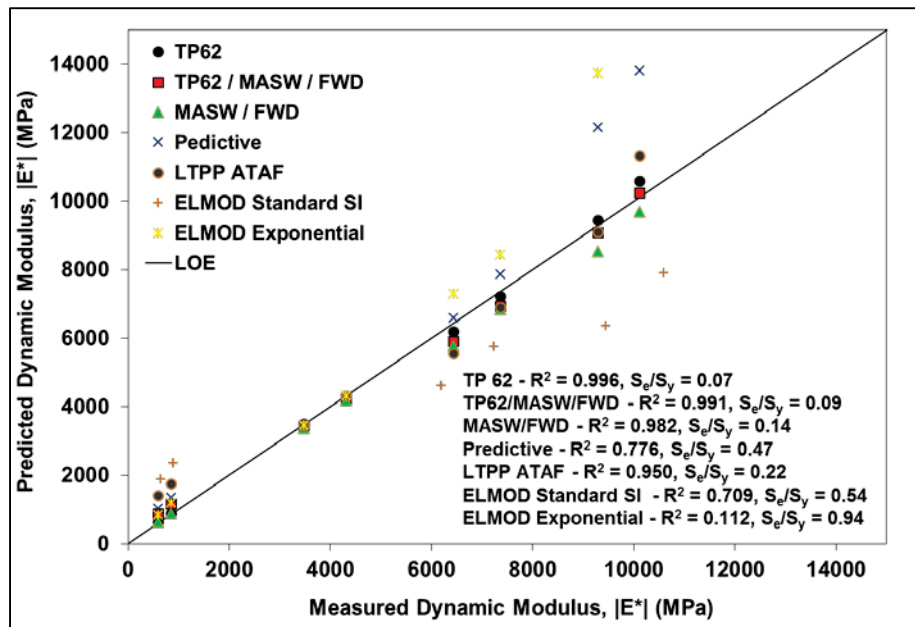


Figure 23 FWD temperature correction Barrington Site.



As previously stated, it was observed during non-destructive data collection and processing that during certain periods within the yearly cycle (October – April) there was a significant reduction in asphalt concrete modulus, noticeable with both MASW and FWD testing. This phenomena was more noticeable at the Barrington Test Site considering that there was significantly more testing performed than at the Miramichi Site. Check cracking was also noted at the Barrington Test Site immediately after construction. The results from all field testing conducted at the Barrington site are summarized on the plot located in Figure 24, which also provides the undamaged master curve constructed using AASHTO TP 62, MASW, and FWD data for reference.

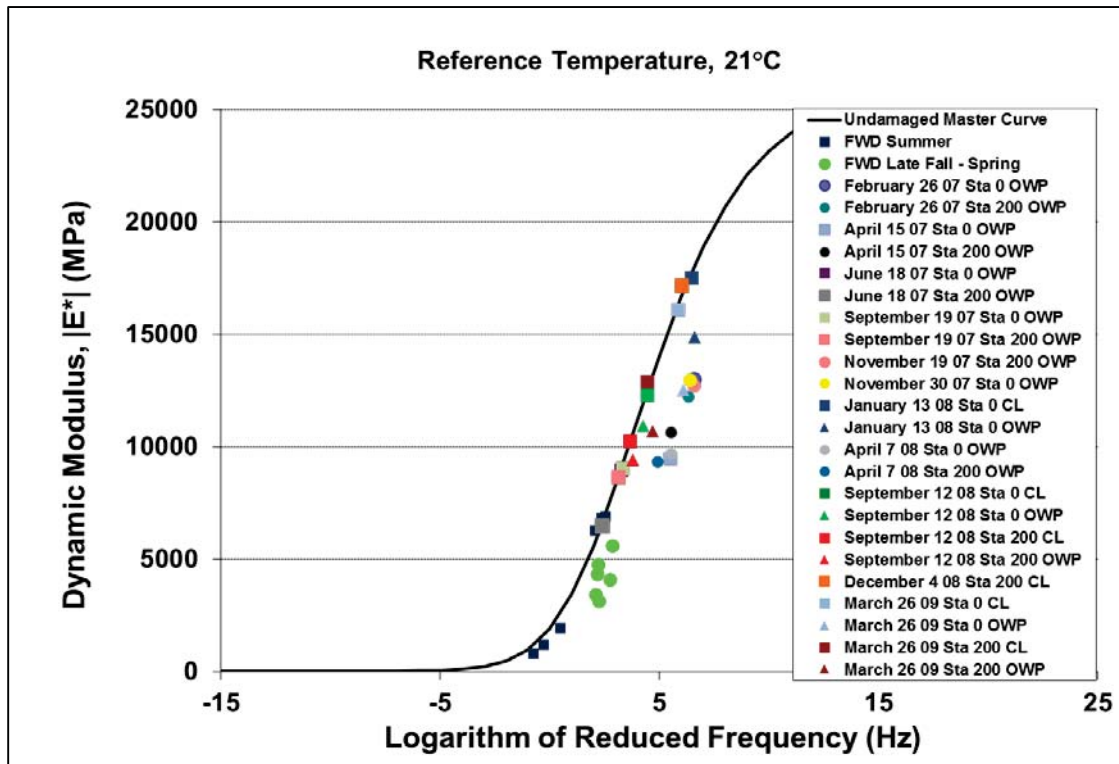


Figure 24 Summary of Seasonal Nondestructive Test Data.

The results displayed in Figure 24 indicate that the asphalt concrete exhibited signs of damage in the outer wheel path during the colder and wetter seasons, while “healing” to what would be considered an undamaged state through the summer. This phenomena was only noticeable in the outer wheel path as there was no reduction in modulus along the

center lane throughout the two year period. The healing effect, which may be attributed to moisture induced damage and fatigue damage, was not studied in this research, however the construction of an in-situ damaged master curve was endeavoured.

A damaged master curve was constructed for the Barrington Test Site using the MEPDG procedure and was compared to the in-situ measured damaged moduli, however the resulting master curve did not fit the field measured data as shown in Figure 25. The equation provided by Seo et al. (2012) (Equation (31)) was also assessed and did provide better results than the MEPDG approach, however they were still not satisfactory. The equation developed by Seo et al. (2012) did not provide coefficients for a PG58-28 binder and was constructed solely for FWD data, therefore an attempt was made to optimize the equation for local conditions and a combination of MASW and FWD data. It was observed during optimization that the equations developed using solely FWD data or solely MASW data were considerably different. The equation coefficients were established by plotting  $\theta_{FWD,MASW}$  versus temperature and performing a polynomial regression. Three sets of coefficients displayed in Table 15 were established, FWD only, MASW only, and FWD/MASW combined. The three experimental master curves developed using the derived equations are also provided in Figure 25 and indicate that the combination of FWD and MASW data provides more suitable results for the full range of test data.

The final evaluation involved constructing two damaged master curves using only the MASW and FWD data points. The first curve was constructed using a similar technique described by the MEPDG, where the undamaged master curve parameters were fixed except the  $\alpha$  parameter. In this case  $\alpha'$  was established and implemented in the damaged master curve. The second master curve was constructed similarly to the original non-destructive only master curve, where all four master curve parameters were solved using the damaged data points. As expected, looking at Figure 25, the master curves based on a combination of MASW and FWD data provide the best fit. Both curves concentrating on reducing the  $\alpha$  parameter of the sigmoidal function provide adequate results, however the master curve constructed to fit the damaged data by optimizing all of the function parameters produced the true in-situ damaged master curve for the season in question.

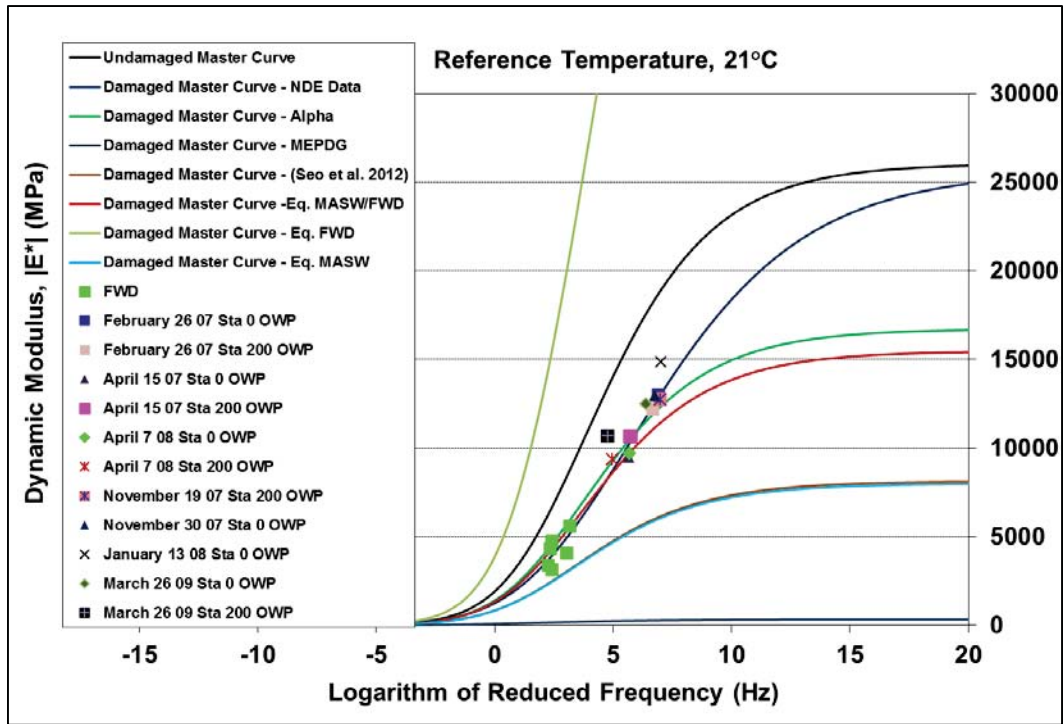


Figure 25 Constructed damaged master curves.

Table 15 Coefficients of the developed predictive equation for establishing  $\alpha'$  for a PG58-28 asphalt binder.

| Data Collection Technique | Coefficients of Equations |            |            |            |
|---------------------------|---------------------------|------------|------------|------------|
|                           | $a_1$                     | $a_2$      | $a_3$      | $a_5$      |
| FWD                       | -9.490E-05                | 8.346E-03  | -1.871E-01 | 1.804E-01  |
| MASW                      | -7.519E-04                | 1.956E-02  | -6.921E-02 | -2.891E+00 |
| FWD / MASW                | 1.971E-04                 | -1.101E-02 | 2.271E-01  | -3.309E+00 |

After analyzing all of the constructed master curves and observing the relatively poor results from the combined MASW and predictive data master curve, it was concluded that an alternative method should be available to transportation agencies for correcting MASW data for locations where FWD test data may not be available, i.e. locations with thin asphalt concrete layers. In an effort to simplify the correction of MASW data to a standard

temperature and design frequency for roadways located throughout Nova Scotia and New Brunswick, without the necessity of the in-situ constructed master curves, standard equations for both the Barrington and Miramichi sites were developed following a similar procedure as described by Oh et al. (2012), where a linear equation was developed to correct field measured PSPA values ranging between 12 and 39.5°C for a site in Florida. The equation developed by Oh et al. (2012) was assessed using data from both the Barrington and Miramichi test sites, however, as expected the equation did not provide satisfactory results, likely due to the differences in the local materials. In addition, the minimum allowable temperature would cause concern for data collection in Atlantic Canada, since the majority of collection may be conducted with temperatures ranging between 4 and 15°C.

Similarly to the method used in determining the master curve parameters, the equation parameters for this study were established by simultaneously solving the coefficients of the polynomial function by optimizing the theoretical model to fit the experimental data by adjusting the coefficients using the “Solver” function in Excel until the least square error was minimized. Multiple functions were assessed, however a cubic function provided the best solution. The standard equation is shown below in Equation (33) and the coefficients for each site are displayed in Table 16.

$$E^*_{MASW(Corrected)} = \frac{E^*_{MASW(Measured)}}{b_1T^3 + b_2T^2 + b_3T + b_4} \quad (33)$$

Table 16 Coefficients of standard equation.

| Site Location    | Coefficients of Equation |                |                |                |
|------------------|--------------------------|----------------|----------------|----------------|
|                  | b <sub>1</sub>           | b <sub>2</sub> | b <sub>3</sub> | b <sub>4</sub> |
| Barrington       | 1.013E-04                | -7.287E-03     | 6.415E-02      | 4.701E+00      |
| Miramichi        | 1.326E-05                | -1.223E-04     | -1.009E-01     | 6.072E+00      |
| Oh et al. (2012) | -                        | -              | 0.0538         | 0.9767         |

To assess the equations, data collected from the Highway 103 Tantallon site was corrected and compared to the master curve predicted values as shown in Table 17. As expected the standard equation developed from the Barrington site provided the best prediction, considering the asphalt concrete at the Tantallon site was constructed with the same PG58-28 binder grade and followed the same NSTIR specification. However, as stated in the introduction, the master curve and resulting standard equation developed for the Barrington site may be more relevant for roadways located in the southwest quadrant of the province since the aggregate source may be somewhat similar. Consequently, the overall assessment is that constructing the master curve non-destructively for each site evaluated will provide the best form of characterization.

Table 17 Frequency and temperature shifted dynamic modulus Tantallon.

| Test Temperature (°C)  |                     | 25.5           | 29.0           | Average        |
|--|---------------------|----------------|----------------|----------------|
| Frequency and Temperature Shifted Dynamic Modulus,  E*  at 21°C and 10 Hz (MPa) (%Error From Mean of Experimental Dynamic Modulus Value) | Barrington Equation | 4094<br>(3.9)  | 4107<br>(4.3)  | 4101<br>(4.1)  |
|  | Miramichi Equation  | 3699<br>(6.1)  | 3555<br>(9.8)  | 3627<br>(7.9)  |
|  | Jeong et al. 2012   | 5731<br>(45.5) | 4716<br>(19.7) | 5223<br>(32.6) |
| AASHTO TP 62 Determined Dynamic Modulus at 21°C and 10 Hz (MPa)  |                     | 3939           |                |                |

## 5.6 CONCLUSIONS

The main objective of this study was to determine if a master curve could be constructed from in-situ dynamic modulus values measured using non-destructive testing techniques and then if it could be implemented to properly shift MASW data to a reference design value. Testing was performed routinely on two test sites over a two year period to obtain

sufficient data for analyses. Based on the findings of this study, the following conclusions can be drawn:

- 1) MASW and FWD field measured dynamic modulus values collected at multiple temperatures may be used for generating the asphalt concrete master curve as opposed to traditional methods. An analysis was performed to evaluate the constructed master curve with standard AASHTO TP 62 testing and a combination of AASHTO TP 62, MASW and FWD testing. This analysis demonstrated that field collected MASW and FWD data are very efficient in constructing the master curve which can later be used to shift MASW data to a standard frequency and temperature.
- 2) For circumstances where FWD data may not be available, for example pavement systems with thin asphalt concrete layers, the master curve cannot be constructed solely with MASW data due to the lack of data points at lower reduced frequencies. The combination of MASW moduli and moduli determined with the predictive equation at 40°C could be used in these circumstances. In an effort to simplify the correction of MASW data for roadways located throughout Nova Scotia and New Brunswick, without the necessity of developing the in-situ constructed master curves, standard equations for both the Barrington and Miramichi sites were developed.
- 3) The non-destructively determined master curve may also be implemented to temperature correct FWD data while providing better results than many standard functions described in the literature.
- 4) MASW and FWD in-situ determined moduli are sensitive to seasonal changes in the asphalt concrete most likely due to moisture induced and fatigue damage and can therefore be used effectively to construct a damaged master curve. Based on the field data, an equation was optimized to provide an alternative approach to constructing the damaged master curve.

- 5) Constructing the master curve using non-destructive data for each individual site being evaluated with will provide the best form of characterization.

## **5.7 REFERENCES**

AASHTO TP 62-03 (2005). “Standard method of test for determining dynamic modulus of hot-mix asphalt concrete mixtures”, American Association of State Highway and Transportation Officials, Washington, D.C.

ASTM D3497-79 (2003). “Standard Test Method for Dynamic Modulus of Asphalt Mixtures”, ASTM International, West Conshohocken, PA. [www.astm.org](http://www.astm.org).

Bai, X. (2004). “Assessment of relationship between dynamic and seismic moduli of asphalt concrete mixtures”, M.Sc. thesis, The University of Texas at El Paso.

Bari, J., Witczak, M.W. (2005). “Evaluation of the effect of lime modification on the dynamic modulus stiffness of hot-mix asphalt”, Transportation Research Record 1929, Transportation Research Board, National Research Council, Washington, D.C., pp. 10-19.

Barnes, C.L. (2008). “Evaluating moisture damage in asphalt concrete using surface waves”, Ph.D. thesis, Dalhousie University.

Barnes, C.L., Trottier, J.-F. (2009). “Evaluating High-Frequency Visco-Elastic Moduli in Asphalt Concrete”, Research in Nondestructive Evaluation, Volume 20, Issue 2, pp.116-130.

Barnes, C.L., Trottier, J.-F. (2010). “Evaluating in-service asphalt concrete damage using surface waves”, International Journal of Pavement Engineering, Volume 11, Number 6, pp. 449-458.

Bonaquist, R., Christensen, D.W. (2005). “Practical procedure for developing dynamic modulus master curves for pavement structural design”, Transportation Research Record 1929, Transportation Research Board, National Research Council, Washington, D.C., pp. 208-217.

Celaya, M., Nazarian, S. (2006). “Seismic testing to determine quality of hot-mix asphalt”, Transportation Research Record 1946, Transportation Research Board, National Research Council, Washington, D.C., pp. 113-122.

Chang, D.-W., Roesset, J.M., Stokoe II, K.H. (1992). “Nonlinear effects in falling weight deflectometer tests”, Transportation Research Record 1355, Transportation Research Board, National Research Council, Washington, D.C., pp. 1-7.

Dougan, C.E., Stephens, J.E., Mahoney, J., Hansen, G. (2003). “E\* dynamic modulus – test protocol – problems and solutions”, Report No. CT-SPR-0003084-F-03-3, Connecticut Transportation Institute, University of Connecticut, Storrs, Connecticut.

Dynatest (2013). Dynatest Elmod 6 program package – Demo Version, Dynatest International, Glostrup, Denmark.

Gudmarsson, A., Ryden, N., Birgisson, B. (2012a). “Application of resonant acoustic spectroscopy to asphalt concrete beams for determination of the dynamic modulus”, Materials and Structures, Vol. 45, pp. 1903-1913.

Gudmarsson, A., Ryden, N., Birgisson, B. (2012b) “Characterizing the low strain complex modulus of asphalt concrete specimens through optimization of frequency response functions”, Journal of Acoustical Society of America, Vol. 132, Issue 4, pp. 2304-2312.



Hakim, B., Brown, S.F. (2006). "Pavement analysis using the FWD: Practical difficulties and proposed simplifications", 10<sup>th</sup> International Conference on Asphalt Pavement, International Society of Asphalt Pavements, Quebec, Canada, August 12-17.

Hasim, M.S., Hameed, A.M., Mustafa, M.S. (1994). "The effect of edge restraint on FWD deflection values tested on asphalt road pavement", 4th International Conference, Bearing Capacity of Roads and Airfields, Minnesota Department of Transportation, Minneapolis, MN, pp. 259-272.

Irwin, L.H. (2002). "Backcalculation: An Overview and Perspective", <http://pms.nevadadot.com/2002presentations/11.pdf>

Kweon, G., Kim, Y.R. (2006). "Determination of asphalt concrete complex modulus with impact resonance test", Transportation Research Record 1970, Transportation Research Board, National Research Council, Washington, D.C., pp. 151-160.

Lacroix, A., Kim, Y.R., Sadat, M., Far, S. (2009). "Constructing the dynamic modulus mastercurve using impact resonance testing", Asphalt Paving Technology, Vol. 78, The Association of Asphalt Paving Technologists, pp. 67-102.

Lukanen, E.O., Stubstad, R., Briggs, R. (2000). "Temperature predictions and adjustment factors for asphalt pavement, Federal Highway Administration, Publication No. FHWA-RD-98-085, McLean, Va.

Lytton, R. L., Germann, F. P., Chou, Y. J., Stoffels, S. M. (1990). "Determining asphaltic concrete pavement structural properties by non-destructive testing." National Cooperative Highway Research Program (NCHRP) Report 327, Transportation Research Board, Washington, D.C.

Maser, K.R., Holland, T.J., Roberts, R., and Popovics, J. (2006). “NDE methods for quality assurance of new pavement thickness”, *The International Journal of Pavement Engineering*, Vol. 7, No. 1, pp. 1-10.

National Cooperative Highway Research Program (NCHRP) (2004). “Guide for mechanistic-empirical design of new and rehabilitated pavement structures” NCHRP 1-37A Design Guide, Washington, D.C., <http://www.trb.org/mepdg/guide.htm> [Accessed 25 January 2010].

Nazarian, S., Tandon, V., Yuan, D. (2005). “Mechanistic quality management of asphalt concrete layers with seismic methods”, *Journal of ASTM International*, Vol. 2, No. 9, October, Paper ID: JAI12256.

Oh, J. H., E. G. Fernando, E.G., Lee, I., Holzschuher, C. (2012). “Correlation of asphalt concrete layer moduli determined from laboratory and non-destructive field tests”, *ASCE Journal of Transportation Engineering*, Vol. 138, No. 3, pp. 361-370.

Park, C.B., Miller, R.D., and Xia, J. (1999). “Multimodal analysis of high frequency surface waves”, *Proceedings of the Symposium of Applied Geophysics in Engineering and Environmental Problems (SAGEEP 1999)*, Oakland, CA, pp.115-121.

Park, D., Buch, N., Chatti, K. (2001). “Effective Layer Temperature Prediction Model and Temperature Correction via Falling Weight Deflectometer Deflections”, *Transportation Research Record 1764*, Transportation Research Board, National Research Council, Washington, D.C., pp. 97-111.

Ping, W.V., Xiao, Y. (2007). “Final Report: Evaluation of the dynamic complex modulus test and indirect diametral test for implementing the AASHTO 2002 Design Guide for Pavement Structures in Florida”, Florida Department of Transportation, BC-352-12, Tallahassee, Florida.

Ryden, N., Park, C.B., Ulriksen, P., and Miller, R.D. (2004). “Multimodal Approach to Seismic Pavement Testing”, *Journal of Geotechnical and Geoenvironmental Engineering*, Vol. 130, No. 6, pp. 636-645.

Ryden, N. (2011). “Resonant frequency testing of cylindrical asphalt samples”, *European Journal of Environmental and Civil Engineering*, Vol. 15, No. 4, pp. 587–600.

Seo, J., Kim, Y., Cho, J., Jeong, S. (2012). “Estimation of in situ dynamic modulus by using MEPDG dynamic modulus and FWD data at different temperatures”, *International Journal of Pavement Engineering*, Vol. 14, Issue 4, pp.1-11.

Ullidtz, P., and Stubstad, R.N. (1985). *Analytical Empirical Pavement Evaluation Using the Falling Weight Deflectometer*”, Transportation Research Record 1022, Transportation Research Board, National Research Council, Washington, D.C., pp. 36-44.

Van Velsor, J.K., Premkumar, L., Chehab, G., Rose, J.L. (2011). “Measuring the complex modulus of asphalt concrete using ultrasonic testing”, *Journal of Engineering Science and Technology Review*, Vol. 4, No. 2, pp. 160-168.

Willett, D.A., Mahboub, K., and Rister, B. (2006). “Accuracy of Ground-Penetrating Radar for Pavement Layer Thickness Analysis”, *Journal of Transportation Engineering*, ASCE, Vol. 132, No. 1, pp. 96-103.

Zhu, H., Sun, L., Yang, J., Chen, Z., Gu, W. (2011). *Developing master curves and predicting dynamic modulus of polymer-modified asphalt mixtures*”, *ASCE Journal of Materials in Civil Engineering*, Vol. 23, No. 2, pp. 131-137.

## **CHAPTER 6      DISCUSSION**

Asphalt concrete master curve construction using MASW and FWD field measured dynamic modulus values collected at multiple temperatures has been presented as a viable method for the construction of in-situ master curves. Seismic surface wave testing has been shown to provide accurate non-destructive estimates of the in-situ asphalt concrete modulus, however since these moduli values are measured at high frequencies and need to be corrected to a reference frequency and temperature for use in pavement design, the adoption of the test method has been limited by the pavement engineering community. As a result, FWD is currently the test method of choice for many highway agencies and as the recommended standard for assessing in-situ pavements as described in the MEPDG. It has been shown in Paper № 1 that seismic surface wave testing can complement FWD testing and provide an overall improved solution where there are known deficiencies when attempting to backcalculate the moduli of certain pavement structures. By providing a simpler technique that is more accessible to transportation agencies for constructing the master curve and correcting the seismic moduli to a standard design frequency, adoption of seismic testing may become prevalent and would enhance pavement evaluation techniques.

The original focus of this research was to implement multiple non-destructive testing techniques including GPR and MASW and to monitor in-situ seasonal changes using instrumented test sections to improve FWD testing in the Canadian Maritime Provinces. Four test sections, three in Nova Scotia and one in New Brunswick were selected as part of a collaborative research effort between academia, government, and industry. As testing progressed, it was noted that MASW moduli would be a valuable complement to FWD testing, however there was a requirement to correct the moduli to a standard design frequency. Consequently, after the development of Paper № 1, where the importance of GPR and the value of MASW moduli values were presented, the focal point of the thesis shifted to enhancing master curve construction for correcting MASW moduli and developing master curves using field data to provide an alternative method to conventional laboratory testing generally not accessible to all transportation agencies.

FWD testing is currently the test method predominantly used in the evaluation of in-situ pavement structures. The FWD provides the capability to backcalculate the moduli of both the bound and unbound layers of the pavement system, however there are factors that can complicate and even obstruct the backcalculation process. Paper № 1 presented a case study where the importance of implementing GPR testing to determine layer thickness into pavement evaluation and rehabilitation design was validated and the use of MASW testing to measure in-situ seismic moduli to complement FWD testing was confirmed. The case study involved performing deflection testing by means of the FWD in addition to GPR and MASW testing along the longitudinal profile of a recently constructed 200 meter test section and across the transverse width of the traffic lane to measure variations in thickness and resultant moduli.

Cores were extracted in the outer wheel path along the test section to calibrate GPR data and to perform dynamic modulus testing for comparison with in-situ measured moduli and for constructing the master curve to correct MASW data to a standard design frequency. The maximum variation in core thicknesses was measured to be 39 mm while the GPR results indicated a 65 mm variation in thickness between the center of the lane and the pavement edge and a 60 mm variation longitudinally along the outer wheel path. As a result there were significant differences between the nearest measured core thickness and the actual thickness measured with GPR when considering the FWD test locations. Backcalculation of the layer moduli was performed first using the core determined thicknesses and then with the GPR measured values resulting in a 40 percent difference in measured asphalt concrete moduli. The backcalculated moduli were then compared to the corrected MASW moduli and the AASHTO TP 62 determined moduli where it was found that the backcalculated moduli determined with GPR provided a better estimate to the other testing techniques.

To reinforce the significance of using the correct thickness and moduli in pavement design, a required overlay thickness was established using the parameters of the AASHTO 1993 Pavement Guide. The difference in modulus and thickness between GPR and non-GPR data in this study resulted in nearly a 50 mm difference in overlay thickness. Through this

study it is recommended that highway agencies make GPR testing a requirement when assessing in-situ pavements and that the GPR data be collected along the exact path of the FWD data collection.

Many trunks, routes and local roads found throughout the provinces of Nova Scotia and New Brunswick have very narrow shoulders with the outer wheel path approaching the edge of the asphalt concrete pavement. It was also determined in Paper № 1 that MASW testing may be used to differentiate between asphalt moduli reductions related to pavement edge effects and actual pavement distress. The recorded FWD deflections increased significantly closer to the pavement edge resulting in a modular decrease suggesting that the backcalculated moduli are not only influenced by the damage across the traffic lane, but also by the lack of shoulder support. The MASW determined moduli at the center of the lane correlated with the undamaged modulus determined using AASHTO TP 62 and only decreased slightly across the lane which could indicate slight amounts of fatigue damage in the wheel path, or perhaps construction flaws as you approach the edge (lack of compaction). Consequently, the difference in backcalculated moduli to MASW moduli generally increased near the edge of the lane. The MASW results are not influenced by the properties or behaviour of the underlying materials as the test focuses solely within the asphalt concrete layer. Therefore the results represent the actual material modulus and not necessarily the modulus required to fit the pavement system providing a method of differentiating between edge effects and actual pavement distress. Since the MASW calculated moduli may be determined to within approximately 20 mm from the surface, the MASW test may also complement the FWD for pavement structures with thin layer asphalts (< 70 mm) by seeding the asphalt modulus in the backcalculation procedure.

The MEPDG does briefly describe some of the benefits of implementing seismic testing for pavement evaluation, however there has been minimal adoption of the technology by transportation agencies or researchers due to the dissimilarity between the higher frequency seismic moduli and the low frequency modulus required in design. The master curve constructed using conventional AASHTO TP 62 testing has provided a method of correcting seismic moduli but the influence of incorporating seismic data with conventional

dynamic modulus data has not been examined. Paper № 2 presents an experimental study in which MASW testing was conducted at multiple temperatures on 70 x 250 x 450 mm asphalt concrete plate specimens, cut from an asphalt concrete pavement produced using standard procedures, and later cored and used to perform AASHTO TP 62 testing. Two additional plate specimens were used to establish the asphalt concrete volumetric parameters for constructing the master curve using dynamic moduli values computed from the predictive equation described in the MEPDG. Master curves were also constructed for data sets consisting of the AASHTO TP 62 dynamic moduli, and a combination of the AASHTO TP 62 data with surface wave based moduli, using four different methods of modelling the shift factor (the MEPDG Model, the Arrhenius Equation, the WLF Equation, and the Second Order Polynomial Equation). Once all of the master curves were constructed, a statistical analysis was performed to assess the viability of the construction techniques by plotting the master curve predicted  $E^*$  versus the laboratory measured  $E^*$  values and calculating goodness of fit statistics. The results indicated that the only master curve that did not provide acceptable results was the Level 3 MEPDG predictive equation without binder data.

The main objective of Paper № 2 was to establish the master curve construction technique that would provide the most reliable method for correcting MASW moduli. To assess the impact of subtle differences among the various master curves, actual MASW data was corrected to standard design values (21°C and 10 Hz) and compared to the measured laboratory values. By comparing the percentage relative error of corrected versus laboratory determined moduli it was concluded that the master curves constructed with a combination of MASW and AASHTO TP 62 data, regardless of shift factor equation, provided the smallest error. Therefore using a combination of dynamic modulus data appears to be significantly more important than the selection of shift factor equation. In general, the evaluation of master curves is limited to performing statistical analysis, therefore to further assess the ability of a master curve to properly shift MASW data to a reference design value, corrected moduli values obtained in the study were implemented into a fatigue analysis using the fatigue model supplied in the MEPDG. This exercise

revealed that small deviations in the corrected moduli that might be overlooked in the statistical analysis may not adequately represent the variations in design parameters.

Upon completion of Paper № 2, where the inclusion of seismic moduli in construction of the master curve was shown to enhance the correction procedure, it was determined that a similar study should be attempted using field measured data and that a master curve be constructed solely from the in-situ data. For transportation agencies that generally collect seasonal FWD data, adding seismic testing to their program could provide an opportunity to construct master curves for those particular sections.

Paper № 3 presents an experimental study in which FWD and MASW testing were performed in tandem over a two year period on two 200 m in-situ test sections with the initial purpose of improving FWD backcalculation and reviewing seasonal characteristics, however the final result developed into constructing in-situ master curves. The first test section was located in Barrington, Nova Scotia, and the other in Miramichi, New Brunswick. These sections were selected due to the differences in asphalt mixture type and geographic location. Core samples were extracted from the roadway approximately one month after completion of the highway section and non-destructive testing, including, GPR, MASW, and FWD commenced shortly after. The extracted core samples were used to calibrate the GPR thickness evaluation and to perform AASHTO TP 62 testing to construct the undamaged master curve for comparison with the in-situ constructed curve. The original asphalt concrete mixture designs, construction records and binder data were implemented into the predictive equation for establishing a predictive master curve. MASW and FWD testing were initially performed in the outer wheel path, however a reduction in modulus from the AASHTO TP 62 undamaged value was observed using both test methods during certain periods throughout the year, most generally between late fall and mid spring. At that point, a comparison evaluation between testing in the outer wheel path and the center of the lane was established. It was observed that the moduli values measured in the center of the lane remained undamaged during that period and that testing in the outer wheel path during summer months provided relatively undamaged values.



Once all of the data was analyzed and tabulated for both the Barrington and Miramichi sites, in addition to the master curves constructed using predictive and AASHTO TP 62 dynamic moduli, master curves were also constructed for data sets consisting of a combination of the AASHTO TP 62 data with surface wave and FWD based moduli, MASW and FWD moduli, and MASW with predictive moduli using the Second Order Polynomial Equation for modelling the shift factor. To assess the viability of the master curve construction techniques, a similar statistical analysis as was performed in Paper № 2 was completed validating the effectiveness of constructing the master curve using solely field measured MASW and FWD data. The non-destructive only curves used to correct MASW data in comparison to the laboratory measured value resulted in percentage errors of similar magnitude to the curves constructed using AASHTO TP 62 and a combination of AASHTO TP 62, MASW, and FWD. It is important to note that since the AASHTO TP 62 testing was performed on undamaged asphalt core specimens, for comparison purposes, the MASW and FWD data used in the master curve construction evaluation was based on undamaged test results, therefore resulting in the use of data collected during summer months or from the center of the lane. In addition, due to time restraints a design analysis as recommended by Paper № 2 was not performed. The predictive equation master curve and the master curve produced with MASW moduli in conjunction with predictive moduli did not produce adequate results for use in design. Consequently, it is recommended that a comprehensive study be undertaken to evaluate the predictive equation parameters for the asphalt concretes currently used in the Maritime Provinces.

In addition to comparing the capability of the non-destructive master curve for correcting MASW data to a useable design frequency, the master curve was also used to correct FWD data for temperature in comparison to some of the standard equations generally used in practice. Many transportation agencies utilize these equations or procedures and realize that there may be a requirement for calibration, but rarely take the initiative. The results of the comparison suggest that the non-destructive master curve can also be implemented in temperature correcting FWD data and that as recommended by Dynatest the standard curves provided with ELMOD do require calibration for local conditions.

As described above, a large portion of the data was not implemented into the master curve construction analysis due to the apparent damage occurring during the colder and wetter months. All of the seismic and FWD moduli collected were plotted in comparison to the undamaged master curve. Reviewing the plot, it was observed that the reduction in stiffness of the damaged moduli were of similar scale and that the data may be used to construct a master curve characterizing the damage. Therefore a master curve with four new sigmoidal function parameters ( $\delta$ ,  $\alpha$ ,  $\beta$ ,  $\gamma$ ) was established using non-destructive moduli in addition to a master curve with only a change to the alpha parameter as outlined in the MEPDG. The MEPDG recommends using FWD measured in-situ moduli to establish a damage factor which is then applied to the alpha sigmoidal parameter creating a damaged master curve. This procedure was also performed but did not produce similar results to the curves constructed using non-destructive data. A second procedure based on FWD data (Seo et al., 2012), where the damage factor described in the MEPDG is revised, was attempted and provided slight improvements to the results. Consequently, a study was performed to optimize the equation described by Seo et al. (2012) to include the seismic surface wave moduli values in addition to the FWD data where it was observed that the equation parameters produced using solely MASW moduli or solely FWD moduli produced erroneous results, while the master curve constructed from parameters established through the combination of MASW and FWD data provided similar results to the non-destructive only master curves.

The final aspect considered in Paper № 3 was the optimization to local conditions of the equation discussed by Oh et al. (2012) to provide a simpler procedure than the master curve for correcting seismic moduli for thin layer pavements. Using the master curve parameters determined for the Barrington and Miramichi test sites two equations were produced. As expected, there were considerable differences between the equations established for each site and in comparison to the equation established by Oh et al. (2012) for a site in Florida due to the variation in construction materials. The equations were then used to correct surface wave moduli collected at a second site located in Nova Scotia and compared to the laboratory determined moduli. The curve constructed from the Barrington site provided the best approximation considering that the same binder was implemented for both asphalt

mixtures. As discussed in Paper № 3, there is an abundance of acceptable asphalt concrete aggregate throughout Nova Scotia, therefore the characterization of one asphalt concrete mixture regardless of binder certainly does not encompass the entire Province. Accordingly, the construction of an in-situ master curve for all sites to be evaluated will provide the best technique for correcting seismic moduli, however in circumstances where that is not viable, establishing a master curve or simplified equation for a nearby site may be satisfactory.

The following provides an example demonstrating the potential benefits of this research. In the case of NSTIR, who are slowly attempting to shift to a mechanistic-empirical pavement design methodology, there is currently no test data available characterizing the dynamic moduli of any asphalt concrete mixture utilized in the province. They currently have 18 test sections where they are conducting seasonal testing to help characterize seasonal effects and would like to characterize the asphalt in-situ, therefore as shown in Paper № 3 supplementing FWD testing with seismic testing throughout the test program would provide them the opportunity to produce master curves for each site. There is also an abundance of shallow bedrock and highly non-linear subgrades located throughout the province complicating the backcalculation process. Utilizing the non-destructively determined master curves for correcting the seismic data would provide a seed modulus for the asphalt concrete simplifying the backcalculation of the unbound layer moduli. If the province established 18 in-situ master curves scattered throughout the province, they may be used in circumstances where tandem in-situ testing could not be supported, i.e. thin asphalt layers.

Simulated multichannel surface wave testing adapted by Barnes and Trottier (2009) was selected as the seismic test method for this research. This non-destructive test method was selected primarily due to the availability of the equipment, however the research had also shown the benefits of using this procedure including enhanced repeatability and the ability to obtain useful phase velocity data at frequencies up to 90 kHz (to within 20 mm of the surface). One of the concerns with the test was the time required to collect and analyze the data, therefore alternative seismic testing procedures could be evaluated to determine the

overall benefits of each and which provides the best approach for constructing the in-situ master curve. It is important to note that the main objective was to utilize a seismic testing procedure that could complement other non-destructive techniques for pavement evaluation. There was no attempt initiated to provide input or to suggest modifications to the testing procedures utilized.

For circumstances where seismic surface wave in-situ testing may not be feasible, conducting MASW testing in the laboratory using extracted plate samples as described in Paper № 2 could be a viable solution. MASW moduli at multiple temperatures could be performed with relative ease but the main drawback becomes the destructive nature of the test. The other concern would be attempting to extract a plate sample on pavement structures with thin asphalt concrete layers. For these instances, the implementation of free-free resonant frequency measurements on core samples of arbitrary size (Ryden, 2011) may produce the desired moduli values in conjunction with the predictive equation. As part of the overall research conducted, resonant frequency testing was performed on core samples extracted from the plate samples tested in Paper № 2. The testing and results are not included in this thesis since this test requires destructive core extraction and the focus was to produce non-destructive master curves. However preliminary results as displayed in Figure 26 provided comparable results to the MASW determined moduli.

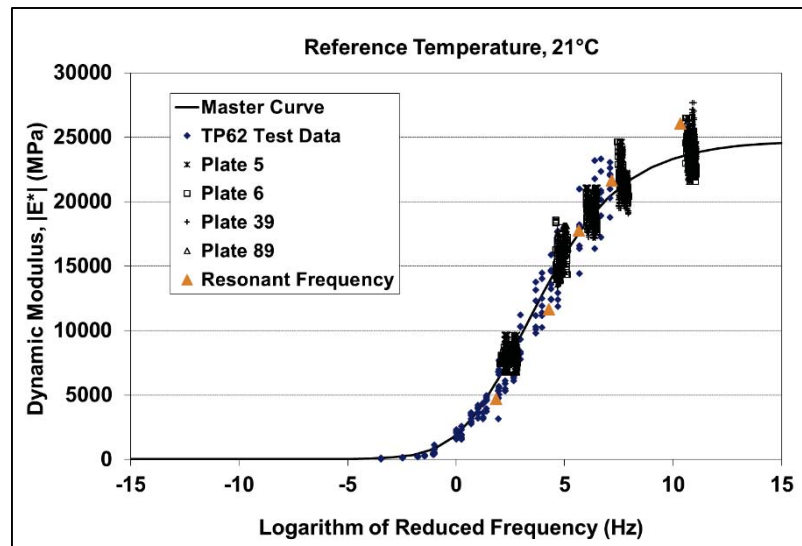


Figure 26 Comparison of MASW and resonant frequency moduli.

## **CHAPTER 7      CONCLUSION**

The research presented in this thesis addressed the requirement to construct an in-situ master curve using MASW and FWD field data collected at a variety of temperatures to make construction of master curves more accessible to agencies without the necessity of conducting destructive core testing. The construction of an in-situ master curve also provides a valuable tool of correcting seismic moduli to a standard frequency which may increase the overall appeal of seismic testing to the pavement community and provide a tool for supplementing routine FWD testing. In general, FWD is the non-destructive test method recommended in design standards and selected by highway agencies for pavement evaluation, however literature has identified some deficiencies in the backcalculation procedure that may be supplemented with GPR and seismic testing including variations in layer thicknesses, edge restraint, shallow bedrock, and thin asphalt concrete layers. Some other key elements that have not been examined in the literature with regards to seismic testing and master curves include the outcome of including in-situ seismic moduli on the constructed master curve parameters, the impact of the shift factor model used in generating the asphalt concrete master curve on seismic moduli correction, validating constructed master curves using design examples in addition to statistical analysis, and the ability to construct an in-situ damaged master curve. The conclusions of this research as described in the three papers are summarized as follows:

- 1) Due to the extreme variations in layer thicknesses associated with pavement construction, GPR testing should be considered by all transportation agencies for measuring continuous layer profiles for pavement design and evaluation, especially when FWD testing is performed. Applying GPR testing in the exact path of the FWD is also important due to the transverse thickness variations that may be observed.
- 2) For roadways where there is no paved shoulder and the outer wheel path falls close to the pavement edge it was determined that MASW may be used to

differentiate between asphalt moduli reductions related to pavement edge effects and actual pavement distress or flaws. The MASW results are not influenced by the lack of shoulder support as compared to the backcalculated results. The MASW reduction in modulus across the lane width coincides with actual damage or flaws within the asphalt layer, while backcalculated moduli values show a reduction due to a combination of damage and lack of shoulder support. The MASW calculated moduli which may be determined to within approximately 20 mm of the surface would provide a valuable complement to FWD testing for pavements with thin layer asphalts.

- 3) Using a combination of dynamic modulus data appears to be significantly more important than the selection of shift factor equation. The MEPDG and polynomial equations seemed to provide the best results, regardless of the dynamic modulus collection technique. This analysis demonstrated the importance of implementing a combination of MASW and AASHTO TP 62 dynamic modulus data to construct master curves to be used in shifting MASW field data to reference temperatures and frequencies if AASHTO TP 62 data is available.
- 4) If MASW data is to be used in pavement analysis and design, the ability of a master curve to properly shift data to a reference design value becomes extremely important as demonstrated by the fatigue analysis in Paper № 2. It is important to validate the master curve statistically, but small deviations in modulus that might be overlooked in the statistical analysis may not adequately represent the variations in design parameters.
- 5) MASW and FWD field measured dynamic modulus values collected at multiple temperatures may be used for generating the asphalt concrete master curve as opposed to traditional. A statistical analysis was used to demonstrate that the master curve constructed with the field collected MASW and FWD

data is highly effective for correcting surface wave moduli to a standard frequency and temperature.

- 6) In circumstances where FWD backcalculated moduli for the asphalt concrete layer are not available, the master curve cannot be constructed solely with MASW data due to the lack of data points at lower reduced frequencies. The combination of MASW moduli and moduli determined with the predictive equation at 40°C could be used, however the results are sub-standard. In an effort to simplify the correction of MASW data for roadways located throughout Nova Scotia and New Brunswick, without the necessity of the in-situ constructed master curves, standard equations for both the Barrington and Miramichi sites were developed.
- 7) The non-destructively determined master curve may also be utilized for temperature correcting FWD data while providing better results than many standard functions described in the literature.
- 8) MASW and FWD in-situ determined moduli are sensitive to seasonal changes in the asphalt concrete most likely due to moisture induced and fatigue damage and can be used effectively for constructing the damaged master curve. Based on the field data, an equation was optimized to provide an alternative approach for constructing the damaged master curve, however generating the non-destructive master curve solely from in-situ test points best fit the measured data.
- 9) Constructing the master curve using non-destructive data for each individual site being evaluated will provide the best form of characterization. In the case of Nova Scotia where there is such an abundance of acceptable aggregate, an in-situ tool to characterize the asphalt concrete master curve is of significant importance.

Through review and discussion of the research findings, the following recommendations are also proposed:

- 1) The full complement of nondestructive testing, GPR, FWD, and MASW, should be performed on multiple pavement structures with an asphalt concrete thickness less than 70 mm to assess the effectiveness of the seismic testing. Obtaining data and completing several rehabilitation pavement designs by seeding the asphalt concrete modulus would help validate the overall effectiveness of the complement of testing and may lead to agencies adapting their testing procedures.
- 2) The test sites used in this research were instrumented with two strain gauges located at the bottom of the asphalt concrete layer. Strains were periodically measured while performing FWD testing, therefore the gauge data may be used to correlate the calculated and field measured strains for confirming the FWD backcalculated moduli values.
- 3) For the construction of master curves using seismic and conventional moduli, future research should explore the influence of several different asphalt concrete mixtures (different aggregate size, binder type, binder content, air voids etc.) on the observed results from this study.
- 4) A comprehensive study should be undertaken to assess the validity of the MEPDG predictive equation for the asphalt mixtures currently used in the Canadian Maritime Provinces. This study should include several different aggregate sources, varying aggregate gradation specifications, asphalt contents, air voids, binder grades, and review aging models. The assessment would require a tremendous amount of conventional laboratory dynamic modulus testing, however this would provide the local agencies with a large database of master curves and typical dynamic modulus values considering there is no historical data.



- 5) Multiple seismic testing techniques should be evaluated for the same pavement structure to determine the pros and cons of each technique in direct comparison. Some of the factors that should be assessed include whether the technique is non-destructive, thickness of asphalt concrete capable of being assessed, ease and speed of testing and processing, repeatability of results, cost of the apparatus, and the capability of constructing an in-situ non-destructive master curve. For the MASW test used in this research, a higher frequency impact source should be implemented to attempt to obtain moduli at shallower depths at higher collection temperatures.
- 6) The study to compare the MASW test results with resonant frequency methods originally commenced during this research should be completed to provide an alternative procedure for assessing thin layer asphalt cores.
- 7) In-situ damaged master curves should be constructed for several pavement structures at various levels of visual distress. This would aid in determining the sensitivity of the in-situ master curve construction. In addition, attempting to delineate damage between asphalt concrete layers and constructing master curves for each may become a useful tool in assessing damage type and severity. A laboratory study may be implemented in this case.
- 8) A comprehensive study should be undertaken to characterize the damage and healing effect observed during the warmer and dryer months. In this instance, testing should be performed at much closer time intervals and cores may be utilized to perform additional laboratory testing or visual assessment to correlate field data. MASW could be used to assess variations in surface wave derived moduli with depth to localize the damage to a particular asphalt concrete lift.

## REFERENCES

AASHTO TP 62-03 (2005). “Standard method of test for determining dynamic modulus of hot-mix asphalt concrete mixtures”, American Association of State Highway and Transportation Officials, Washington, D.C.

Achenbach, J.D. (1973). *Wave Propagation in Elastic Solids*, North Holland Publishing Company, Amsterdam/New York.

Al-Qadi, I.L., and Lahouar, S. (2004). “Ground penetrating radar: State of the practice for pavement assessment”, *Materials Evaluation*, American Society for Nondestructive Testing, Vol. 62, No. 7, pp. 759-763.

American Association of State Highway and Transportation Officials. (1993). “AASHTO Guide for Design of Pavement Structures”, Washington, D.C.

ASTM C 215 (2008). “Standard test method for fundamental transverse, longitudinal, and torsional frequencies of concrete specimens”, ASTM International, West Conshohocken, PA. [www.astm.org](http://www.astm.org).

ASTM D3497-79 (2003). “Standard Test Method for Dynamic Modulus of Asphalt Mixtures”, ASTM International, West Conshohocken, PA. [www.astm.org](http://www.astm.org).

Bai, X. (2004). “Assessment of relationship between dynamic and seismic moduli of asphalt concrete mixtures”, M.Sc. thesis, The University of Texas at El Paso.

Bari, J., Witzczak, M.W. (2005). “Evaluation of the effect of lime modification on the dynamic modulus stiffness of hot-mix asphalt”, *Transportation Research Record 1929*, Transportation Research Board, National Research Council, Washington, D.C., pp. 10-19.

Barnes, C.L. (2008). "Evaluating moisture damage in asphalt concrete using surface waves", Ph.D. thesis, Dalhousie University.

Barnes, C.L., Trottier, J.-F. (2009). "Evaluating High-Frequency Visco-Elastic Moduli in Asphalt Concrete", *Research in Nondestructive Evaluation*, Volume 20, Issue 2, pp.116-130.

Barnes, C.L., Trottier, J.-F. (2010). "Evaluating in-service asphalt concrete damage using surface waves", *International Journal of Pavement Engineering*, Volume 11, Number 6, pp. 449-458.

Biswas, K.G., Pellinen, T.K. (2007). "Practical methodology of determining the in situ dynamic (complex) moduli for engineering analysis", *ASCE Journal of Materials in Civil Engineering*, Vol. 19, No. 6, pp.508-514.

Bonaquist, R., Christensen, D.W. (2005). "Practical procedure for developing dynamic modulus master curves for pavement structural design", *Transportation Research Record 1929*, Transportation Research Board, National Research Council, Washington, D.C., pp. 208-217.

Celaya, M., Nazarian, S. (2006). "Seismic testing to determine quality of hot-mix asphalt", *Transportation Research Record 1946*, Transportation Research Board, National Research Council, Washington, D.C., pp. 113-122.

Chang, D.-W., Roesset, J.M., Stokoe II, K.H. (1992). "Nonlinear effects in falling weight deflectometer tests", *Transportation Research Record 1355*, Transportation Research Board, National Research Council, Washington, D.C., pp. 1-7.

Dongre, R., Myers, L., D'Angelo, J., Paugh, C., Gudimettla, J. (2005). "Field evaluation of Witczak and Hirsch models for predicting dynamic modulus of hot-mix asphalt", Journal of the Association of Asphalt Paving Technologists from the Proceedings of the Technical Sessions, Vol. 74, 2005.

Dougan, C.E., Stephens, J.E., Mahoney, J., Hansen, G. (2003). "E\* dynamic modulus – test protocol – problems and solutions", Report No. CT-SPR-0003084-F-03-3, Connecticut Transportation Institute, University of Connecticut, Storrs, Connecticut.

Dynatest (2013). Dynatest Elmod 6 program package – Demo Version, Dynatest International, Glostrup, Denmark.

Gudmarsson, A., Ryden, N., Birgisson, B. (2012a). "Application of resonant acoustic spectroscopy to asphalt concrete beams for determination of the dynamic modulus", Materials and Structures, Vol. 45, pp. 1903-1913.

Gudmarsson, A., Ryden, N., Birgisson, B. (2012b) "Characterizing the low strain complex modulus of asphalt concrete specimens through optimization of frequency response functions", Journal of Acoustical Society of America, Vol. 132, Issue 4, pp. 2304-2312.

Hadidi, R., Gucunski, N., Zaghoul, S., Vitillo, N., Shoukouhi, P. (2006). "Development of paving layer moduli temperature correction models for seismic pavement analyzer (SPA) in New Jersey", The 85<sup>th</sup> Transportation Research Board Annual Meeting, Washington, D.C., January 22-26.

Hakim, B., Brown, S.F. (2006). "Pavement analysis using the FWD: Practical difficulties and proposed simplifications", 10<sup>th</sup> International Conference on Asphalt Pavement, International Society of Asphalt Pavements, Quebec, Canada, August 12-17.

Hasim, M.S., Hameed, A.M., Mustafa, M.S. (1994). "The effect of edge restraint on FWD deflection values tested on asphalt road pavement", 4th International Conference, Bearing Capacity of Roads and Airfields, Minnesota Department of Transportation, Minneapolis, MN, pp. 259-272.

Heisey, J.S., Stokoe II, K.H., and Meyer, A.H. (1982). "Moduli of pavement systems from spectral analysis of surface waves", Transportation Research Record 852, Transportation Research Board, National Research Council, Washington, D.C., pp. 22-31.

Irwin, L.H. (2002). "Backcalculation: An Overview and Perspective", <http://pms.nevadadot.com/2002presentations/11.pdf>

Jones, R. (1955). "A vibration method for measuring the thickness of concrete road slabs in situ", Magazine of Concrete Research, Vol 7, No. 20, pp.97-102.

Kweon, G., Kim, Y.R. (2006). "Determination of asphalt concrete complex modulus with impact resonance test", Transportation Research Record 1970, Transportation Research Board, National Research Council, Washington, D.C., pp. 151-160.

Lacroix, A., Kim, Y.R., Sadat, M., Far, S. (2009). "Constructing the dynamic modulus mastercurve using impact resonance testing", Asphalt Paving Technology, Vol. 78, The Association of Asphalt Paving Technologists, pp. 67-102.

Loizos, A., and Plati, C. (2007). "Accuracy of pavement thickness estimation using different ground penetrating radar analysis approaches", NDT & E International, Elsevier Science, Vol. 40, No. 2, pp. 147-157.

Lukanen, E.O., Stubstad, R., Briggs, R. (2000). "Temperature predictions and adjustment factors for asphalt pavement, Federal Highway Administration, Publication No. FHWA-RD-98-085, McLean, Va.

Lytton, R. L., Germann, F. P., Chou, Y. J., Stoffels, S. M. (1990). "Determining asphaltic concrete pavement structural properties by non-destructive testing." National Cooperative Highway Research Program (NCHRP) Report 327, Transportation Research Board, Washington, D.C.

Maser, K.R., Holland, T.J., Roberts, R., and Popovics, J. (2006). "NDE methods for quality assurance of new pavement thickness", *The International Journal of Pavement Engineering*, Vol. 7, No. 1, pp. 1-10.

Mirza, M.W., Witczak, M.W. (1995). "Development of a global aging system for short and long term aging of asphalt cements", Annual Meeting of the Association of Asphalt Paving Technologists, The Association of Asphalt Paving Technologists, March, pp. 393-430.

National Cooperative Highway Research Program (NCHRP) (2004). "Guide for mechanistic-empirical design of new and rehabilitated pavement structures" NCHRP 1-37A Design Guide, Washington, D.C., <http://www.trb.org/mepdg/guide.htm> [Accessed 25 January 2010].

Nazarian, S., Stokoe II, K. H., Hudson, W.R. (1983). "Use of Spectral Analysis of Surface Waves Method for Determination of Moduli and Thicknesses of Pavement Systems", *Transportation Research Record 930*, Transportation Research Board, National Research Council, Washington, D.C., pp. 38-45.

Nazarian, S., Yuan, D., Tandon, V. (1999). "Structural field testing of flexible pavement layers with seismic methods for quality control", *Transportation Research Record 1654*, Transportation Research Board, National Research Council, Washington, D.C., pp. 50-60.

Nazarian, S., Tandon, V., Yuan, D. (2005). "Mechanistic quality management of asphalt concrete layers with seismic methods", *Journal of ASTM International*, Vol. 2, No. 9, October, Paper ID: JAI12256.

Oh, J. H., E. G. Fernando, E.G., Lee, I., Holzschuher, C. (2012). “Correlation of asphalt concrete layer moduli determined from laboratory and non-destructive field tests”, ASCE Journal of Transportation Engineering, Vol. 138, No. 3, pp. 361-370.

Park, C.B., Miller, R.D., and Xia, J. (1998). “Imaging dispersion curves of surface waves on multi-channel record”, Kansas Geological Survey, 68<sup>th</sup> Annual International Meeting of the Society of Exploration Geophysicists, Expanded Abstracts, pp. 1377-1380.

Park, C.B., Miller, R.D., and Xia, J. (1999). “Multimodal analysis of high frequency surface waves”, Proceedings of the Symposium of Applied Geophysics in Engineering and Environmental Problems (SAGEEP 1999), Oakland, CA, pp.115-121.

Park, D., Buch, N., Chatti, K. (2001). “Effective Layer Temperature Prediction Model and Temperature Correction via Falling Weight Deflectometer Deflections”, Transportation Research Record 1764, Transportation Research Board, National Research Council, Washington, D.C., pp. 97-111.

Pellinen, T.K., Witczak, M.W., and Bonaquist, R.A. (2004). “Asphalt mix master curve construction using sigmoidal fitting function with non-linear least squares optimization”, Recent Advances in Materials Characterization and Modeling of Pavement Systems, American Society of Civil Engineers Geotechnical Special Publication No. 123, pp. 83-101.

Ping, W.V., Xiao, Y. (2007). “Final Report: Evaluation of the dynamic complex modulus test and indirect diametral test for implementing the AASHTO 2002 Design Guide for Pavement Structures in Florida”, Florida Department of Transportation, BC-352-12, Tallahassee, Florida.

Roesset, J.M., Chang, D.W., Stokoe II, K.H., Aouad, M. (1990). “Modulus and thickness of the pavement surface layer from SWSW tests”, Transportation Research Record 1260, Transportation Research Board, National Research Council, Washington, D.C., pp. 53-63.

Rowe, G.M., Sharrock, M.J. (2011). “Alternate shift factor relationship for describing temperature dependency of viscoelastic behavior of asphalt materials”, Transportation Research Record 2207, Transportation Research Board, National Research Council, Washington, D.C., pp. 125-135.

Ryden, N., Ulriksen, P., Park, C.B., Miller, R.D., Xia, J., and Ivanov, J. (2001). “High frequency MASW for non-destructive testing of pavements-accelerometer approach”, Proceedings of the Symposium on the Application of Geophysics to Engineering and Environmental Problems (SAGEEP 2001), Environmental and Engineering Geophysical Society, Annual Meeting, Denver, RBA-5.

Ryden, N., Park, C.B., Ulriksen, P., and Miller R.D. (2003). “Lamb wave analysis for non-destructive testing of concrete plate structures ”, Proceedings of the Symposium on the Application of Geophysics to Engineering and Environmental Problems (SAGEEP 2003), San Antonio, TX, April 6-10, INF03.

Ryden, N. (2004). “Surface wave testing of pavements”, Ph.D. thesis, Lund University.

Ryden, N., Park, C.B., Ulriksen, P., and Miller, R.D. (2004). “Multimodal Approach to Seismic Pavement Testing”, Journal of Geotechnical and Geoenvironmental Engineering., Vol. 130, No. 6, pp. 636-645.

Ryden, N., Park, C.B. (2006). “Fast simulated annealing inversion of surface waves on pavement using phase-velocity spectra”, Geophysics, Vol. 71, No. 4, pp. R49-R58.

Ryden, N. (2011). “Resonant frequency testing of cylindrical asphalt samples”, European Journal of Environmental and Civil Engineering, Vol. 15, No. 4, pp. 587–600.



Seo, J., Kim, Y., Cho, J., Jeong, S. (2012). "Estimation of in situ dynamic modulus by using MEPDG dynamic modulus and FWD data at different temperatures", *International Journal of Pavement Engineering*, Vol. 14, Issue 4, pp.1-11.

Shahin, M. (1994). "*Pavement Management for Airports, Roads, and Parking Lots, 2<sup>nd</sup> Edition*", Springer, New York, N.Y.

Singh, D., Zaman, M., Commuri, S. (2012). "Evaluation of dynamic modulus of modified and unmodified asphalt mixes for different input levels of the MEPDG", *International Journal of Pavement Research and Technology*, Chinese Society of Pavement Engineering, Vol. 5, No.1, pp. 1-11.

Ullidtz, P., and Stubstad, R.N. (1985). "Analytical Empirical Pavement Evaluation Using the Falling Weight Deflectometer", *Transportation Research Record 1022*, Transportation Research Board, National Research Council, Washington, D.C., pp. 36-44.

Van Velsor, J.K., Premkumar, L., Chehab, G., Rose, J.L. (2011). "Measuring the complex modulus of asphalt concrete using ultrasonic testing", *Journal of Engineering Science and Technology Review*, Vol. 4, No. 2, pp. 160-168.

Walubita, L.F., Alvarez, A.E., Simate, G.S. (2011). "Evaluating and comparing different methods and models for generating relaxation modulus master-curves for asphalt mixes", *Construction and Building Materials*, Vol. 25, pp. 2619-2626.

Willett, D.A., Mahboub, K., and Rister, B. (2006). "Accuracy of Ground-Penetrating Radar for Pavement Layer Thickness Analysis", *Journal of Transportation Engineering*, ASCE, Vol. 132, No. 1, pp. 96-103.

Witczak, M.W., and Bari, J. (2004). "Development of a E\* master curve database for lime Modified Asphaltic Mixtures", <http://www.lime.org/Publications/MstrCurve.pdf>

Yuan, D., Nazarian, S., Chen, D.-H., Hugo, F. (1998). "Use of seismic pavement analyzer to monitor degradation of flexible pavements under Texas mobile load simulator", Transportation Research Record 1615, Transportation Research Board, National Research Council, Washington, D.C., pp. 3-10.

Zhu, H., Sun, L., Yang, J., Chen, Z., Gu, W. (2011). Developing master curves and predicting dynamic modulus of polymer-modified asphalt mixtures", ASCE Journal of Materials in Civil Engineering, Vol. 23, No. 2, pp. 131-137.